



Czech Technical University in Prague

Faculty of Civil Engineering

Pavement Structures Permanent Deformation and Surface Roughness

Habilitation

December 2020

Ing. Josef Žák, Ph.D.

Acknowledgement:

I would like to thank my family, my wife Kateřina and both of my sons Adam and David, for their patience, encouragement and understanding that I did not spend more time with them during the time they were growing up.

I would like to thank to my colleague, prof. Renata Heralová, for her support as well as life mentors prof. Carl L. Monismith, RNDr. Jiří Stastna, prof. Ludo Zanzotto, prof. John Harvey and Dr. James Signore for their willingness to share their wisdom. I would like to express my special acknowledgement as well to my colleagues Ing. Jan Suda, Ph.D. and Dr. Erdem Coleri for their cooperation, as well as to many colleagues from the Department of Management and Economics, Department of Road Structures at CTU in Prague and Institute of Information Theory and Automation at the Czech Academy of Sciences.

Last but not least to the Ministry of Industry and Trade of the Czech Republic, whose grants enabled several experiments and to the J. William Fulbright Commission, whose grant helped to realize the results published in this work as well.

Table of contents

1	Introduction	1
1.1	Foreword	1
1.2	Asphalt mixtures shear properties	2
1.3	Energy dissipation in asphalt mixtures	3
1.4	Permanent deformation simulation	4
1.5	Pavement roughness.....	5
1.6	Summary	7
1.6.1	Uniaxial Shear Tester	7
1.6.2	ResiSkan.....	12
1.6.3	Software for pavements reconstructions.....	15
2	Scientific works	18
2.1	Žák, J., Monismith, C.L., Coleri, E.,Harvey, J. T., Uniaxial Shear Tester – new test method to determine shear properties of asphalt mixtures, 2017.....	18
2.2	Žák, J., Suda, J., Uniaxial Shear Tester – test methodology, 2020.....	36
2.3	Žák, J., Suda, J., Ryjáček, P., Polymer Modification Technologies and Asphalt Mixtures Fatigue Resistance in Pavement Structures, 2016.....	57
2.4	Žák, J., Suda, J., Laboratory Design and Testing of Asphalt Mixtures Dissipating Energy, 2019.....	68
2.5	Žák, J., Coleri, E., Harvey, J., Incremental rutting prediction with asphalt mixture shear properties, 2018.....	85
2.6	Žák, J., Shear Accumulated Equilibrium Compliance as Permanent Deformation Susceptibility Parameter, 2020.....	102
2.7	Žák, J., On Laser Scanning, Pavement Surface Roughness and International Roughness Index in Highway Construction, 2016.....	123
2.8	Šroubek, F., Šorel, M., Žák, J., Obr, V., Precise International Roughness Index Calculation, 2020.....	137

1. Introduction

1.1. Foreword

Highways may in many aspects be seen as veins of our civilization. They form a vital network for transportation. Area vitality in terms of transportation is a primary factor in industrial development. The presence of capacity transport infrastructure is a development factor of the territory.

Highways are owned in most European countries by the governments; however smaller portions of this property are private. Highways are assets, regardless of ownership. Design, construction and maintenance of these assets is of key importance for all developed countries, and private owners. This work focuses on asphalt pavements which with the respect to construction and maintenance cost form the largest part of these assets.

This work addresses selected phenomena in the field of asphalt pavements. It mainly focusses on two phenomena: permanent deformation and roughness of pavements.

Permanent deformation has a surface manifest. The permanent deformation surface manifest, which is studied in this work, is present in the form of rutting. Rutting occurs in the wheel paths and is perceived as surface depressions and pavement shearing along the edges of the rut. The rutting may be caused by subgrade, material characteristics including insufficient compaction of the asphalt layer. Especially during high surface temperatures, the most serious distress mode is the rutting phenomenon.

The research conducted focused on the permanent deformation of well compacted asphalt layers, thus studying the material properties which define the resistance of asphalt mixtures to permanent deformation. In this field, shear properties form a key domain as is described in selected papers. However, the option to measure shear properties of asphalt mixtures is very limited. Especially in European countries, the proper testing device is not available. Mostly shear properties of asphalt mixtures are indirectly determined from other test methods or entirely overlooked. The current practice is focused on an empirical test method called the Hamburg Wheel Tracking Test (HWTT) or simplified as Wheel Tracking Test. This test method is fully empirical, and many countries have implemented the test results in the asphalt mix design methodology. The test method requires a unique test device and sample preparations. Its empirical basis is proven by the non-presence of HWTT characteristics in any of asphalt pavement design methodology. Simply the correlation between the HWTT and pavement rutting is not well expressible mathematically in relation to traffic loading and in situ performance. The newly developed test device called Uniaxial Shear Test and its development process and applications are described in selected papers.

Each traffic loading of the asphalt layer causes a change in the shape. This deformation is partly reversible (elastic) and partly irreversible (permanent). Selected papers focus on the energy dissipation and its effect of asphalt mixture resistance to permanent deformation. By studying the dissipation principle and its utilization on asphalt mixture design materials with high resistance to permanent deformation was developed.

Roughness is the other phenomena addressed in this work. Permanent deformation in asphalt layers is not the only factor in pavement roughness. Technological indiscipline during construction, unbound pavement layers and subgrade characteristics, as well as freeze and thaw cycles and overall pavement deterioration manifest in pavement surface unevenness. Many methods to measure pavement roughness are used worldwide. Among these, the rod and level and International Roughness Index (IRI) are the most frequently used test methods. The IRI is broadly recognized as the indicator of highway utility and as the characteristic that correlates well with convenience of transport and its quality. The research reported focusses on modern methods of data acquisition and IRI calculations. Methodology to utilize the IRI calculations from data acquired by laser scanning is presented. Moreover, the precise IRI calculation is proposed as is described in selected papers. The methodology to calculate the IRI from laser scan data and utilized IRI calculations was implemented in design software which is being used for reconstruction designs in industrial applications.

1.2. Asphalt mixtures shear properties

The lack of a device to measure shear properties of asphalt mixtures led to the development of the Uniaxial Shear Test (UST). UST is an assembly of Universal Testing Machines or Nottingham Asphalt Testers which are standard equipment for European laboratories. The test device is capable of testing samples prepared in laboratory as well as asphalt mixtures taken directly from the pavement. From the measured data, the linear-viscoelastic parameters can be derived. The following papers describe the development of the test device as well as two testing methods. Repeated Shear Tests and Uniaxial Shear Frequency Sweep Tests are described in these works.

It was found that the Repeated Shear Test might be a surrogate for the Repeated Shear Test at Constant Height performed in SuperPave Shear Test (SST). The correlation between SST and UST is assessed based on a correlation coefficient of the Frequency Sweep Test and Repeated Shear test at Constant Height.

The UST have been sold to several laboratories abroad. The document called “methodology” was written for the purpose of using the test device by laboratory technicians. It was the intention to prepare such a methodology following similar content and form as technical standards have, as this is a common document for laboratory technicians and it will allow simpler understanding and use. The document entitled “Uniaxial Shear Tester – Test methodology” was submitted to the head of the national TNK147 technical committee for consideration. This work includes the description of testing principles, test equipment, preparation of testing specimens, tempering, stress configuration and data collection and results calculations. Test protocols and recommended data acquisition stages are annexes of this document. Hopefully, this methodology will serve the needs of laboratory technicians and standardize the testing procedure in laboratories.

I’m including following works as part of this topic:

Žák, J., Monismith, C.L., Coleri, E, Harvey, J. T., Uniaxial Shear Tester – new test method to determine shear properties of asphalt mixtures, Road Materials and Pavement Design. 2017, 18 87-103. ISSN 1468-0629. WoS: 000393204700005, Scopus: 2-s2.0-85007392068

Žák, J., Suda, J.; Uniaxial Shear Tester – Test methodology; Submitted to the TNK147 technical committee for consideration, Czech Standardization Agency, 2020.

1.3. Energy dissipation in asphalt mixtures

Asphalt mixtures are basically composed of irregular aggregates with a small amount of asphalt binder and a low volume fraction of air voids. The aggregate and asphalt binder are renewable natural resources and composition of both have to be carefully designed so that the maximum potential of these resources is utilized.

The demand for better performing asphalt mixtures becomes more important with increasing volumes and traffic loads. Municipalities, airports and road administrations are paying extra attention to the asphalt mixture durability and its resistance to loading. Although asphalt forms only a small part of the asphalt paving mix, it determines the viscoelastic properties of these materials. Quite often, the asphalt binder is modified either chemically or by blending it with various polymeric modifiers. Modified asphalt binders are materials with superior properties. Suitable closeup methodologies shall be used for the analysis of such materials. Empirical methods of designing asphalt mixtures leave much room for improvement to fully utilize the potential of source materials. The methods based on dissipation energy approach are innovative methods that properly address material characteristics. The development in Universal Testing

Machines, sensors and data acquisitions techniques enabled the use of these innovative techniques to analyze material properties in detail so that resulting materials can better serve the needs of transportation.

Basically, one can say that the investigation of the asphalt mixture properties reveals more about the high-temperature and fatigue properties of asphalt mixtures than more common approaches.

Both conventional and innovative techniques were used for the asphalt mixture design in the following works. Articles included in this work address the dissipating energy interpretation methodologies for fatigue resistance of asphalt mixtures. Assessments of pavement design parameters were determined by the dissipating energy method and Uniaxial Shear Test. As a result, the asphalt mixture with superior properties was designed. This asphalt mixture is currently produced at various asphalt plants across the Czech Republic and the trademark of the asphalt mixture is owned by the general contractor.

The following articles are included in this work to report the undertaken research in this field:

Žák, J.; Suda, J.; Ryjáček, P., Polymer Modification Technologies and Asphalt Mixtures Fatigue Resistance in Pavement Structures, In: *Geo-China 2016: Innovative and Sustainable Solutions in Asphalt Pavements*. Reston, VA: American Society of Civil Engineers, 2016. pp. 11-18. GSP. ISSN 0895-0563. ISBN 978-0-7844-8005-2. WoS: 000389419400002, Scopus: 2-s2.0-84983085605

Žák, J.; Suda, J., Laboratory Design and Testing of Asphalt Mixtures Dissipating Energy, In: *Advances and Trends in Engineering Sciences and Technologies III: Proceedings of the 3rd International Conference on Engineering Sciences and Technologies*. Boca Raton: CRC Press, 2019. p. 739-744. ISBN 9780367075095. Scopus: 2-s2.0-85068410215

1.4. Permanent deformation simulation

The impact of traffic loading is a major cause for pavement rutting. Sewer transport, stopping or standing vehicles are the aspects which submit asphalt mixtures to the high loading. It is a difficult task for a civil engineer to design an asphalt pavement that will resist heavy traffic loading.

In some respects, pavements made of asphalt mixtures reach their limits, and other technologies, like concrete pavements, must be selected to withstand heavy traffic loading. The limit is given by asphalt mixtures properties and their resistance to permanent deformation. Thus, it was the intention to increase this limit of asphalt pavements by deep study of asphalt mixture properties and aspects that affect the asphalt mixtures resistance to permanent deformation.

From the mechanical point of view the rutting is an accumulation of permanent deformation. The calculation of permanent deformation is not present in the Czech pavement design methodology. The paper entitled “Incremental rutting prediction with asphalt mixture shear properties” which was selected for this work utilizes the Californian pavement design methodology. The intention of this paper is not to argue about the need to capture this distress in design methodologies but to evaluate the possibility to utilize the data measured in laboratory by Uniaxial Shear Test for pavement rutting predictions. This evaluation is supported as well by comparisons of pavement rutting predictions calculated from the Super Pave Shear test and simulation of various pavement in three climates.

The other paper entitled “Shear accumulated equilibrium compliance as permanent deformation susceptibility parameter” uses the same laboratory data. This work aims to present the procedure that might be used to derive material characteristic, accumulated equilibrium compliance, which describes the asphalt pavement deformation susceptibility. The intention is to propose one parameter that might help the professional community to compare between various scenarios and result in a design of asphalt pavement that will resist higher traffic loadings.

Both published papers use the asphalt mixture shear properties measured in laboratory by the Uniaxial Shear Test.

Following publications were selected in this work to focus on selected topics in the field of asphalt pavement permanent deformation:

Žák, J.; Coleri, E.; Harvey, J., Incremental rutting prediction with asphalt mixture shear properties, In: Solving Pavement and Construction Materials Problems with Innovative and Cutting-edge Technologies. Basel: Springer, 2018. p. 13-24. ISSN 2366-3405. ISBN 978-3-319-95791-3.

Žák, J., Shear accumulated equilibrium compliance as permanent deformation susceptibility parameter, In: Construction and Building Materials, ISSN: 0950-0618, 2020, In Press <https://doi.org/10.1016/j.conbuildmat.2020.121510>

1.5. Pavement roughness

Roughness is the surface manifest of permanent deformation. The only technique which is used to evaluate the pavement permanent deformation during its lifetime in situ is basically the roughness measurement. Unfortunately, pavement engineers do not focus on the permanent deformation of asphalt mixtures itself, but on its presence in the form of roughness that is a combination of other conditions as well. Not only the traffic loading, and asphalt mixtures permanent deformation as discussed in previous

paragraphs causes the roughness of pavement structures. Weather conditions, freeze and thaw cycles, subgrade characteristics are the aspects which result in pavement deteriorations which are present on the surface.

In practice, it is the role of engineers to tackle this multi aspectual process and select the appropriate pavement maintenance strategies. Due to roughness not only ride quality is affected but also vehicle tire contact with asphalt pavement is reduced. Surface water run-off is limited and especially where pavement ruts form a depression which accumulates water. This water presence on the pavement may lead to vehicle aquaplaning. Pavement roughness decreases traffic safety.

The roughness can be assessed visually, by survey techniques, measured by road and level and several profilographs and Response Type Road Roughness Meters were developed to evaluate the pavement surface geometry. Several characteristics to evaluate the pavement surface conditions were developed as well from these measurements: International Roughness Index, Quarter-car Index, Profilograph Index, Present Serviceability Rating, Profilographs, road and level surface smoothness (table reports), and many other characteristics are used for quality control and road maintenance purposes.

Automation in the civil construction and design is of crucial importance. Regular roughness measurements across the highway network are of key importance for the selection of proper maintenance methods. The use of laser scanning methods is spreading as well across civil engineering. The following paper entitled "On Laser Scanning, Pavement Surface Roughness and International Roughness Index in Highway Construction" was selected to expand the topic of roughness by this effective method for large data acquisitions. This method is suitable for the pavement roughness measurement as a quality control criteria and as well as regular surface checks that shall be performed by administrating agencies. The paper discusses the utilization of methodology that proposes the in-situ laser scanning, point cloud data filtering, longitudinal profile extraction and derivation of International Roughness Index and rod and level roughness by utilization of algorithms implemented in RIRI programs. This methodology is further compared with common approaches of rod and level measurements and precise leveling.

The paper entitled "Precise International Roughness Index Calculation" further evolves the work presented in the previously listed article. Commonly used principles for International Roughness Index calculation are based on uniform samples evenly distributed on the pavement surface. The laser scan captures the pavement surface geometry by non-uniform sampling. To overcome this obstacle the RIRI program filters the non-uniform samples by moving average which provides certain inaccuracy in the results. The proposed algorithm in the second paper can calculate the International Roughness Index

from any non-uniform samples. To check the correctness of the proposed algorithm the original methods were compared with newly proposed on selected data measured in situ.

These articles were included in the habilitations thesis:

Žák, J., On Laser Scanning, Pavement Surface Roughness and International Roughness Index in Highway Construction.” In Euroasphalt & Eurobitume Congress 2016. Prague Czech Republic, 2016.

Šroubek, F., Šorel, M., Žák, J., Obr, V.; 2020; Precise International Roughness Index Calculation, Submitted to Journal of Computing in Civil Engineering, ISSN: 0887-3801, 2020.

1.6. Summary

The scientific research, its importance, topicality, and findings are described in the selected articles. It is not an intention to rephrase or generalize the conclusions in listed papers in this paragraph.

These scientific works have resulted as well in industrial applications. Therefore, in this paragraph the industrial applications of these research works are reported.

1.6.1. Uniaxial Shear Tester

The Uniaxial Shear test is a device which has been patented in 2016 first in the Czech Republic. The owner of the patent is the Czech Technical University of Prague (CTU in Prague) and Regents of the University of California (Regents of Uof), USA.

The test device can be used as an accessory of the Universal Testing Machine or in some countries the so-called Nottingham asphalt tester. The aim is to use this device as widely as possible so that it can be used for accurate asphalt mixtures designs.

Since the first patent was filed, the Uniaxial Shear tests have been sold by CTU in Prague and Regents of UofC to:

- University of Waterloo & Golden Associates Ltd., Canada
- The Council for Scientific and Industrial Research (CSIR), South Africa
- TipTop China Limited, China

The licenses to distribute this test device have been signed with:

- TipTop China Limited, China, 2020
- Unico.ai s.r.o., 2020

The first Uniaxial Shear tester prototype, which was used mainly for research purposes, is shown in Figure 1. This prototype is currently present at the Pavement Research Center at the University of California, Berkeley and Department of Road Structures, Czech Technical University in Prague.

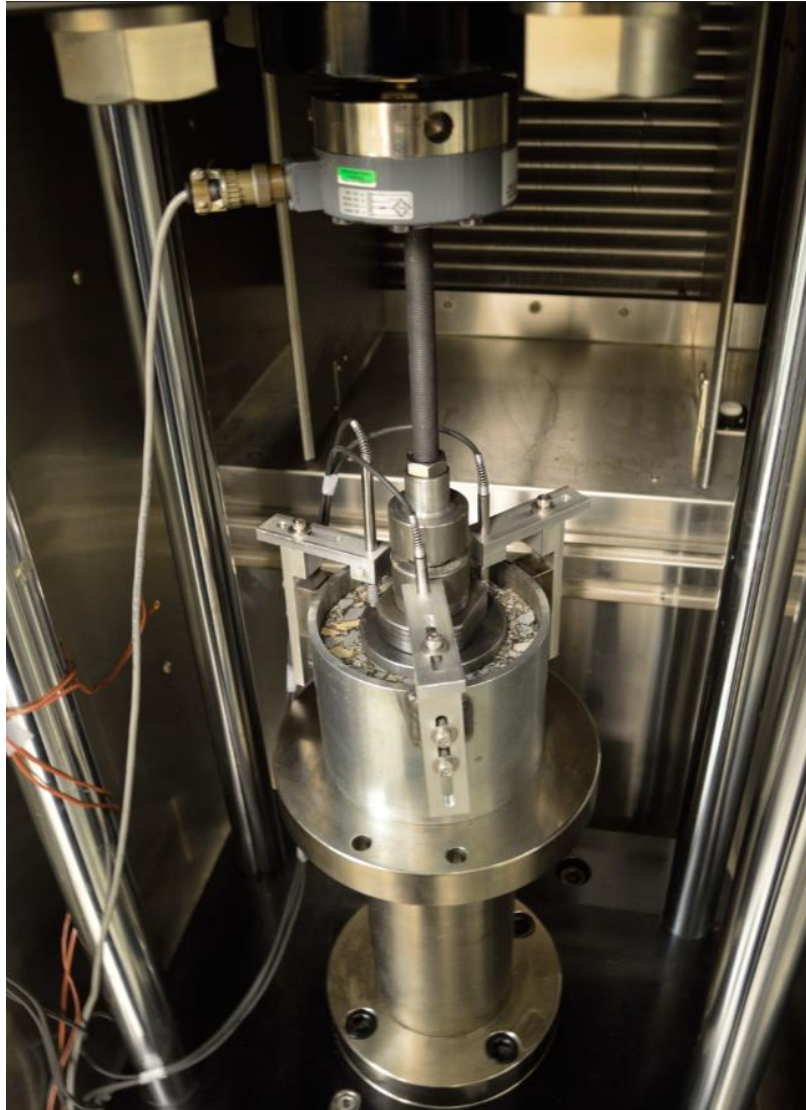


Figure 1. The Uniaxial Shear Tester (1st prototype) in temperature chamber at the University of California, Berkeley, 2016

The testing temperature is usually either 50°C or 60°C. The sample is heated inside the Universal Testing Machine temperature chamber. Consequently, the operation of tested specimen removal and placement of new ones must be performed quickly by a laboratory technician. The second prototype is the result of cooperation with industrial designer Jakub Stedina. The aim was to change the Uniaxial Shear Tester design so that laboratory technicians can easily insert and extrude specimens, the whole test device will be lighter, and LVDT transducers will be easily placed at its position. The second prototype is shown in

Figure 2 and 3. The bottom part remained the same and is made of stainless steel, the upper part is manufactured in a 3D printer and equipped with a “fast clip” which allows to remove and place back the whole assembly.



Figure 2. The Uniaxial Shear Tester (2nd prototype) visualization, 2019



Figure 3. The Uniaxial Shear Tester (2nd prototype) placed in the temperature chamber at Department of Road Structures, Czech Technical University in Prague, 2020

Until today the Uniaxial Shear Test has been granted the following patents:

1. patent no. CZ306155 (B6), titled Device for measuring shear properties of asphalt mixtures, based on an application filed with the Industrial Property Office in the Czech Republic on 09 July 2015, published on 24 August 2016 and granted on 13 July 2016.
2. patent no. US10386280 (B2), titled Device for measuring shear properties of asphalt mixtures, filed on 21 June 2016 with the United States Patent and Trademark Office in the United States of America published on 19 July 2018 and granted on 20 August 2019;
3. patent no. AU2016289265 (B2), titled Device for measuring shear properties of asphalt mixtures, filed on 21 June 2016 with the IP Australia, published on 21 December 2017 and granted on 22 October 2020;

and has been the subject of the following pending patent registration applications:

1. patent registration application no. CA2989673 (A1), titled Device for measuring shear properties of asphalt mixtures, filed on 21 June 2016 with the Canadian Intellectual Property Office and published on 12 January 2017, as of the date of this Agreement the Canadian Intellectual Property Office has not decided on granting the patent;
2. patent registration application no. CN107850517 (A1), titled Device for measuring shear properties of asphalt mixtures, filed on 21 June 2016 with the China National Intellectual Property Administration and published on 27 March 2018, as of the date of this Agreement the China National Intellectual Property Administration has not decided on granting the patent;
3. patent registration application no. SA518390714 (A), titled Device for measuring shear properties of asphalt mixtures, filed on 9 January 2018 with the Saudi Patent Office, as of the date of this Agreement the Saudi Patent Office has not decided on granting the patent;
4. patent registration application no. EP3329245 (A1), titled Device for measuring shear properties of asphalt mixtures, filed on 21 June 2016 with the European Patent Office and published on 6 June 2018, as of the date of this Agreement the European Patent Office has not decided on granting the patent; and
5. patent registration application no. WO2017005229 (A1), titled Device for measuring shear properties of asphalt mixtures, filed on 21 June 2016 with the World Intellectual Property Organization and published on 12 January 2017, as of the date of this Agreement the World Intellectual Property Organization has not decided on granting the patent.

1.6.2. ResiSkán

The aim to design an asphalt mixture that will have a high resistance to permanent deformation resulted in cooperation between Czech Technical University in Prague, Brno University of Technology and Skanska a.s. The developed asphalt mixture was named ResiSkán. The trademark ResiSkán is owned by Skanska a.s. The production of ResiSkán is secured at several asphalt plants across the Czech Republic, see Figure 1.

For the design of ResiSkán, the Uniaxial Shear Test was used as well as dissipating energy principles described in paragraph 1.3 and published in selected papers.

Developed asphalt mixtures that dissipate energy are manufactured in several asphalt plants.

For the development of this asphalt mixture the first Uniaxial Shear Tester shown in Figure 1 was utilized.

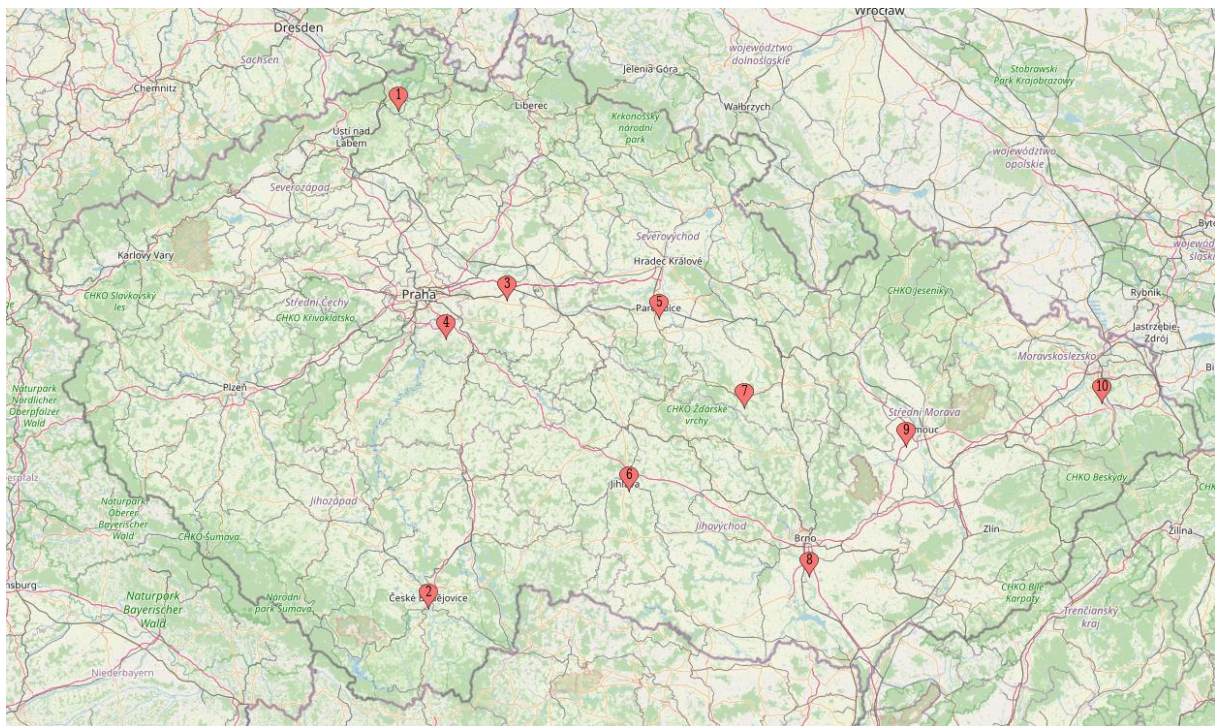


Figure 4. Locations of asphalt plants where the ResiSkán production is secured, (Map data ©OpenStreetMap)

The developed asphalt mixture was used on several construction sites. The following photographs are examples of projects that the author is aware of. With regard to the production of the mixture in several places, the author is no longer aware of all the locations where the asphalt mixture was laid.

The asphalt mixture was developed in 2019, at this time the Skanska a.s. company issued two utility models. The first utility model describes an asphalt mixture for wearing course. The second utility model

describes a combination of the wearing course and base layer. These utility models are co-owned by Skanska a.s., the Czech Technical University in Prague and the Brno University of Technology.

The first project that used the newly developed asphalt mixture was a road reconstruction in Polička, on Zákrejsova street. See figure 5. This road is loaded by heavy transportation from closed pits and mechanization repair shops. The aim of this test section was to assess the conditions of asphalt pavement during the paving. This test section was paved without any special difficulties. The pavement was regularly checked during its first year in service. As the test section does not exhibit any deterioration after its first year in service it was decided that the ResiSkan is going to be utilized for other projects. Poděbradská street, in Prague, Figure 6, is street located in Prague which exhibits permanent deformation even after several reconstructions. The ResiSkan was laid down on this project in autumn 2020, Brandova street, Figure 7, is the road with sewer traffic loading caused by trolley buses and the Rajhrad rest station at D52 Motorway, Figure 8, is loaded especially by stopping trucks. The performance of ResiSkan is going to be observed regularly at these projects. Hopefully, the high resistance to permanent deformation is going to be proved during the life-time.



Figure 5. First highway paved with ResiSkan in Polička in 2019.



Figure 6. Highway paved with ResiSkan, Poděbradská street, Prague 2020.



Figure 7. Paving the Brandova street in Brno with ResiSkan in 2020.



Figure 8. Paving the rest station Rajhrad at D52 motorway with ResiSkan in 2020.

1.6.3. Software for pavements reconstructions

Automation in civil construction and design is of crucial importance. The industrial applications from scientific work reported in selected papers are in the form of two softwares. The first software was entitled “RIRI” which is an abbreviation of Roughness and International Roughness Index. The graphical user interface is shown in Figure 9. The software was used to calculate roughness and International roughness index for pavement reconstructions in the Czech Republic. Examples are Patočkova street, Českobrodská street and Papírenská street in Prague and a highway in Česka Rybná.

Based on the response to the articles, I have recorded requests for software from the Department of Civil and Environmental Engineering, University of Nebraska–Lincoln, USA; IMIE in Nantes, France; Stahl Sheaffer Engineering, LLC, USA; IIT Kanpur, India; Softwareontwikkelaar, Advin BV, Netherlands; NCC Industry, Sweden until 2018 and several others later on. Request for the software download after 2018 were fulfilled without the user registration.

The new algorithm for International Roughness Calculation was used for pavement reconstruction design of few small highways in the Czech Republic. Kunratická spojka street can be listed from larger projects and especially the Highway 17 Sudbury project. Highway 17 Sudbury was 12km of 4-6 lane highway in Canada. The innovative pavement rehabilitation method was used as published in several professional and local newspapers, see Figure 10.

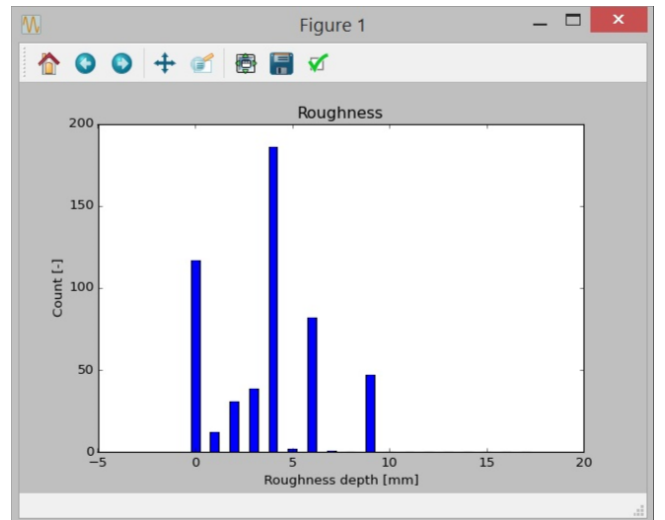
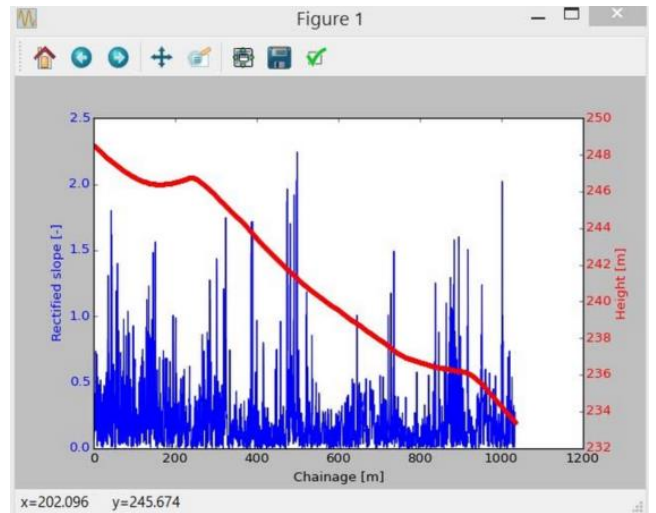
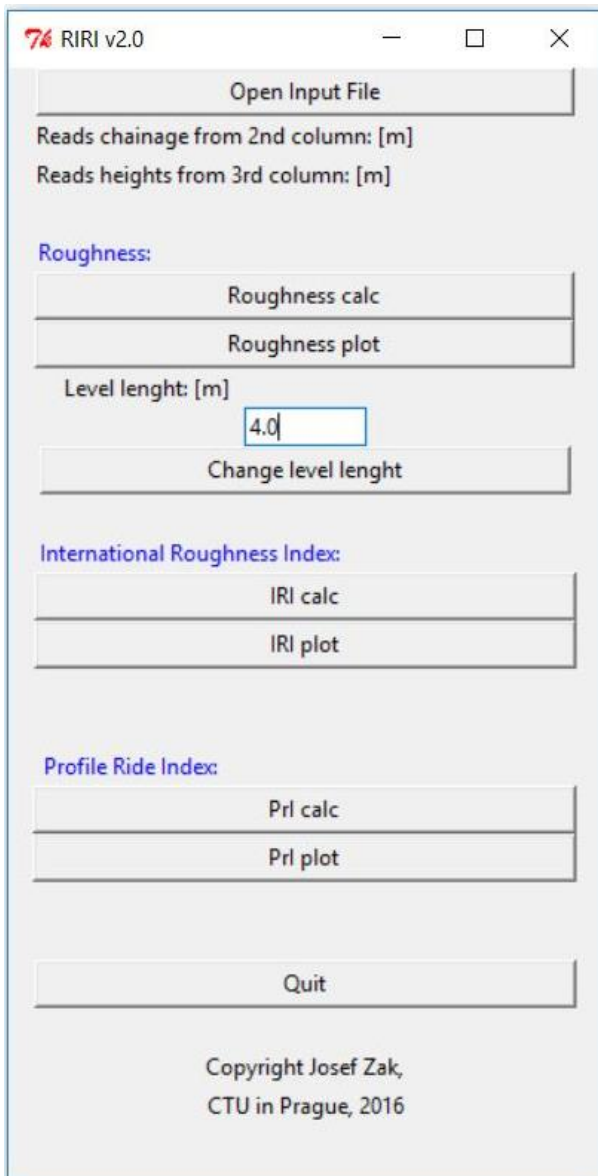


Figure 9. Graphical user interface RIRI program.



Figure 10. ROADBuilder front page. (ROADBuilder, The Ontario Road Builders' Association, Media Edge, Canada, 2020)

2. Scientific works

- 2.1. Žák, J., Monismith, C.L., Coleri, E., Harvey, J. T., Uniaxial Shear Tester – new test method to determine shear properties of asphalt mixtures, 2017.**

Authors' contribution percentage:

70% Žák, J.,

10% Monismith, C.L.,

10% Coleri, E.,

10% Harvey, J. T.

Uniaxial Shear Tester – New Test Method to Determine Shear Properties of Asphalt Mixtures

Josef Zak^a, Carl L. Monismith^b, Erdem Coleri^c, John T. Harvey^d

^a CTU in Prague, Faculty of Civil Engineering, Department of Road Structures, Thakurova 7, Prague, Czech Republic.

^b University of California, Berkeley, Faculty of Civil and Environmental Engineering, Institute of Transportation Studies, 1353 S 46th St, Bldg. 480, Richmond, CA, USA.

^c Oregon State University, School of Civil and Construction Engineering, 101 Kearney Hall, Corvallis, OR, 97331, USA

^d University of California Pavement Research Center, Department of Civil and Environmental Engineering, University of California, Davis, Davis, CA, 95616, USA.

The main focus of the paper is to present the concept of a newly developed Uniaxial Shear Tester (UST) and to investigate the correlation between results from the UST and the Superpave Shear Tester (SST), a tool broadly recognized for asphalt mix design and rutting susceptibility evaluation. In this study, the UST testing principles, finite element analysis of stresses, and comparison of measured data are presented. The correlation was assessed on the basis of two tests, the repeated shear test and the small amplitude oscillation test also referred as the shear frequency sweep test. It was shown that the material characteristics determined from UST and SST are highly correlated. The dependencies are discussed in the sense of linear correlation and correlation coefficients. Test variability is discussed in the paper.

Keywords: Asphalt mixture shear properties, Superpave Shear Tester, Uniaxial Shear Tester, repeated shear test, shear frequency sweep test

1. Introduction

One of criteria for flexible pavement design is permanent deformation. Its occurrence has a significant effect on surface water runoff and ride quality, and, most importantly, traffic safety.

Permanent flexible pavement deformations, in the form of rutting, are the combination of the irreversible deformation occurring in the subgrade, and the granular unbound material and asphalt mixture layers.

The setting of pavement design criteria for characterizing asphalt mixture premature failure in regard of resistance to permanent deformation has been studied by researchers for decades. The Marshall Stability and the Hveem Stabilometer (Monismith, 2012) were among the forerunners of current test methodologies designed to determine specifically the asphalt mixture susceptibility to permanent deformation. These

have been replaced in many countries by newer broadly recognized test methods such as the Superpave Shear Tester, the Hamburg Wheel Tracking Test, and the Repeated Load Triaxial Test.

The Hamburg-Wheel Tracking Device (HWTB) is a test method used in both the US and Europe to assess the susceptibility of asphalt mixtures to permanent deformation. The standardized test methodology is utilized under different conditions, specimens submerged in water or cooled by air are tested at 50 or 60°C in the CEN countries (European Committee for Standardization) and similar types of conditions are used in many US states. The Wheel Tracking Slope or Proportional Rut Depths values are further limited for various asphalt mixtures in national material specifications, although the determination of performance related rheological parameters from the HWTB is troublesome (Zak et al., 2013). For those HWTB experiments that are conducted with specimens submerged in water, it is hard to separate the effects of moisture damage and rutting resistance on total surface deformation.

McLean suggested in his work (McLean, 1974) that the permanent deformation of asphalt concrete (AC) layers is caused by the densification (change in the volume) and shear deformation (shape distortion) of AC under repeated traffic loads. In the case of well compacted asphalt mixtures, the densification has a comparatively small influence on the rutting. Further available information suggests that the shear deformation is the predominant rutting mechanism (Monismith, Deacon, & Harvey, 2000). X-ray CT images of asphalt samples before and after heavy vehicle testing (HVS), (Coleri et al., 2012) have also showed that shear related deformation is controlling the long term rutting performance of the test sections while densification was a contributor at the very earlier stages of trafficking.

The permanent deformation response of asphalt mixtures was broadly studied as part of SHRP and reported in (Monismith et al., 1994). One of the research outcomes was the development of the Superpave Shear Tester (SST). The test device is capable of testing both laboratory prepared specimens and cores taken from the pavement, typically with a diameter of 150 to 200 mm and height of 50 to 75 mm, with the possibility of testing prismatic specimens as well (Coleri et al., 2012). Through the application of different loading schemes, tests like the Repeated Shear Test at Constant Height, Shear Frequency Sweep at Constant Height, and Simple Shear Test at Constant Height can be performed. All tests are conducted at a constant temperature.

The validity of measured shear properties was further assessed in situ during the WesTrack project (Monismith et al., 2000) where mechanistic-empirical models were developed to represent the behavior of the pavement test sections in the accelerated pavement testing experiment using full-scale trucks. Such models are further utilized as a performance models that relates the laboratory measured shear properties of asphalt mixtures with the in-situ asphalt mixture performance (Deacon et al., 2002).

The utilization of the asphalt mixture shear properties as mix design parameters was reported in (J. T. Harvey et al., 2014) and utilized in many projects since the SST device development including the reconstruction of I-710 in Long Beach (Monismith et al. 2009) and subsequent high value reconstruction projects in California. Rut depth prediction models were studied in the NCHRP 719 report (Von Quintus et al., 2012). In this comprehensive report, four transfer functions / performance models are assessed and differences between the Repeated Load Triaxial and Simple Shear Testing are summarized. The Repeated Shear Test at Constant Height was proved as a suitable test to predict the rutting performance of asphalt mixtures run in accordance with (AASHTO T 320-07, 2011). The rut depth transfer functions, utilizing the Repeated Shear at Constant Height Test, are implemented in CalME and MEPDG pavement design programs (Ullidtz et al., 2010; Von Quintus et al., 2012).

Another test device to measure the shear properties of asphalt mixtures was developed by the GEMH-GCD Laboratory at Limoges University and France's Eurovia Research Center. (Diakhaté et al., 2011). The so called Double Shear Tester (DST) is able to perform shear tests on asphalt mixture slabs with dimensions of 50x70x125mm into which four 10-mm high notches are cut near the loaded central part (60mm in width) in order to generate and localize the shear band (Petit, Millien, Canestrari, Pannunzio, & Virgili, 2012). The aim of developing the DST device was to measure the tack coat properties of asphalt mixture layers and bound in-between AC layers. The loading conditions of the DST enable the application of both monotonic and cyclic conditions (Diakhaté et al., 2011). However the DST has limitations to be used for HMA shear properties determination.

The Leutner Shear Test was also developed to determine the shear properties of asphalt mixtures. This was one of the earliest works reporting the measurement of shear properties of asphalt mixtures, (Molenaar, Heerkeng, & Verhoven, 1986). The idea of applying the shear load by two loading platens into one plane was further extended by the modification of the Leutner Shear Test resulting in the development of the Layer-Parallel Direct Shear Test (Raab & Partl, 2004), the Simple Shear Test Device (Sholar, Gale, Musselman, Upshaw, & Moseley, 2002) and the Shear Box (Canestrari, Ferrotti, Partl, & Santagata, 2005). The localization of the shear plane is given by the position of loading platens perpendicular to the core axis of symmetry. The practicability of such devices is limited and is suitable for the measurement of shear properties between two layers.

2. Uniaxial shear tester

The lack of equipment allowing the measurement of asphalt mixture shear properties in Europe and the desire to simplify the equipment compared with the SST were the motives behind this research project. Common laboratories are equipped with Universal Testing Machines (UTM) also known as Nottingham Asphalt Testers in Europe. The Uniaxial Shear Tester (UST, see Figure 1) is an assembly that is inserted into the UTM chamber. Either a servo-hydraulic or a pneumatic press may be used to apply the shear load. The load cell measures the force values and the attached LVDT's measure the steel insert deflection.

The UST is less expensive due to the UTM's simpler construction and more applicable for many other required laboratory tests than is the single purpose SST. The SST device keeps the sample height constant with a second hydraulic piston while applying the shear load, which creates a difficult control problem.

For the UST, a hollow cylindrical specimen, as shown in Figure 2, is placed inside a steel cylinder and the load is applied through the knee joint on a steel insert placed in the center of the hollow cylindrical specimen. The dimensions of the specimen are 150mm diameter and typically height of 50mm. The steel insert is pushed down through the specimen and excites the shear load in the tested asphalt mixture. The steel cylinder restricts the asphalt mixture horizontal strain at the lateral area. Thus, the horizontal (confining) pressure, given by the material deformation characteristics itself, occurs on the lateral sides of the specimen due to the prevented horizontal lateral deformations. The UST test assembly is axisymmetric along the vertical axis. To determine the material properties, the vertical deflection of the steel insert is measured by three LVDTs located along 120° on the steel insert. The derivation of the equation used to calculate the mechanical properties from the measured applied force and deflection can be found in (Zak, 2014). The axisymmetric shear stress in the left half of the specimen is presented in figure 1. The Von Mises stress criterion was selected to present the effect of lateral (confining) pressure. Both figures were prepared by performing linear elastic finite element (FE) analysis in the ABAQUS software. The FE modeling input parameters were following: Asphalt mixture ($E=308\text{MPa}$ (corresponding approximate temperature 50°C), $\nu=0.4$), Steel ($E=210\text{GPa}$, $\nu=0.3$). Contact properties between asphalt mixtures and steel were set as hard normal behavior with the tangential friction coefficient equal to 0.09 (Zak & Valentin, 2013). The steel insert was loaded by 1850N.

The final shape and size of the individual elements of the UST assembly are the result of the assessment of the base three variants (a) without the hole in the specimen, b) with the hole in the center of the specimen and gluing of the insert, c) with the center hole and insert with load-spreading washer - final

variant). The size of individual elements have been optimized using digital prototyping methods and analyzes of the resulting stresses and strains using FEM.

It should be noted that during specimen mounting in the UST device gluing is not needed, unlike the SST. The UST sample mounting is therefore quicker and less costly. By omitting the specimens gluing process the measured properties variance is not affected by the variation of glue type or operator experience. The center hole is cored using standard laboratory coring equipment with diamond core bit with the 50mm external diameter. The core bit is centered using a thick steel plate placed on top of the specimen with the 51mm hole during coring.

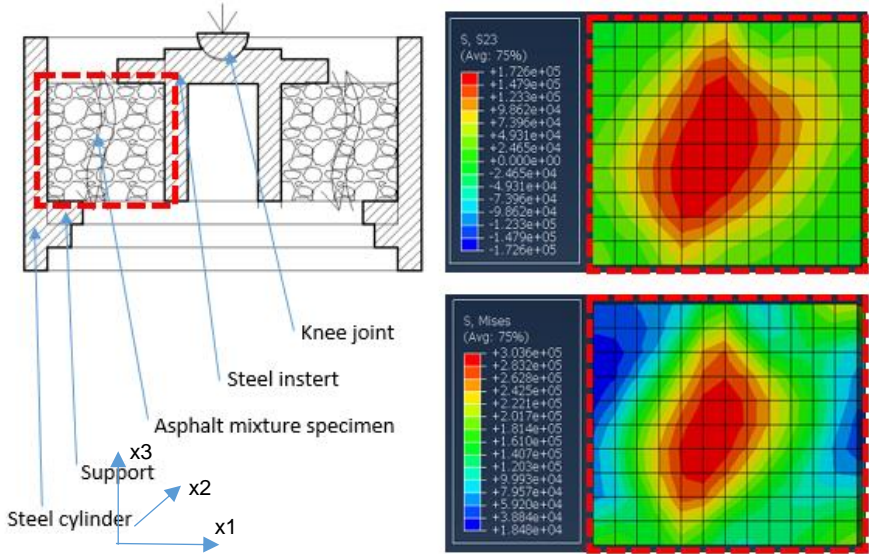


Figure 1. Uniaxial Shear Tester (cross section, shear stress [Pa], Von Mises stress [Pa])



Figure 2. Uniaxial Shear Tester (top view, hollow cylindrical specimen, UST placed in UTM chamber)

2.1. Specimen preparation and material specification

SST and UST specimens taken from the pavement and specimens prepared in the laboratory were tested in this research project. Blocks were sawn from a pavement test section at UCPRC, Davis. Cylinders were cored from the blocks and the final specimens were cut from a specific asphalt mixture layer using a double bladed saw, which ensured parallel specimen faces. For SST, the cut specimens were glued to steel platens and tested in accordance with (AASHTO T 320-07, 2011). For UST, a hole 50mm in diameter was cored in the center of the cylinders using a standard core bit in the laboratory. The core bit was centered on the specimen with the use of a thick steel plate with 51mm center hole placed on top of the sample during coring.

Laboratory specimens were prepared with the Superpave Gyrotory Compactor. A cylinder 135mm high and 150mm in diameter was produced, which would yield two test specimens. Such an “ingot” was sliced with the water cooled table saw mounted with standard diamond blade. Preparation of the specimens for testing was the same as for the specimens taken from the pavement. The final hollow cylinder is 150mm in external diameter, 50mm thick with the cored 50mm hole in the center.

Five asphalt mixtures were used during the research project. Mix #1 was 19 mm hot mix asphalt (HMA) containing 4.8% of the PG 64-10 neat asphalt binder, 25% of reclaimed asphalt and 0.9% of hydrated lime as an anti-strip additive. The material was prepared in the asphalt plant and batches of the material were taken from the construction site. Mix #2 was 19 mm HMA containing 5% of the PG 64-28PM polymer modified asphalt binder and 15% of reclaimed asphalt and 0.9% of hydrated lime. Mix #2 was also prepared in the asphalt plant and taken from the construction site. Mix #3 was 12.5 mm gap-graded rubberized hot-mix asphalt, RHMA-G, with 7% of the PG 64-10 asphalt binder and a 4% air void content. Mix# 3 was also prepared in the asphalt plant. Blocks of Mix #3 were taken from the UCPRC test section and the specimens were prepared using the above described procedure. Mix #4 was ACO 11+ 50/70 (designated in accordance with (ČSN EN 13108-1, 2008)), the asphalt concrete mixture used for wearing courses with 5.6% of an asphalt binder of the 50/70 penetration grade. The air void content was 3.5% and the mix design was done in accordance with (ČSN EN 13108-1, 2008). Mix #5 was prepared from the same material as Mix #2 but with the targeted 96% degree of compaction relative to briquette bulk specific gravity (California Test 308, 2000). The average specimen’s air void content was 7.6%.

The testing matrix was designed so that the validation of the measured asphalt mixture properties was done over a broad range of mixture properties. Thus, it covers:

- samples taken from the pavement and samples prepared in the laboratory,
- polymer modified, rubberized and conventional binders,

- the mix design according to Czech amend to European specification and Caltrans material specifications,
- well compacted and poor compacted mixtures,
- variety of aggregate sources.

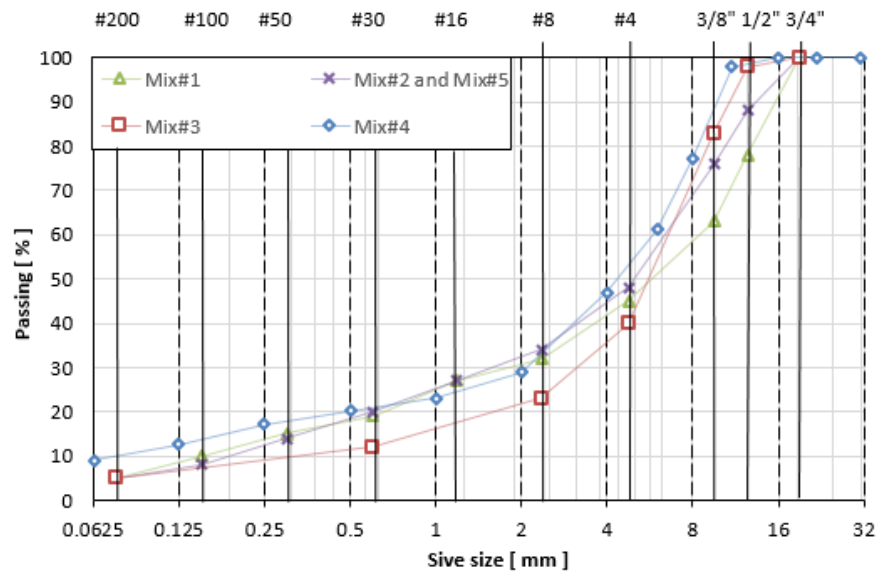


Figure 3. Asphalt mixture grading curve

3. Experiments

The main purpose of the laboratory testing was to first obtain data from the newly developed UST device and, second to statistically evaluate the similarities between the UST device and the currently used SST. Five replicates were tested for each asphalt mixture and in case of repeated shear tests and three in case small amplitude oscillation tests.

3.1. Repeated shear tests

Repeated loading seems to be the most suitable material testing approach to determine the asphalt mixture resistance to permanent deformation. The suitability of the analysis determining the portions of recoverable and non-recoverable strains changing over time with the application of repeated loading and unloading has been demonstrated by many researchers (Bahia et al., 2001; D'Angelo et al., 2007; Harvey et al., 2001; Monismith et al., 1994). The Repeated Simple Shear Test at Constant Height (RSST-CH) was performed in accordance with (AASHTO T 320-07, 2011). The equivalent test procedure, Uniaxial Repeated Shear Test (URST), compound from 30,000 cycles containing haversine shear pulses 69kPa

for 0.1s followed by 0.6s of rest periods, was developed and performed for the same number of samples using UST. The test temperature was maintained at 50°C.

An example of mined test data from URST is presented in following figures. Figure 4 shows determined characteristic denotations. As can be seen from the presented figures (5-9), all measured characteristics have a very low scatter. The resilient moduli, relative peak strain and permanent strain increments reach their steady state values for most of the cases after 100 to 300 loading cycles. Also, the absolute peak strain and accumulated permanent strain reach their steady state increments after the first 100 to 300 loadings. The typical trend of shear strain of five replicates is presented in figure 10.

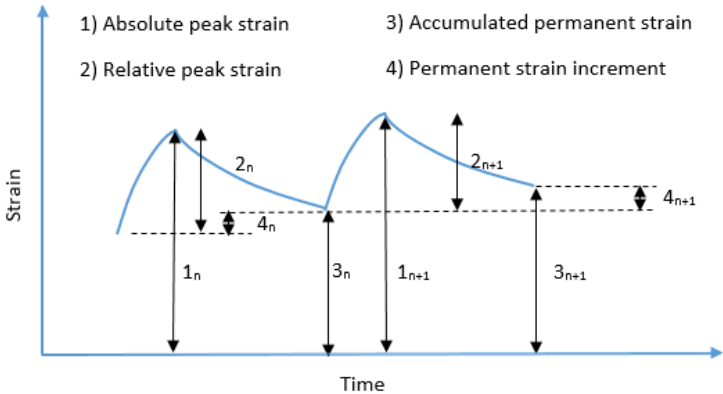


Figure 4. The key to material properties derivation

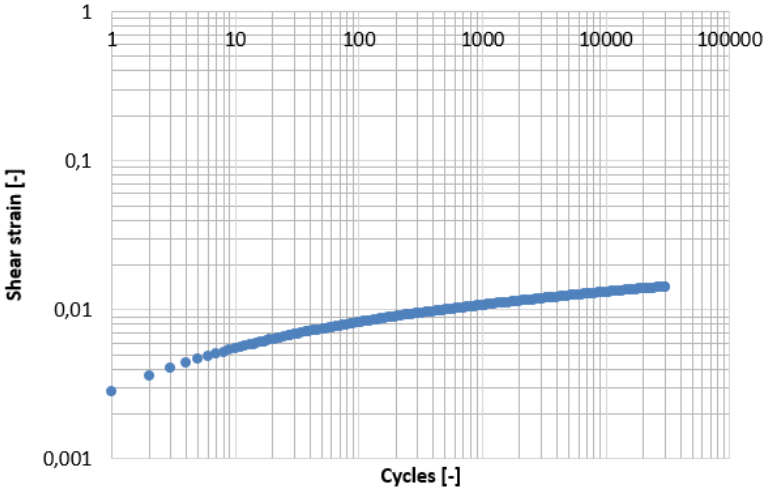


Figure 5. Absolute resilient peak strain

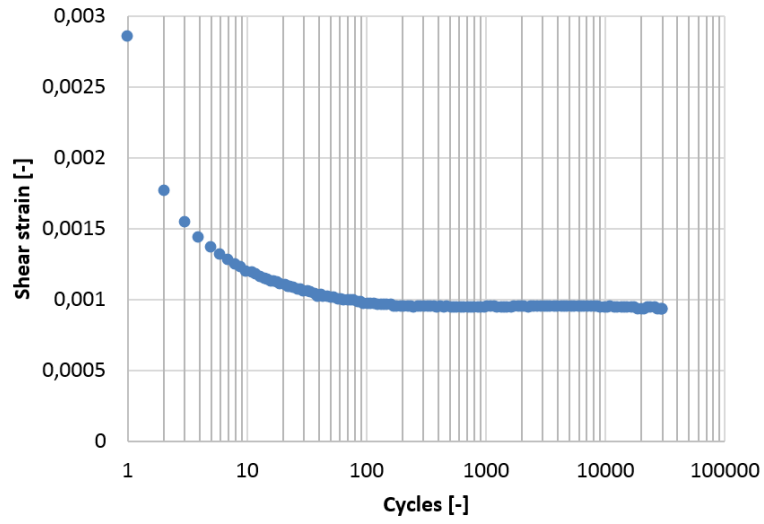


Figure 6. Relative peak resilient strain

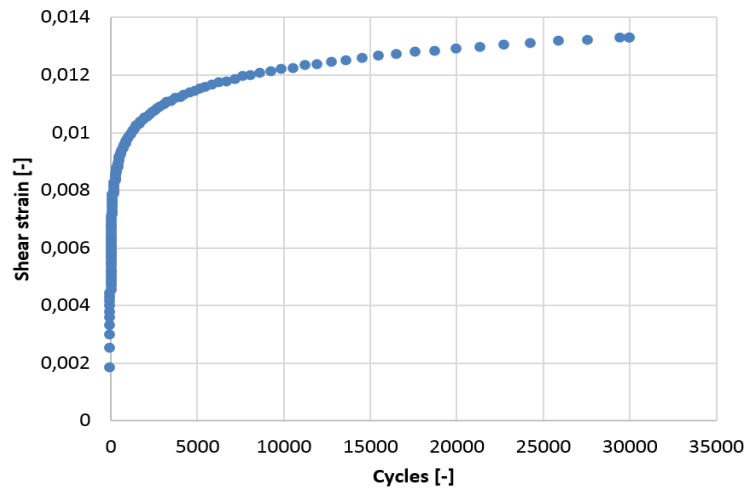


Figure 7. Accumulated permanent strain

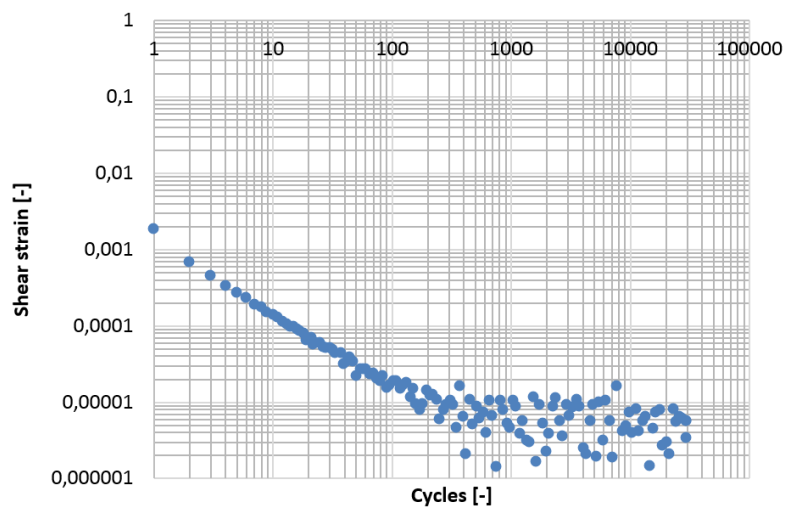


Figure 8. Permanent strain increment

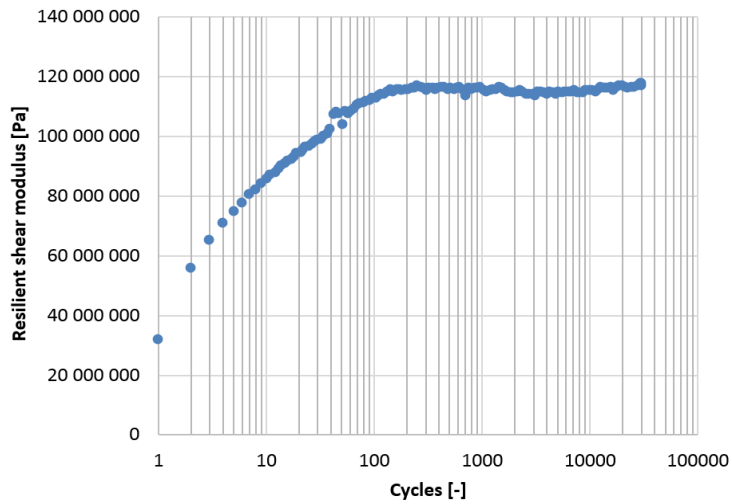


Figure 9. Resilient modulus

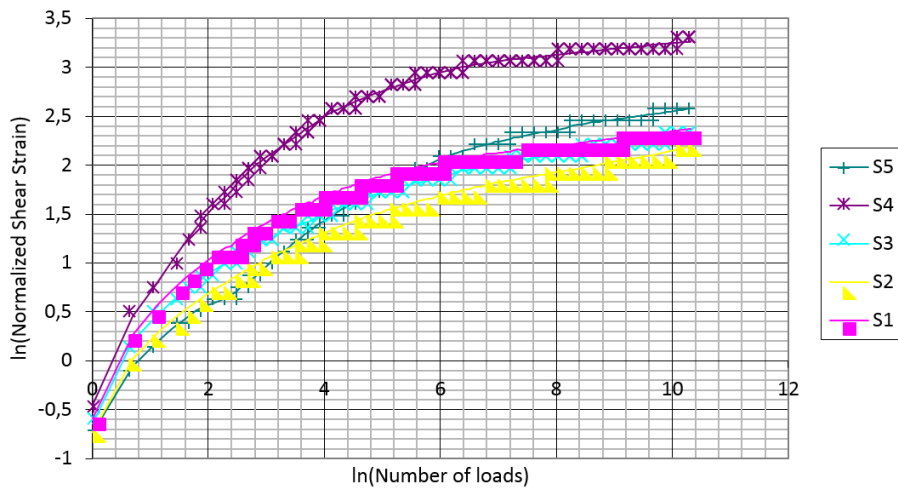


Figure 10. Shear strain for five replicate tests (Mix #2 3/4" HMA PG 64-28PM)

The correlation between the parameters developed from RSST-CH (SST) and URST (UST) test results are presented in Figure 11. The resilient modulus was determined as a portion of shear stress and relative peak strain at 100th cycle. Even if the shear resilient modulus may not be a good rutting performance indicator (J. Harvey et al., 2002), the shear resilient moduli of the asphalt mixtures reached their steady state after 100 cycles thus such a value can be considered as a representative elastic characteristic for the pavement strain calculation. The correlation coefficient of linear regression between the resilient moduli values measured by RSST-CH and URST was equal to 0.71.

The accumulated shear strain has been fitted with a second order polynomial function. The same parameters of the polynomial function can be obtained from the linear fitting in the log-log scale. The slope

of such a fitted curve, in the secondary phase, is called the m-value and has been found to correlate well with the field rutting performance parameters (Witczak et al., 2002). The correlation between UST and SST m-values is presented in figure 4 and the correlation coefficient is 0.82.

One of the quality measures relating the pavement rutting performance to in laboratory measured characteristics is also the number of cycles to 5% permanent shear strain which SHRP research indicated corresponded to a 12.5 mm rut depth (Monismith et al. 1994). To capture one more point from the accumulated permanent shear strain, the number of loading repetitions to 3% was also studied. The usability of such a parameter for the pavement rutting performance was shown in WesTrack and I-710 projects (Monismith et al., 2000, 2009). The statistical relationship can be expressed with very good correlation coefficients equal to 0.98 and 0.84 respectively.

The Weibull curves can be applied for the regression of accumulated permanent shear strain (Tsai et al., 2005; Tsai et al., 2003). Firstly, the three stage Weibull approach has been utilized for the measured data analysis. The determined accumulated permanent shear strain does not exhibit the tertiary stage rutting either in the case of the RSST-CH or in the case of the URST. Therefore, the two stage Weibull approach has been found to be appropriate for both. The exponent of the Weibull regression second phase was determined for RSST-CH and URST. The measure of linear correlation is a correlation coefficient equal to 0.93.

Looking at the overall material performance, Mix #1 19mm HMA with the PG64-28PM polymer modified asphalt binder has the best material performance in regard of resistance to permanent deformation. The second best quality was obtained by Mix #2 19 mm HMA PG64-10. Even if Mix #5, 3/4" HMA PG64-28PM 96%DC, was compacted only to 96% of bulk specific gravity, it is placed in the imaginary third position among the studied materials' rutting susceptibility. It also shows the high resistance of polymer modified asphalt binders to permanent deformation. Through determined material characteristics close to each other, a stronger rutting potential of mixes #3 and #4, RHMA-G PG64-10 and ACO 11+ 50/70 was identified. The described sequence of material characteristics can be concluded from all the presented charts and studied material characteristics except for resilient moduli. It proves that the resilient modulus may not be a good rutting performance indicator (J. Harvey et al., 2002).

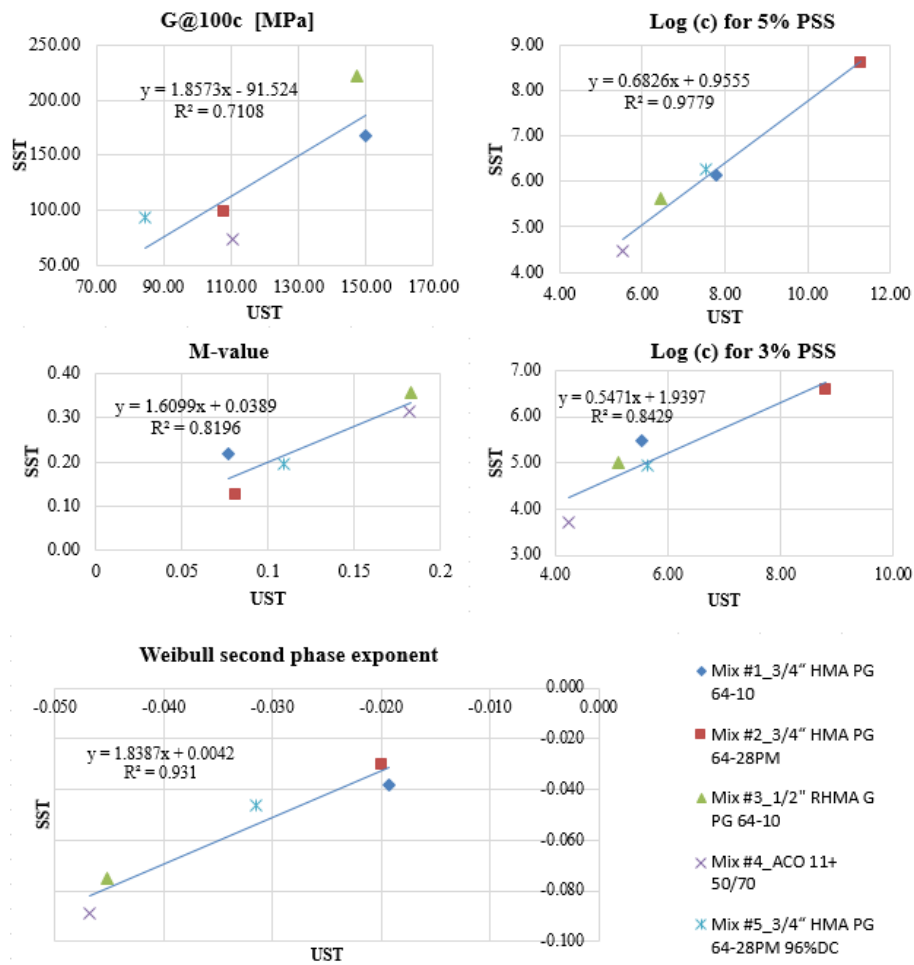


Figure 11. Correlation between SST and UST

3.1.1. Variability

The variability of both the RSST-CH and URST test was studied. The calculated means are presented in Figure 4. To study the dispersion from the mean, the standard deviation was computed. The standard deviation is one of the repeatability measures. The standard deviation was calculated for each asphalt mixture type and the average standard deviation as the in laboratory test repeatability is presented in the last column of table 1. The standard deviations (SD) of the measured resilient modulus and the m-value for the URST test are smaller and higher for cycles to 5% Permanent Shear Strain (PSS), respectively, as can be seen from table 1.

UST		Mix #1	Mix #2	Mix #3	Mix #4	Mix #5	Average
Standard deviation	Resilient modulus	9	19.7	16	8.1	12.1	12.98
	M-value	1.70E-02	2.00E-02	3.10E-02	2.10E-02	2.00E-02	0.02
	5% PSS	1.20E+08	1.20E+11	3.00E+06	2.10E+05	2.90E+10	2.98E+10
Coefficient of variation	Resilient modulus	0.06	0.18	0.11	0.07	0.10	10.4%
	M-value	0.22	0.25	0.17	0.07	0.18	18.0%
	5% PSS	1.91	0.64	1.08	0.60	1.01	104.9%
SST		Mix #1	Mix #2	Mix #3	Mix #4	Mix #5	Average
Standard deviation	Resilient modulus	16.2	11.7	92.6	10.1	28.1	31.74
	M-value	4.60E-02	1.50E-02	4.10E-02	3.20E-02	3.10E-02	0.033
	5% PSS	6.70E+06	2.10E+09	1.50E+05	2.40E+04	4.90E+08	5.19E+08
Coefficient of variation	Resilient modulus	0.10	0.12	0.42	0.14	0.21	19.5%
	M-value	0.21	0.12	0.11	0.10	0.12	13.4%
	5% PSS	1.49	2.15	0.82	0.81	1.29	131.0%

Table 1. Correlation between SST and UST

3.2. Shear Frequency Sweep (Small Amplitude Oscillation)

A sinusoidal load is applied on top of the tested sample in the perpendicular direction to the tested cylindrical sample axis during the Shear Frequency Sweep Test at Constant Height (SFST-CH) in accordance with (AASHTO T 320-07, 2011). The applied loading passes through zero to alternately positive and negative values and the delayed material response is measured.

The Uniaxial Shear Frequency Sweep Test (USFST), run in UST, has a different form in the case of small amplitude oscillation testing than in SFST-CH. The loading is applied on the sample in the direction of the tested hollow cylindrical sample axis, the same direction as that in which the specimen is compacted and loaded by traffic. The load pushes the steel insert through the specimen exciting the shear load in the tested sample. Therefore, the applied loading varies from zero to positive values and the delayed material response is not affected that the machine would pull back the steel insert.

Ideally, Small Amplitude Oscillation Tests were executed in the control strain mode with the strain amplitude set within the linear viscoelastic range. However, the desired sinusoidal shape of the applied stress was poorly attained and the tuning of the Proportional-integral-derivative (PID) controller will have to become a necessity for each individual test. The reason seems to be that the material properties become part of the machine control loop. The displacement response was generated through material properties, consequently the PID values for the machine loop control are dependent on the material properties in the control strain mode.

Thus, the control stress mode has been found as an appropriate solution to overcome the obstacles with the PID value tuning in the control signal loop of the strain mode. The settings of the SFST-CH were established in previous work (Harvey et al., 2000). First, SFST-CH was performed. The same SFST-CH

settings as in (J. Harvey et al., 2000) were used in this article. Further, the data were analyzed and from the tests performed on asphalt mixtures #1, #2 and #3 average stresses with dependence on temperature and frequency were computed. The SFST-CH stresses were afterwards fitted with the s-type function, (Tschoegl, 1989), and the stresses were calculated for the use in USFST performed in UST. More details about stress fitting of small amplitude shear oscillation can be found in (Zak, 2014).

Both asphalt mixture shear frequency sweep tests were done in a broad range of temperatures from -15°C to 75°C and a frequency domain of 0.01÷10Hz in the case of SST and 0.01-40Hz in the case of UST. The Time-Temperature Superposition (TTS) was performed for all the asphalt mixtures at the reference temperature of 15°C. The reduced frequency $\omega' = aT^* \omega$ was described by the Williams-Landel-Ferry relation. No vertical shifting was needed for all the studied TTS mixes. Both the phase angle and the shear moduli were shifted with the same horizontal shift factors.

The typical behavior of the measured asphalt mixture characteristics is shown in figure 12 for Mix #1 (3/4" HMA PG64-28PM) master curve. All the tested mixes displayed a similar behavior, i.e. the complex shear modulus, G^* , starts from its plateau at low frequencies and increases with reduced frequencies. The G^* also reaches its plateau at high frequencies / low temperatures in the case of USFST. The absolute maximum of G^* was not even found at -15°C in the case of SFST-CH. The real part of the shear modulus, G' , and the loss shear modulus, G'' , reaches its absolute maximum in the displayed domain of reduced frequencies in the case of USFST. Similarly, the loss tangents of all the materials reached their absolute maximum well before their moduli did in the case of USFST. The G^* positively correlates between both tests. The variation in the trends of a real part of the shear modulus, G' , and the loss modulus, G'' , is caused by the negative correlation of the phase angle.

It must be emphasized that the different trend of the phase angle was found in previous work (J. Harvey et al., 2000). If the trend of the phase angle, measured by SFST-CH from (J. Harvey et al., 2000) is utilized in this article, the phase angle will be positively correlating with the trend of the phase angle measured by the USFST presented in this article. Such an assumption will resolve the difference in phase angle trend. From the behavior of dynamic material functions, it is clear that all the materials behave as linear viscoelastic solids (in the tested domain). This can be clearly seen in figure 12, where there is no upturn in $\text{tg}(\delta)$ (tangents of phase angle) to the higher values for the behavior of the loss tangent at the lowest reduced frequencies (highest temperature), usually indicating the flow of the material (Zak et al., 2013).

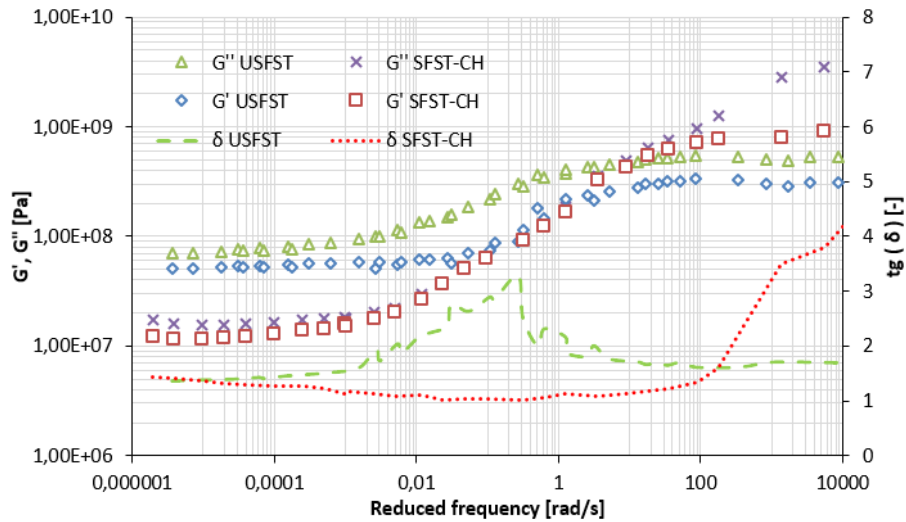


Figure 12. Mix #1 (3/4\"/>

4. Conclusions

The results from two test devices and two test methodologies performed are presented in this article. The main focus of the paper is to present measured data from the newly developed Uniaxial Shear Tester and to assess the correlation with the established Superpave Shear Tester developed in 1990s. The correlation is presented through the linear correlation of determined material properties. It can be concluded that measured material parameters for UST and SST tests are highly correlated. The coefficient of determination values are higher than 0.7, namely the resilient shear modulus -0.71, the logarithm of cycles to 5% permanent shear strain - 0.98, the logarithm of cycles to 3% permanent shear strain - 0.84, the m-value - 0.82 and the Weibull second phase exponent 0.93. The test results' variability may be considered as similar, or slightly lower in the case of UST, for selected material characteristics.

The other test methodology discussed in this paper is the Small Amplitude Oscillation Shear Test, also referred to as the Frequency Sweep Shear Test. It was found that the complex shear moduli measured by UST and SST devices positively correlate over the measured domain. The phase angle does not exhibit the same positive correlation. We assume that the observed differences are caused by the differences in the shearing direction as discussed in the introduction of paragraph 3.1.

The UST provides promising results. Even so, the validation of the new laboratory test method's ability to predict the rutting performance under in situ conditions should be further investigated.

The UST device is a simpler and lower cost alternative to SST device and has promising value to the community because it allows performance testing of as-built pavements for rutting susceptibility and in laboratory asphalt mixture shear properties determination.

Acknowledgements:

This work was supported by Competence Centers program of Technology Agency of the Czech Republic (TA CR), project no. TE01020168 and by both United States and Czech Republic governments through J. William Fulbright Commission.

5. References

- AASHTO T 320-07. (2011). *Standard Method of Test for Determining the Permanent Shear Strain and Stiffness of Asphalt Mixtures Using the Superpave Shear Tester (SST)*. American Association of State Highway and Transportation Officials.
- Bahia, H. U., Hanson, D. I., Zeng, M., Zhai, A., Khatri, M. A., & Anderson, R. M. (2001). *Characterization of Modified Asphalt Binders in Superpave Mix Design*. Transportation Research Board — National Research Council, National Academy Press Washington, D.C.
- California Test 308. (2000). *Method of Test Bulk Specific Gravity and Density of Bituminous Mixtures*. Department of Transportation Engineering Service Center, Transportation Laboratory 5900 Folsom Blvd. Sacramento, California 95819-4612.
- Canestrari, F., Ferrotti, G., Partl, M. N., & Santagata, E. (2005). *Advanced Testing and Characterization of Interlayer Shear Resistance*. Transportation Research Record: Journal of the Transportation Research Board, (1929). doi:10.3141/1929-09
- Coleri, E., Harvey, J. T., Yang, K., & Boone, J. M. (2012). *A Micromechanical Approach to Investigate Asphalt Concrete Rutting Mechanisms*. Construction and Building Materials, 30, 36–49. doi:10.1016/j.conbuildmat.2011.11.041
- ČSN EN 13108-1. (2008). *Bituminous mixtures - Material specification - Part 1: Asphalt Concrete*. Czech Office for Standards, Metrology and Testing.
- D'Angelo, J., Kluttz, R., Dongré, R., Stephens, K., & Zanzotto, L. (2007). *Revision of the Superpave high temperature binder specification: The multiple stress creep recovery test* (Vol. 76, pp. 123–162). Presented at the Asphalt Paving Technology: Association of Asphalt Paving Technologists-Proceedings of the Technical Sessions.
- Deacon, J., Harvey, J., Guada, I., Popescu, L., & Monismith, C. (2002). *Analytically Based Approach to Rutting Prediction*. Transportation Research Record: Journal of the Transportation Research Board, 1806(-1), 9–18. doi:10.3141/1806-02
- Diakhaté, M., Millien, A., Petit, C., Phelipot-Mardelé, A., & Pouteau, B. (2011). *Experimental investigation of tack coat fatigue performance: Towards an Improved Lifetime Assessment of Pavement Structure Interfaces*. Construction and Building Materials, (25). doi:doi:10.1016/j.conbuildmat.2010.06.064
- Harvey, J., Guada, I., & Long, F. (2000). *Effects of Material Properties, Specimen Geometry, and Specimen Preparation Variables on Asphalt Concrete Tests for Rutting* (Vol. 69). Presented at the Association of Asphalt Paving Technologists Technical Sessions, 2000, Reno, Nevada, USA.
- Harvey, J., Guada, I., Monismith, C., Bejarano, M., & Long, F. (2002). *Repeated Simple Shear test for Mix Design: A Summary of Recent Field and Accelerated Pavement Test Experience in California*. Presented at the Ninth International Conference on Asphalt Pavements, Copenhagen, Denmark.
- Harvey, J. T., Signore, J., Wu, R. Z., Basheer, I., Hollikati, S., Vacura, P., & Holland, T. J. (2014). *Integration of Mechanistic-Empirical Design and Performance Based Specifications: California Experience to Date*. In 12th ISAP Conference on Asphalt Pavements. Raleigh, North Carolina.
- Harvey, J., Weissman, S., Long, F., & Monismith, C. (2001). *Tests to evaluate the stiffness and permanent deformation characteristics of asphalt/binder-aggregate mixes, and their use in mix design and analysis* (Vol. 70, pp. 576–604). Presented at the Association of Asphalt Paving Technologists Technical Sessions, 2001, Clearwater Beach, Florida, USA.
- McLean, D. B. (1974). *Permanent deformation characteristics of asphalt concrete*. PhD Thesis, University of California, Berkeley.
- Molenaar, A. A. A., Heerkeng, J. C. P., & Verhoven, J. H. M. (1986). *Effects of Stress Absorbing Membrane Interlayers*. Annual Meeting of Association of Asphalt Paving Technologist.

- Monismith, C., Deacon, J. A., & Harvey, J. (2000). *WesTrack: Performance Models for Permanent Deformation and Fatigue*. Pavement research Center; Institute of Transportation Studies, University of California, Berkeley.
- Monismith, C. ., Harvey, J., Tsai, B. W., Fenella, L., & Signore, J. (2009). *Summary Report: The Phase 1 I-710 Freeway Rehabilitation Project: Initial Design (1999) to Performance after Five Years of Traffic (2009)*. University of California, Davis & Berkeley.
- Monismith, C. L. (2012). *Flexible Pavement Analysis and Design-A Half-Century of Achievement*. In *Geotechnical Engineering State of the Art and Practice* (pp. 187–220). American Society of Civil Engineers.
- Monismith, C. L., Hicks, R. G., Finn, F. N., Sousa, J., Harvey, J., Weissman, S., ... Paulsen, G. (1994). *Permanent Deformation Response of Asphalt Aggregate Mixes*, 1–437.
- Petit, C., Millien, A., Canestrari, F., Pannunzio, V., & Virgili, A. (2012). *Experimental study on shear fatigue behavior and stiffness performance of Warm Mix Asphalt by adding synthetic wax*. *Construction and Building Materials*, 34, 537–544. doi:10.1016/j.conbuildmat.2012.02.010
- Raab, C., & Partl, M. N. (2004). *Interlayer Shear Performance: Experience with Different Pavement Structures*. Presented at the 3rd Eurasphalt & Eurobitume Congress, Vienna: EAPA-European Asphalt Pavement Association.
- Sholar, G. A., Gale, C. P., Musselman, J. A., Upshaw, P. B., & Moseley, H. L. (2002). *Preliminary Investigation of a Test Method to Evaluate Bond Strength of Bituminous Tack Coats*. State of Florida Materials Office.
- Tsai, B. W., Bejarano, M. O., Harvey, J. T., & Monismith, C. L. (2005). *Prediction and Calibration of Pavement Fatigue Performance Using Two-Stage Weibull Approach*. *Journal of the Association of Asphalt Paving Technologists*, (74), 697–732.
- Tsai, B. W., Harvey, J., & Monismith, C. (2003). *Application of Weibull Theory in Prediction of Asphalt Concrete Fatigue Performance*. *Transportation Research Record: Journal of the Transportation Research Board*, 1832(-1), 121–130. doi:10.3141/1832-15
- Tschoegl, N. W. (1989). *The Phenomenological Theory of Linear Viscoelastic Behavior: An Introduction*. Berlin, Germany: Springer-Verlag.
- Ullidtz, P., Harvey, J. T., Basheer, I., Jones, D., Wu, R., Lea, J., & Lu, Q. (2010). *CalME, a Mechanistic-Empirical Program to Analyze and Design Flexible Pavement Rehabilitation*. *Transportation Research Record: Journal of the Transportation Research Board*, 2010(2153), 143–152. doi:10.3141/2153-16
- Von Quintus, H., Mallela, J., Bonaquist, R., Schwartz, C. W., & Carvalho, R. L. (2012). *Calibration of Rutting models for structural and Mix Design*. Washington, D.C.: Transportation Research Board - National Research Council.
- Witczak, M. W., Kaloush, K., Pellinen, T., El-Basyouny, M., & Von Quintus, H. (2002). *Simple Performance Test for Superpave Mix Design* (NCHRP Report 465). Transportation Research Board - National Research Council. Retrieved from http://onlinepubs.trb.org/onlinepubs/nchrp/nchrp_rpt_465.pdf, Accessed July 22, 2014.
- Zak, J. (2014). *Numerical Characterization of Asphalt Mixtures Properties - Dissertation*. CTU in Prague, Faculty of Civil Engineering.
- Zak, J., Stastna, J., Zanzotto, L., & MacLeod, D. (2013). *Laboratory Testing of Paving Mixes – Dynamic Material Functions and Wheel Tracking Tests*. *International Journal of Pavement Research and Technology*, (6), 147–154. doi:10.6135/ijprt.org.tw/2013.6(3).147
- Zak, J., & Valentin, J. (2013). *Test Method for Measuring Friction Characteristics between Asphalt Mixture and Steel*. In *Proceedings of the Ninth International Conference on the Bearing Capacity of Roads, Railways and Airfields* (Vol. 9th, pp. 585–593). Trondheim: Akademika Publishing.

2.2. Zak, J., Suda, J., Uniaxial Shear Tester – test methodology, 2020.

Authors' contribution percentage:

50% Žák, J.,

50% Suda, J.

Test methods for hot mix asphalt – UST2020CZ

Determining the shear properties of asphalt mixtures using Uniaxial Shear Test – Uniaxial Repeated Shear Test (URST)

Bestimmung der Schereigenschaften von Asphaltmischungen - Scherswellversuch

Détermination des propriétés de cisaillement des enrobés bitumineux - Essai de cisailment cyclique

This methodology for determining the shear properties of asphalt mixtures exists in two language versions (English, Czech).

This methodology is not the responsibility of the CEN or the ACLU. This technical regulation is not part of the set of standards for testing asphalt mixtures.

Methodology development:

Ing. Josef Žák, Ph.D.

Ing. Jan Suda, Ph.D.

Foreword

The lack of devices to measure the shear properties of asphalt mixtures in Europe and the attempt to simplify the equipment compared to that used in North American countries called the Superpave Shear Tester (SST) were motives for development of the new device. Testing laboratories are equipped with Universal Testing Machines (UTMs), also known as Nottingham asphalt tester (NAT). Compared to SST, the Uniaxial Shear Test (UST) device is of cheaper productional and operational costs due to its simpler design and its complementary use with UTM as a device eligible for a variety of other laboratory tests. Therefore, it is not a single-purpose device such as SST. This methodology is written down to establish the conditions for testing the shear properties using UST device and describes the test methodology for repeated shear tests, respectively. The UST can be used as well for other types of tests, e.g. a Uniaxial Shear Frequency Sweep Test (dynamic test), which is not the subject of this methodology.

1. Introduction

In developed countries one of the criteria for flexible pavement design is an assessment of pavement structure susceptibility to permanent deformation. The occurrence of permanent deformation has a significant impact on the serviceability, surface water run-off, ride quality and, most importantly, the traffic safety.

Permanent road deformations in flexible pavements in the form of ruts are a combination of irreversible deformation occurring in the subgrade, granular unbound material and asphalt mixture layers.

The Hamburg Wheel Tracking Test Device (HWTDD) is a test method used in both the United States and Europe to assess the sensitivity of asphalt mixtures to permanent deformations. The standardized test method is used under various conditions, samples immersed in water or cooled by air are tested at 50 or 60 °C in CEN (European Committee for Standardization) countries, and similar conditions are used in many US states. The values of the Proportional Ruth Depth (PRD) or the Wheel Tracking Slope (WTS) are standardized in national technical regulations and standards for different asphalt compacted layers, although the determination of mechanical-physical (rheological) parameters from HWTDD is very difficult (Zak et al., 2013). HWTDD tests are as well in some cases conducted with submerged samples and is therefore difficult to separate the effect of damage due to the presence of water and the effect of resistance to permanent deformation from the overall test results.

McLean was one of the first to state in his work (McLean 1974) that the permanent deformation of the asphalt compacted layers (AC) is caused by compression (volume change) and the shear deformation (shape distortion) as an effect of repeated traffic loads. In the case of well-compacted asphalt mixtures,

compaction has relatively little effect on the formation of permanent deformations. Thus, shear deformation is the predominant repetitive mechanism that results in permanent deformations (Zak et al. 2016). X-ray CT images of samples of asphalt compacted mixtures before and after loading by heavy trucks (E. Coleri et al. 2012) also showed that shear-related deformations a major impact on the formation of permanent deformations in roadways, while compression (volume change) contributes in the earliest stages of traffic loading to the road structure (after the road has been put into service) .

Permanent deformations of asphalt compacted layers have been the subject of extensive SHRP research described in Monismith et al. (1994). One of the research results was the development of the Superpave Shear Test (SST) test device. The SST is able to test laboratory-prepared samples and borehole samples taken from the roadway, typically with a diameter of 150 to 200 mm and a height of 50 to 75 mm, with the possibility of testing also prismatic samples (Coleri et al. 2012). Using different load patterns it is possible to perform various tests such as repetitive loop test by repetitive loads at constant specimen height and dynamic loop test at constant specimen height. All tests shall be carried out at a constant temperature.

The validity of the measured mechanical-physical properties was further evaluated *in-situ* during the WesTrack project (Monismith et al. 2000), where mechanistic-empirical models were developed that represent the behavior of roadway test sections in accelerated experimental testing using fully loaded trucks. Such models are further used as a performance models that relate the laboratory-measured results to the behavior of asphalt compacted layers *in-situ* (Deacon et al. 2002; Zak et al. 2018).

The use of shear properties of asphalt compacted layers as parameters of roadway construction was described in Harvey et al. (2014) and used in many projects since the development of SST device including the reconstruction of I-710 in Long Beach (Monismith and Harvey 2009) and a number of other reconstruction projects in California. Track depth prediction models were developed in NCHRP 719 analysis (Von Quintus et al. 2012). Four models are assessed in this comprehensive report and the differences between the repeated load tests are summarized. The shear test by repeated loading at a constant specimen height has proven to be a suitable test for predicting the performance of asphalt mixtures carried out in accordance with AASHTO T 320-07 2011.

2. Cited normative documents and standards

The following referenced normative documents are necessary for the use of this document. For dated links only quoted editions apply, for undated links applies the last edition of the reference document (including changes).

EN 12697-6 Bituminous mixtures - Test methods for hot mix asphalt - Part 6: Determination of bulk density of bituminous specimens

EN 13108-20 Bituminous mixtures – Material specifications – Part 20 : Type testing

EN 12697-27 Bituminous mixtures - Test methods - Part 27: Sampling

EN 12697-29 Bituminous mixtures - Test methods for hot mix asphalt - Part 29: Determination of the dimensions of a bituminous specimen

EN 12697-30 Bituminous mixtures - Test methods for hot mix asphalt - Part 30: Specimen preparation by impact compactor

EN 12697-31 Bituminous mixtures - Test methods - Part 31: Specimen preparation by gyratory compactor

EN 12697-33 Bituminous mixtures - Test methods for hot mix asphalt - Part 33: Specimen prepared by roller compactor

3. Object of the document

This methodology describes a test method to compare asphalt mixtures or to assess the suitability of the mixture in terms of assessing the increase of accumulated permanent deformation and derived parameters.

The method covers a procedure for preparing and testing hot mix asphalt (HMA) to determine the shear parameters in relation to the permanent deformations of asphalt mixtures in a uniaxial repeated shear test with horizontal deformation limitation. HMA mechanical-physical parameters are derived by evaluation of the measured deformations from loading.

In this test, cylindrical test specimens prepared in the laboratory or samples taken from roadway boreholes are subjected to uniaxial repeated shear stress. The maximum aggregate grain size is 22 mm.

Note: This method correlates with the SST device according to AASHTO T 320-07.

4. Terms and definitions

For the purposes of this methodology, the following terms and definitions apply:

4.1. accuracy class

allowed error of measurement in the sensor signal expressed as percentage

4.2. contact area

the area of the load plate touching the test specimen

4.3. permanent strain

permanent axial strain after one load cycle

4.4. accumulated permanent strain ϵ_{sp}

accumulated permanent strain after n-times repeated load cycles

4.5. increment permanent strain ϵ_p

permanent shear strain increment after n-times repeated cycles (n being between 5 000 and 10 000)

4.6. absolute peak strain ϵ_a

absolute strain value for the nth load cycle (see Figure 4)

relative peak strain ϵ_r

strain value induced by the respective load cycle (see Figure 4)

4.7. shear plane S_p

theoretical plane where the maximum shear stress under load is distributed,

$$(S_p = 2\pi H r_{sp})$$

4.8. radius to shear plain center r_{sp}

distance from the axis of symmetry to the surface of the shear plane in meters ($r_{sp} = 0,06$ m)

4.9. logarithm regression

a regression model that is linear in parameters but describes a nonlinear relationship between variables;

this regression contains only one independent variable, but it occurs in different powers

4.10. holding load

a load of test specimen weight under unloading (min. 25 N)

4.11. haversine

derived goniometric function $(1-\cos)/2$

4.12. Conversion factor C_f , multiplier m , coefficient Δ_{power}

coefficients were determined in a simulation of a uniaxial shear test based on analysis of linear elastic finite elements (FE) in software ABAQUS ($C_f = 24,604$, $m = 1,063$, $\Delta_{power} = 1,08$)

4.13. precision

the closeness of conformity between independent test results obtained under pre-specified conditions. Conformity depends only on the distribution of random errors and is unrelated to the actual or specified value. The degree of conformity is usually expressed by non-conformity and is calculated as the standard deviation of the test results. A smaller conformity is reflected in a larger standard deviation. The "independent test results" are those unaffected by any previous result on the same or a similar test sample. The quantitative degree of conformity depends crucially on predetermined conditions. Repeatability and reproducibility conditions are subsets of extreme pre-specified conditions.

4.14. micro strain

a unit of relative strain $\varepsilon = 10^{-6}$, which is usually given as a percentage (%) or as a dimensionless number ($\mu\text{m/m}$)

4.15. shear resilient modulus G

the shear modulus is defined as the ratio of the stress deviator to the reversible deformation in dynamic tests; this type of module is used for tests with fast-acting load (haversine load)

5. Test principle

The repeated shear test determines the shear parameters in relation to the formation of permanent deformations in asphalt mixtures. The tempered cylindrical test specimen with a hole is inserted into a steel socket with an inner flange. A steel insert is then inserted into an opening between two parallel load plates. The entire set is placed on a pedestal and three LVDT probes are installed at an angle of 120° . A stress is then applied to the hemisphere-shaped joint at the center of the steel insert. The steel insert is pushed down through the specimen of the asphalt mixture producing a shear stress and deformation. The steel socket limits the horizontal deformation of the asphalt mixture in the sides which characterizes the influence of the surrounding material.

6. Test equipment

6.1. Uniaxial Shear Tester (UST)

Uniaxial Shear Tester (see Figure 1) consists of a cylindrical steel socket with an insert, a steel spacer ring, and holders for LVDT sensors with the possibility of shifting. The UST testing assembly is axially symmetrical along a vertical axis.

Following picture is on of the Uniaxial Shear Test variants. The support, loading piston, LVDT sensors are it regularly equipment of Universal Testing Machines. The connection between loading piston and the steel insert may vary. In the picture two variants are present (knee joint and hemisphere).

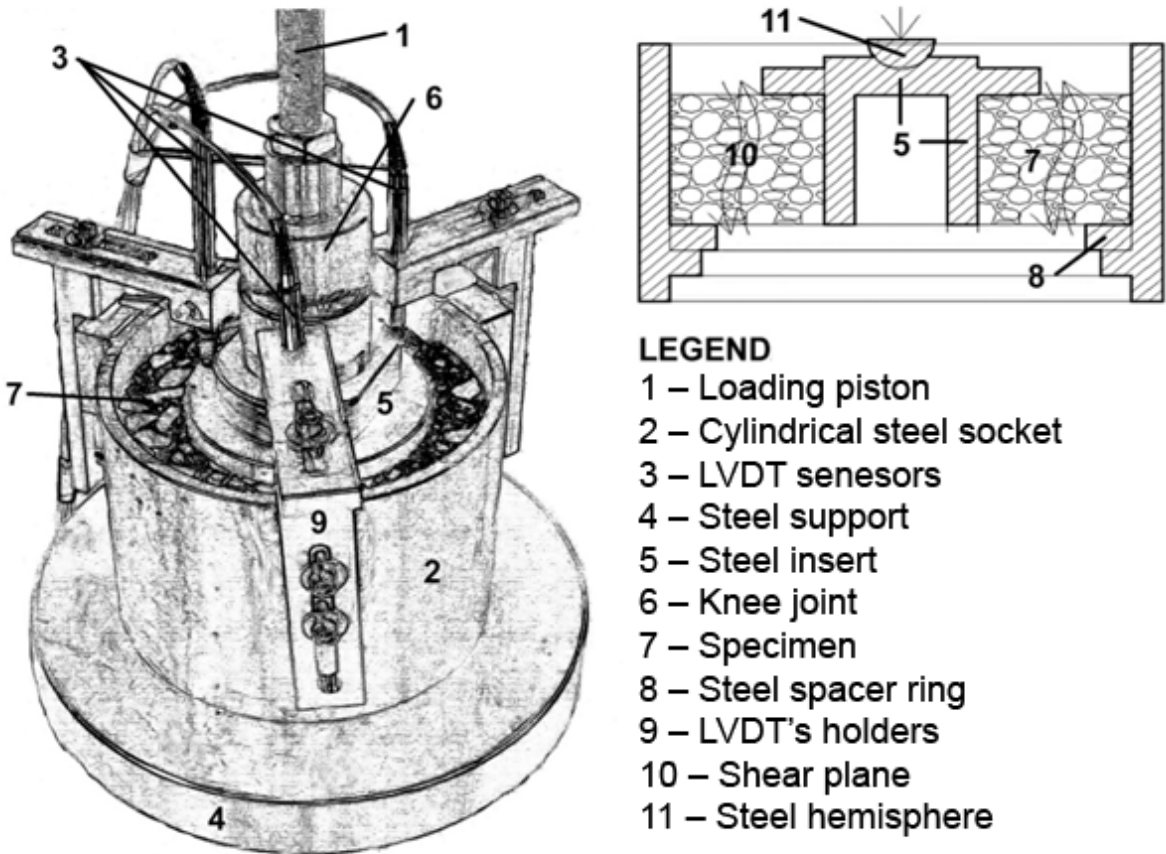


Figure 1. Uniaxial Shear Tester (UST) – a testing assembly

6.2. Loading device

Either a servohydraulic or pneumatic press capable of exerting a force of 2000 N with a precision of $\pm 5\%$ can be used to deliver the shear strain. The electromechanical press with same parameters is allowed to be used as well. The test loading device must be capable of generating harmonic loading pulses of the selected frequency. All components must be constructed of stainless steel. The press must be part of a control and measurement system set that includes a computer and software for controlling, reading, and collecting the necessary data. The control system must ensure that the controlled physical parameters (force) do not oscillate out of defined boundaries during the test. It is recommended that the control system include a generator of programmable functions and a control circuit through which the selected load signal can be generated. The stress device movement control system must allow the specimen to be controlled so that it meets the specified requirements for displacement and stress load. The control system should ensure that a controlled displacement of the test sample does not induce vibrations during the test.

6.3. Displacement sensors

The deformation measuring system must be equipped with three displacement sensors for measuring and recording the deformation of the specimen. The sensors must comply with accuracy class 0.2. The measuring range of the sensors must not be less than 10 mm. It is recommended to check the specifications given by the supplier because the dynamic behavior of sensors and electronic measuring equipment can cause measurement errors that are significantly higher than the maximum allowed values. Another important factor to consider is whether the electronic equipment is adequately protected against the influence of external interfering electrical and magnetic sources capable of causing measurement errors.

6.4. Strain gauge

Strain gauge with a measuring range of at least $\pm 2\ 000\text{ N}$ and an accuracy of 1%. The force is measured in the middle, between two central supports. The resonant frequency of the strain gauge and the coupled moving mass should be at least 10 times higher than the test frequency.

6.5. Tempering chamber

The control chamber is used to maintain the specified temperature of the specimen. Temperature control accuracy is $\pm 0,5\text{ }^{\circ}\text{C}$ or greater. It is advisable to select tempering chambers of sufficient size to allow other samples to be tempered in the chamber during the test.

6.6. Necessary measuring and auxiliary devices, and accessories

Weights and other devices to determine the bulk density according to EN 12697-6.

Vernier caliper or other suitable device for determining the dimensions of a cylindrical test specimen according to EN 12697-29.

Drying oven with adjustable temperature from 15 °C to 25 °C.

Storage space with adjustable temperature between 5 °C and 25 °C.

7. Preparation of a test specimen

At least 5 test specimens are prepared for the test. Each specimen must be cylindrical. The contact area of the test specimen must be flat and parallel to each other. If this is not the case, the test specimen must be excluded. The seating surfaces of the test fixture should be parallel and perpendicular to the vertical axis of the specimen (e.g. the right angle shall not be inclined by more than 2° to 3°). For a routine control of the plane surface run the hand over the contact area of the specimen. It is considered suitable if the surface is smooth and free of defects, otherwise it must be grinded. After grinding, the specimen must be dried at a temperature not exceeding 25 °C. The specimen is considered dry after a minimum of 8 hours of drying, and if two consecutive weighing with a 4-hour break in between differ by less than 0.1%.

The following dimensions, which are obtained by measuring a dry test specimen according to EN 12697-6 procedure D according to ČSN EN 12697-29 using a Vernier caliper, must be followed:

- The test specimen shall typically have a height of 50 mm and a diameter of 150 mm (see Figure 2).
- The height of the test specimen shall not differ by more than 2,0 mm and the diameter by more than 0,1 mm.
- The cylindrical hole in the middle of the test piece must be made by a core bore of diameter 50 (±0,2) mm.

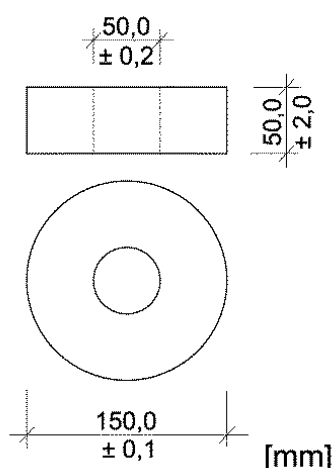


Figure 2. Test specimen dimensions / Example - typical test specimen / test specimen after grinding

The test may be conducted on:

- Test specimens prepared in the laboratory by the gyrator according to CSN EN 12697-31.

- Test specimens taken as cores from a laboratory-prepared slab of asphalt mixture according to CSN EN 12697-33.
- Specimens prepared from test samples taken as a drill core from the roadway according to CSN EN 12697-27.
- Test specimens prepared in the laboratory by the impact compactor according to CSN EN 12697-30.

The method of compacting the test specimen has a significant effect on the test results. For type tests the method of compaction is specified in ČSN EN 13108-20.

The bulk density of the test specimen is determined according to ČSN EN 12697-6.

In the case of test specimens taken as a roadway bore core and if the height of an individual test specimen is insufficient, it still may be used. This information, however, must be recorded in the test report. It is not permissible to stack two samples on top of each other.

No damage to the test specimen shall occur during all stages of sampling, transport, and preparation prior to testing. During transport and at the time of storage the plate or bore core is fully secured to prevent deformation or damage.

8. Tempering

Store the test specimens at 5 °C to 25 °C. The specimens shall be secured against displacement and shall not be stored on top of each other to prevent any kind of damage. The test must not be performed earlier than 2 days after preparation of the specimen in the laboratory or after compaction of the road layer from which the bore core has been taken. If necessary, the test pieces shall be brushed or washed. The test pieces must be dried to constant weight at room temperature.

The test must be carried out at 50°C or 60°C. The samples' test temperature shall be stabilized within $\pm 0,5$ °C for at least 3 hours and no more than 7 hours. It is an advantage if the temperature can be stabilized for the prescribed time in the tempering chamber.

9. Stress configuration and data collection

The stress applied in the repeated shear test is serious of following cycles. One cycle contains 0.1 s haversine shear pulse followed by the 0.6 s rest period. The stress diagram is shown in Figure 3. The typical value for axial load is 1750 N (corresponding to a shear stress of approximately 97,4 kPa) per

specimen with 150 mm in diameter. A contact stress of at least 50 N must be maintained throughout the test.

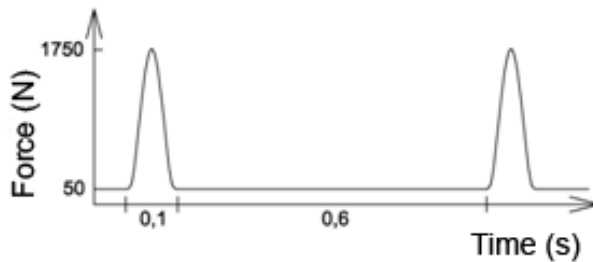


Figure 3. Haversine pulse – loading and unloading time

Data recording must be performed automatically during the test, preferable at critical points and load times, or at the point of maximum pulse load and at the end of the unload time, i.e. as close as possible to the next load pulse. It is measured at least after the applied load pulses listed in Annex B. It is recommended to measure the deformation at a fixed time during the cycle (loading / unloading) or to automatically obtain the global maxima and minima in a defined load cycle. As part of data collection, it is necessary to obtain the following data:

- number of the loading cycle n
- maximum value of the force in (N) of the n^{th} cycle ($F_{\max,n}$)
- minimum value of the force in (N) of the n^{th} cycle ($F_{\min,n}$)
- maximum deformation in (mm) of the n^{th} loading cycle for LVDT sensors 1, 2, 3 ($\epsilon_{a,n}$)
- minimum deformation in (mm) of the n^{th} loading cycle for LVDT sensors 1, 2, 3 ($\epsilon_{r,n}$)

Critical points of the material's response to load pulses are shown in Figure 4. From the measured deformations it is possible to derive and calculate the required values of deformation according to the following relations (1) and (2):

$$\epsilon_{p,n} = \epsilon_{ap,n} - \epsilon_{ap,n-1} \tag{1}$$

$$\epsilon_{r,n} = \epsilon_{a,n} - \epsilon_{p,n} \tag{2}$$

Parameters of the material's response to a loading pulse are shown in Figure 4.

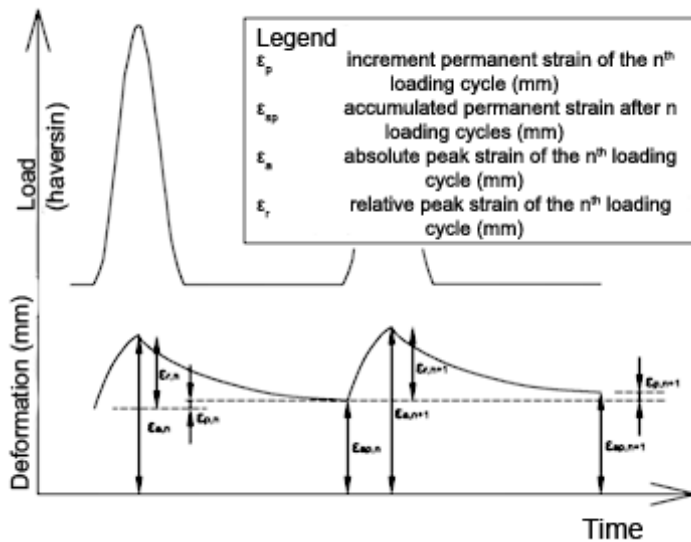


Figure 4. General scheme of the loading cycle and deformation during repeated shear test

10. Test procedure

At least 5 test specimens must be used for the standard Uniaxial Shear Test. The test temperature must be kept constant throughout the test within $\pm 0,5 \text{ }^\circ\text{C}$, the standard test temperature being $50 \text{ }^\circ\text{C}$ or $60 \text{ }^\circ\text{C}$. An inner flange is inserted into the cylindrical steel socket. Subsequently, the sample is inserted axially symmetrically into the steel socket so that the specimen contacts the flange tightly. If necessary, the specimen must be grinded. Then a steel insert is inserted tightly into the hole of the test specimen and 3 LVDT sensors are placed so that they are evenly distributed at an angle of 120° . The steel insert is subsequently inserted into the specimen central hole. Then the test set is placed back in the tempering chamber and allow to temper for 20 minutes. The stress piston is then placed in the contact position and 100 conditioning stress pulses are performed, which have the same parameters as in the test itself. The whole test runs in the controlled load stress mode.

At the end of the conditioning stress load, the sample must be left unloaded for 5 minutes. Subsequently, the stress loading is performed according to the repeated shear test. During this test, both the stress profile and the deformation of the selected cycles are recorded (see Annex B).

Note: If the deformation is greater than the range of the LVDT sensors, the test must be terminated. This information shall be included in the test report.

11. Calculation and results expression

First, determine the coefficient of test specimen thickness according to the relation (3):

$$C_T = \frac{50}{H} \quad (3)$$

where

C_T coefficient of the specimen's thickness (-)

H average thickness of specimen (mm) according to EN 12697-29

The accumulated permanent strain for all load cycles is calculated from the measured data and plotted against the stress cycles. The accumulated permanent deformation is calculated according to the equation (4):

$$\varepsilon_{apS,n} = 1000 \cdot C_T C_f \sum_{1 \leq n \leq 30000} \varepsilon_{p,n} \quad (4)$$

where

$\varepsilon_{apS,n}$ accumulated permanent strain for n^{th} stress cycle ($\mu\text{m}/\text{m}$)

C_f conversion coefficient (-)

Incremental permanent strain is calculated according to relation (5):

$$\text{IPS} = \frac{\varepsilon_{apS,10000} - \varepsilon_{apS,5000}}{5} \quad (5)$$

where

IPS incremental permanent strain ($\mu\text{m}/\text{m}/10^3$)

$\varepsilon_{apS,10000}$ absolute value of accumulated permanent strain after 10 000 stress cycles (m/m)

$\varepsilon_{apS,5000}$ absolute value of accumulated permanent strain on after 5 000 stress cycles (m/m)

The number of cycles up to the specified value of the accumulated permanent strain is calculated by a simple linear regression with one explanatory variable; the relation between the dependent and the

independent variable is logarithmic. The shape of the regression function is given according to the equation (6):

$$N_{\varepsilon\%} = a \varepsilon_{apS,n}^b \quad (6)$$

where

$N_{\varepsilon\%}$ number of cycles up to the percentual value of accumulated permanent strain (-)

a, b regression function parameters (-)

After logarithm we obtain the equation $\log N_{\varepsilon\%} = \log a + b \log \varepsilon_{apS,n}$ and with substitution $y^* = \log N_{\varepsilon\%}$, $a^* = \log a$, $x^* = \log \varepsilon_{apS,n}$ we obtain an equation for simple linear regression (7):

$$y^* = a^* + bx^* \quad (7)$$

Unknown parameters a^* , b estimates are calculated by equations (8) a (9):

$$a^* = \bar{y}^* - b\bar{x}^* \quad (8)$$

$$b = \frac{\sum(x_i^* - \bar{x}^*)y_i^*}{\sum(x_i^* - \bar{x}^*)^2} \quad (9)$$

The number of stress cycles to accomplish 1%, 3% or 5% deformation is calculated by the following equations (10), (11) and (12):

$$N_{1\%,\varepsilon} = \left(\frac{0,01}{10^{a^*}}\right)^{\frac{1}{b}} \quad (10)$$

$$N_{3\%,\varepsilon} = \left(\frac{0,03}{10^{a^*}}\right)^{\frac{1}{b}} \quad (11)$$

$$N_{5\%,\varepsilon} = \left(\frac{0,05}{10^{a^*}}\right)^{\frac{1}{b}} \quad (12)$$

Relative value of shear module (MPa) is calculated by the equation (13):

$$G_{sr,n} = m \frac{F_{max,n}}{(\varepsilon_{r,n})^{\Delta_{power} C_t}} \cdot 10^{-6} \quad (13)$$

where

m multiplier (-)

Δ_{power} coefficient (-)

$F_{max,n}$ the maximum force at n^{th} stress cycle (N)

$\varepsilon_{r,n}$ relative strain at n^{th} stress cycle (m)

Note: To calculate the shear stress it is necessary to consider the shear surface S_p .

12. Test Protocol

In the test protocol there must be a reference to this methodology and all the following information about the samples and test results:

12.1. Information about test specimens and test conditions

The test protocol must contain the following information about the specimens:

- a) type and origin of test asphalt mixture;
- b) the designation of mixtures and materials;
- c) identification number of specimens;
- d) preparation method of a test specimen: in the laboratory (with reference to the relevant European or other standard) or by taking the bore core from the roadway;
- e) mean value of the test specimen diameter, in mm;
- f) density (SSD), in grams per cubic centimeter to the nearest 0,001 g / cm³;
- g) other circumstances (including number of samples discarded);
- h) test temperature

12.2. Test results

The test protocol must contain the following information about the specimens:

- i) density (SSD), in grams per cubic centimeter to the nearest 0,001 g / cm³;
- j) shear module at 1 000 stress cycles [MPa];

- k) regression parameters of accumulated permanent strain;
- l) number of cycles needed to reach 1%, 3% and 5% of permanent deformation [-]
- m) permanent strain at 5 000, 10 000, and 30 000 stress cycles, eventually;
- n) incremental permanent strain;
- o) The accumulated permanent shear strain curve for all test specimens and the average accumulated shear strain curve shall be plotted at the appropriate scale.

13. References

- AASHTO T 320-07. 2011. „Standard Method of Test for Determining the Permanent Shear Strain and Stiffness of Asphalt Mixtures Using the Superpave Shear Tester (SST)". American Association of State Highway and Transportation Officials.
- Bahia, H. U., D.I. Hanson, M. Zeng, A. Zhai, M.A. Khatri, a R.M. Anderson. 2001. *Characterization of Modified Asphalt Binders in Superpave Mix Design*. Transportation Research Board — National Research Council, National Academy Press Washington, D.C.
- Coleri, E., R.Z. Wu, J.T. Harvey, a J. Signore. 2012. „Calibration of incremental-recursive rutting prediction models in CalME using Heavy Vehicle Simulator experiments". In , 471–81.
- Coleri, Erdem, John T. Harvey, Kai Yang, a John M. Boone. 2012. „A micromechanical approach to investigate asphalt concrete rutting mechanisms". *Construction and Building Materials* 30 (květen): 36–49. <https://doi.org/10.1016/j.conbuildmat.2011.11.041>.
- D'Angelo, J., R. Kluttz, R. Dongré, K. Stephens, a L. Zanzotto. 2007. „Revision of the Superpave high temperature binder specification: The multiple stress creep recovery test". In , 76:123–62.
- Deacon, John, John Harvey, Irwin Guada, Lorina Popescu, a Carl Monismith. 2002. „Analytically Based Approach to Rutting Prediction". *Transportation Research Record: Journal of the Transportation Research Board* 1806 (1): 9–18. <https://doi.org/10.3141/1806-02>.
- Harvey, J. T., J. Signore, R.Z. Wu, I. Basheer, S. Hollikati, P. Vacura, a T.J. Holland. 2014. „Integration of Mechanistic-Empirical Design and Performance Based Specifications: California Experience to Date". In *12th ISAP Conference on Asphalt Pavements*. Raleigh, North Carolina.
- Harvey, J., S. Weissman, F. Long, a C. Monismith. 2001. „Tests to evaluate the stiffness and permanent deformation characteristics of asphalt/binder-aggregate mixes, and their use in mix design and analysis". In , 70:576–604.
- McLean, David Brian. 1974. *Permanent deformation characteristics of asphalt concrete*. PhD Thesis, University of California, Berkeley.
- Monismith, C. L., a J. T. Harvey. 2009. „The Ideal Asphalt Pavement: Pavement: Design". *Journal of the Association of Asphalt Paving Technologists* 78: 903–40.
- Monismith, C. L., R. G. Hicks, F. N. Finn, J. Sousa, J. Harvey, S. Weissman, J. Deacon, J. Coplantz, a G. Paulsen. 1994. „Permanent Deformation Response of Asphalt Aggregate Mixes", *srpen*, 1–437.
- Monismith, C.L, J. A. Deacon, a John Harvey. 2000. *WesTrack: Performance Models for Permanent Deformation and Fatigue*. Pavement research Center; Institute of Transportation Studies, University of California, Berkeley.
- Ullidtz, Per, J. T. Harvey, Imad Basheer, David Jones, Rongzong Wu, Jeremy Lea, a Qing Lu. 2010. „CalME, a Mechanistic-Empirical Program to Analyze and Design Flexible Pavement Rehabilitation". *Transportation Research Record: Journal of the Transportation Research Board* 2010 (2153): 143–52. <https://doi.org/10.3141/2153-16>.

Von Quintus, Harold, Jagannath Mallela, Ramon Bonaquist, Charles W. Schwartz, a Regis L. Carvalho. 2012. *Calibration of Rutting models for structural and Mix Design*. Washington, D.C.: Transportation Research Board - National Research Council.

Zak, J. 2012. „IRIS Rheo-Hub, Program description". ČVUT, FSv, Department of Road Structures. <http://silnice.fsv.cvut.cz/predmety/stpk/IRIS.pdf> DOI:10.13140/RG.2.1.3931.1523.

Zak, J, E Coleri, a J. T. Harvey. 2018. „Incremental Rutting Simulation with Asphalt Mixture Shear Properties". In *Solving Pavement and Construction Materials Problems with Innovative and Cutting-edge Technologies*, 13–24. Hangzhou, China: Springer, Cham. https://doi.org/10.1007/978-3-319-95792-0_2.

Zak, J., C. L. Monismith, E Coleri, a J. T. Harvey. 2017. „Uniaxial Shear Tester - Test Method to Determine Shear Properties of Asphalt Mixtures". *Road Materials and Pavement Design Journal*, 87–103. <https://doi.org/10.1080/14680629.2016.1266747>.

7

14. Annex A

UST2020EN

The test of resistance of asphalt mixtures to permanent deformations was performed according to:

Zak, J., C. L. Monismith, E Coleri, a J. T. Harvey. 2017. „Uniaxial Shear Tester - Test Method to Determine Shear Properties of Asphalt Mixtures". Road Materials and Pavement Design Journal, 87–103.

Test methods for hot mix asphalt: UST2020EN - Determining the shear properties of asphalt mixtures using Uniaxial Shear Test – Uniaxial Repeated Shear Test [URST]

Uniaxial Repeated Shear Test

Customer:	Asphalt mixture:
Specimen manufactured:	Asphalt binder:
Test performed by:	Date of test:
Number of specimens tested:	Number of load cycles:
Date of manufacture of test specimens:	Test specimen preparation method:

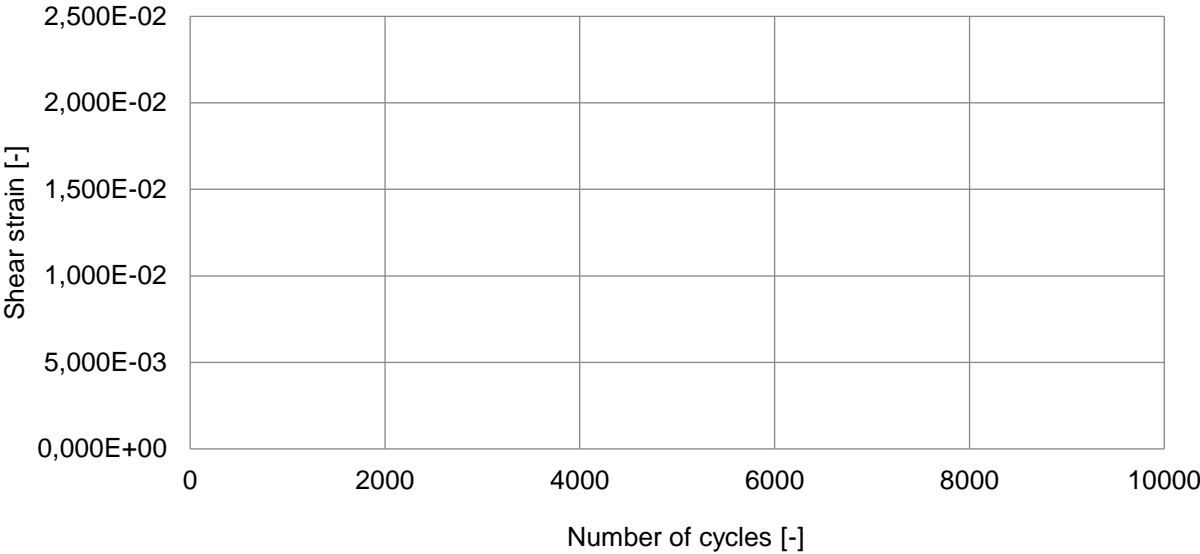
Note:

Load = 1750 N [50 N]

Pulse [haversine] - 0,1 s pulse load time + 0,6 s unloading time

Specimen identification	Specimen Nr.	Specimen Nr.	Specimen Nr.	Specimen Nr.	Specimen Nr.	Specimen Nr.
Diameter [mm]						
Thickness [mm]						
Bulk density [g/cm ³]						
Shear module @ 1000c [MPa]						
Regression of accumulated permanent strain [-]	Parameter A					
	Parameter B					
Number of cycles to reach shear strain [-]	1 % γ					
	3 % γ					
	5 % γ					
	at 5000 cycles					
Permanent strain [$\mu\text{m}/\text{m}$]						
	at 10000 cycles					
Incremental permanent strain [$\mu\text{m}/\text{m}/103$]						

Accumulated permanent shear strain



Specimen Nr. Specimen Nr. Specimen Nr. Specimen Nr. Specimen Nr. Specimen Nr. Average

-- End of protocol --

15. Annex B

Table 2 gives the recommended stress cycles to be used for data acquisition. These values are recommended to be used only for the purpose of simplification, reduction of the test results file size, and easy interpretation of results. The difference between number of following cycles depends on the function $\ln(y)=a+bx$.

1	54	480	4278
2	58	512	4563
3	61	546	4866
4	65	583	5189
5	70	621	5534
6	74	663	5901
7	79	707	6293
8	85	754	6711
9	90	804	7157
10	96	857	7633
11	103	914	8140
12	109	975	8681
13	117	1039	9257
14	124	1108	9872
15	133	1182	10000
16	142	1261	10724
17	151	1344	11464
18	161	1434	12255
19	172	1529	13100
21	183	1630	14004
22	195	1739	14970
23	208	1854	16003
25	222	1977	17106
27	237	2109	18286
28	252	2249	19548
30	269	2398	20896
32	287	2558	22338
34	306	2727	23879
37	327	2909	25526
39	348	3102	27287
42	371	3308	29169
44	396	3528	30000
47	422	3762	
51	450	4012	

Table 2. Recommended stress cycles for data acquisition (record) during the test

2.3. Žák, J., Suda, J., Ryjáček, P., Polymer Modification Technologies and Asphalt Mixtures Fatigue Resistance in Pavement Structures, 2016.

Authors' contribution percentage:

60% Žák, J.,

20% Suda, J.,

10% Ryjáček, P.

Polymer Modification Technologies and Asphalt Mixtures Fatigue Resistance in Pavement Structures

Josef Zak^a, Jan Suda^a, Pavel Ryjacek^a

^a Czech Technical University in Prague, Faculty of Civil Engineering, Thakurova 7, 160 00 Prague, Czech Republic. Corresponding author's email: josef.zak@fsv.cvut.cz

This paper focuses on polymer modification technologies and pavement durability in relation to fatigue resistance, providing a critique of several common mix design practices and recommendations based on recent research findings in relation to pavement field performance. The authors present specific data measurements from the laboratory of fatigue resistance behavior for asphalt mixtures with various bituminous binders: neat, polymer-modified, and chemically-modified asphalt binders. Results show differences in calculated pavement design lifespans when a 50% loss modulus as a standard concept is employed in contrast to a dissipated energy concept. The authors also describe the variability of asphalt mixture fatigue resistance and the stochastic method for calculating a proportional coefficient. Proportional coefficient implementation in pavement design methodologies may enhance consistency in pavement design lifespan predictions and subsequent in-situ performance. The methodology presented in this paper can be utilized to analyze the longevity of the material on steel bridges as will be envisaged in the research project.

1. Introduction

An asphalt mixture's resistance to fatigue is a crucial material parameter that affects the lifespan of an entire pavement structure (De La Roche 2001; Monismith 2012; Harvey et al. 1997; SHRP-A-404 1994; Fiedler, Mondschein, and Zak 2013). Fatigue response measured in the laboratory, however, sometimes does not provide a realistic prediction of in-situ fatigue behaviors. The reliability of such laboratory tests depends on appropriate simulation of real pavement conditions, including proper detection of tipping (failure) points and proper assessment of shift factors (i.e., laboratory→real pavement). The highest tensile strain in pavement is mostly observed on the lower side of the last bituminous layer. Therefore, heavy repetitive loading can provoke the appearance of a fatigue-cracking phenomenon development proceeding from the bottom upwards to the surface, often referred to as bottom-up cracking (Tangela et al. 1990). Despite this, numerous road pavement structures manifest cracks that are not related to bottom-up cracking, arising on the surface of pavement and propagating downward, so-called top-down cracking (Molenaar 2007). In both types of cracking—wherever it occurs (in an entire pavement structure or in

individual layers within a structure) the ability of pavement mixtures to resist cracking is often assessed by a laboratory fatigue test (Zak, Valentin, and Mondschein 2013). As it is a key characteristic entering the design methodologies of pavements in countries across the continents, discussions of individual methods, their exact descriptions, the applicability and usability of these tests or on their alternative versions are continuously occurring in the professional community.

In this paper, the authors use the 50% loss modulus concept and the dissipated energy concept for neat and selected modified asphalt binders in order to observe differences in fatigue responses for selected binder modification technologies and to calculate differences in fatigue resistance. The authors also present data calculated using a recently developed stochastic methodology that measures pavement performance in the laboratory (Zak, Monismith, and Jarušková 2014). The appropriateness of utilizing a dissipated energy method for characterizing resistance to fatigue in pavement design methodologies is also discussed.

Many factors contribute to cracking due to hot-mix asphalt (HMA) fatigue during the lifespan of any pavement structure, including irreversible oxidation processes in the asphalt binders, ultraviolet (UV) radiation, winter maintenance, load amplitude, the quality of an installed HMA layer, asphalt/aggregate adhesion, and moisture susceptibility. Regarding HMA compaction, the lifespans of flexible pavements with a 96% degree of compaction are a quarter of those with a 100% degree of compaction (Zak and Luxemburk 2012; Monismith et al. 2009).

2. Mix and pavement design

According to the small deformation theory, the highest stresses from a tire passing on the pavement surface occur in the surface course (Long 2001). With respect to the above mentioned it seems that the current optimal process is to use a polymer modified binder instead of increasing the binder content in this layer. The bottom asphalt bound layer should be optimized for fatigue resistance by increasing binder content and with the use of economically effective asphalt binder modification technologies.

The HMA tested hot mix asphalt can be characterized as ACO 11+ in accordance with the Czech standard for bituminous mixtures/asphalt concrete (ČSN EN 13108-1 2008), where a dense graded asphalt mixture is used in the surface layer. The binder content was 5.4% of total mass and the air void content was 3.5% as determined by the saturated surface-dry (SSD) method. Since the material tested was based on one aggregate structure (i.e., design), the study was not affected by variation of any other variable except the type of asphalt binder. The aggregate used was amphibolite. For the study, five types of binders were selected. Their characteristics and subsequently-used denotations are summarized in Table 1 above.

3. Test Methodology

Fatigue resistance tests were conducted in the laboratory using 4PBB-PR, a commonly used and recognized test method, in control strain mode. The testing temperature was 15°C and the loading frequency was 20Hz. The test device and methodology were in accordance with the standard test methods used in European Commission for Standardization (CEN) countries (ČSN EN 12697-24+A1 2007) and the United States (ASTM designation D7460-10 2010).

Currently, assessing the fatigue response of asphalt mixtures in the laboratory is often conducted by assessing the viscoelastic performance of pavement structures. Some examples include accessing complex deviatoric (E^* , G^*) and hydrostatic moduli (K^*) and applying the dissipated energy concept to the analysis of fatigue properties in asphalt mixtures. A detailed discussion of the utilization of the dissipated energy theory and a description of the calculation methods can be found in Zak, Valentin, and Mondschein (2013)

Denotation	50/70	35/50	50/70+PPA	50/70+SBS	50/70+Elvaloy
Modification	-	Oxidation/ Blowing	Poly- phosphoric acid	SBS	Elvaloy + PPA
Polymer content [%]	-	-	0.3	5	2+0.3
Ring and Ball test [°C]	47	61	49	74	65
Penetration [1/10mm]	67	37	62	48	49
DSR fail T [°C] real PG	-	-	68	80	84
DSR fail RTFOT T [°C]	64	83	66	75	80
MSCR; RTFOT Jnr 3,2 at 76°C [kPa ⁻¹]	23.62	1.60	13.72	1.65	1.00

Table 1. Asphalt binder properties.

Here, the authors investigated the differences between the fatigue properties of materials determined using the 50% loss modulus and energy dissipation and validated the idea that the difference between the resistances of asphalt mixtures with polymer modified binders is made more striking by the application of the dissipated energy concept compared with the 50% loss modulus.

The dissipated energy concept focuses on the transition between Phase II and Phase III rather than on setting the resistance empirically at a value equal to 50% loss. Because this transition may occur either before or after 50% loss of the stiffness modulus, the order of material characteristics with respect to resistance to fatigue may also change.

4. Test results

4.1. 50% Modulus Loss

One of the input characteristics of pavement designs is the number of cycles determined using the Wöhler curve with respect to stress values computed by multilayer theory. If we choose a reference number of cycles equal to one million, as is utilized in Czech and French design methodologies, an equivalent stress can be determined using the Wöhler curve. Such a parameter is, in both methodologies, denoted as ϵ_6 . Because it is in proportion to the computed elastic strain inside a parenthetical power law by the slope of the Wöhler curve, any change in ϵ_6 has a crucial effect on the calculated service life for a given HMA mix.

The ranking of the different material mixtures in terms of resistance to fatigue can be seen in the Figures 1 and 2 above. The differences in properties caused by polymer and chemical modifications are obvious. Because our tests were designed only to investigate asphalt binder modifications and not other factors, the resulting differences are apparent. When assessed with the 50% loss modulus concept, the resistance to fatigue was very slightly influenced by the addition of polyphosphoric acid.

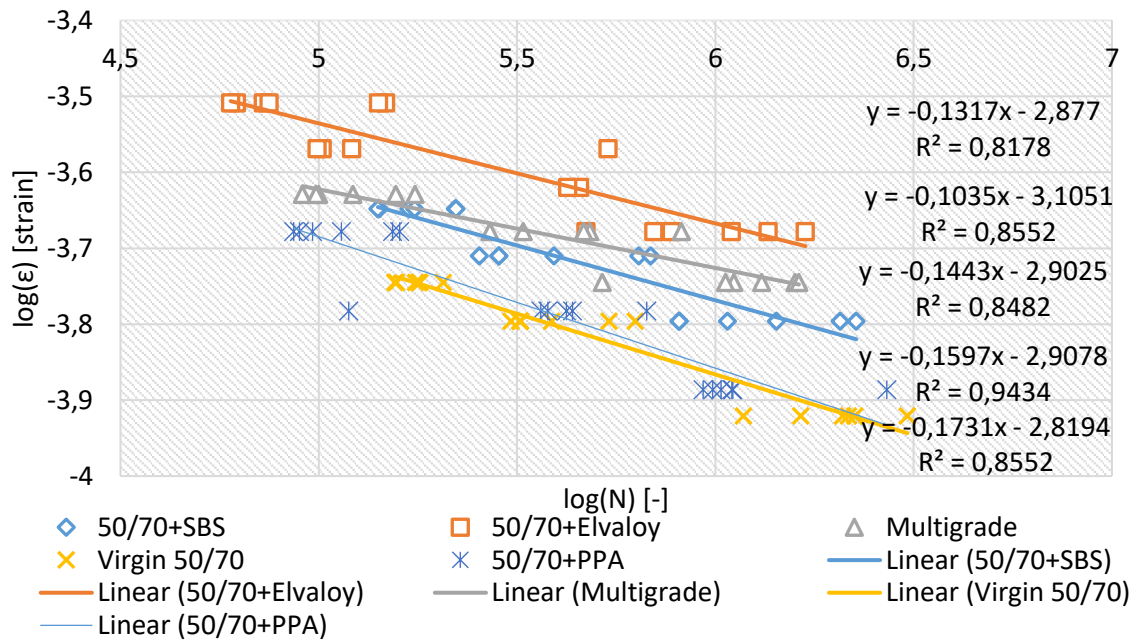


Figure 1. Resistance to fatigue of studied mixtures determined by 50% loss modulus method.

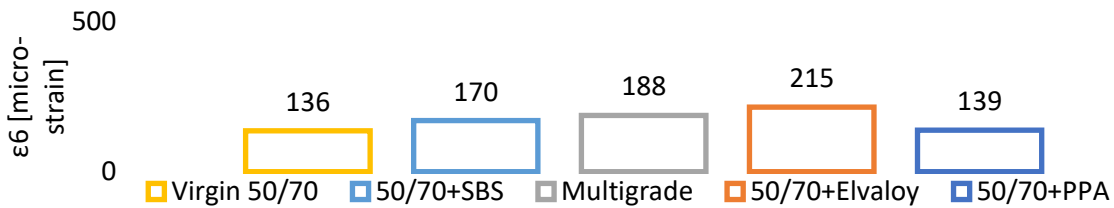


Figure 2. Pavement design parameter ϵ_6 determined by 50% loss modulus method [micro strain].

4.2. Dissipated Energy

From the known dissipated energy interpretation methodologies, the so-called Pronk & Hopman method was chosen (Hopman, Kunst, and Pronk 1989). We selected this test method because of its ability to evaluate both modified and unmodified asphalt binders. Additional details about other possible methods can be found in Zak, Valentin, and Mondschein (2013) and Souliman et al. (2012). The transition point between Phases II and III was determined by calculating the regression coefficient of Phase II and by linear regression. The point where the regression coefficient starts to exceed a value 0.995 is considered the transition point between crack initiation and propagation.

If we look at the laboratory data in Figures 3 and 4, the ranking of assessed materials remains unchanged in comparison to the 50% loss modulus method. From the measured values, the polymer modified group has markedly better resistance to fatigue, especially the asphalt mixture with Elvaloy polymer. If we compare chemical modification (i.e., oxidation) of the two polymers used, the styrene-butadiene-styrene

(SBS) polymer performed worse than the Elvaloy polymer. The addition of polyphosphoric acid distinctly changed the Wöhler curve slope, although its influence on ϵ_6 was minimal. Such diversity in results was not visible when the 50% loss modulus concept was employed.

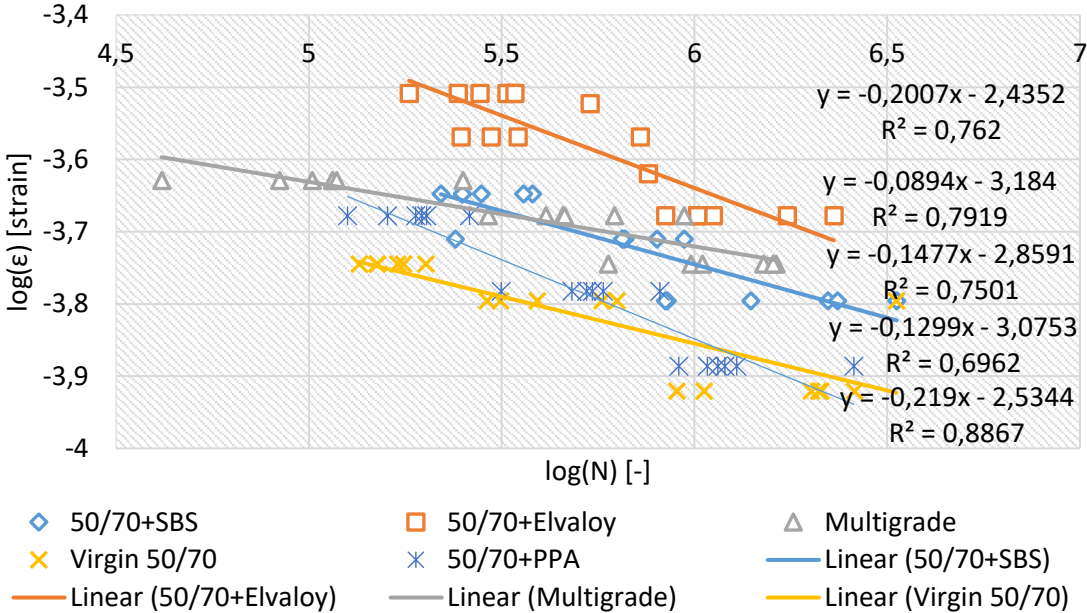


Figure 3. Resistance to fatigue of the studied mixtures determined by Pronk & Hopman method.

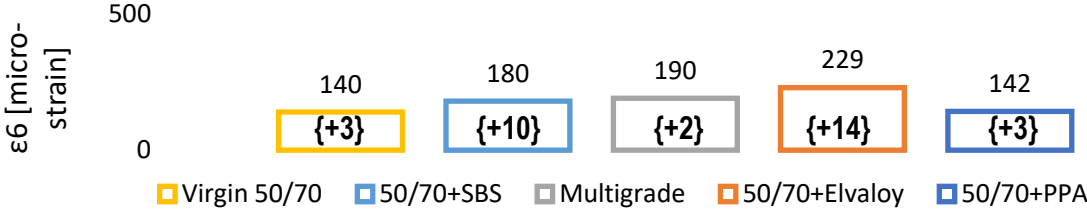


Figure 4. Pavement design parameter ϵ_6 determined by Pronk & Hopman method [micro strain]; difference from 50% loss modulus in curly brackets.

The differentiation when employing the dissipated energy method yielded better results than we originally supposed. The difference between the smallest and highest values of ϵ_6 with the use of the Pronk & Hopman method is 13% higher than the difference observed with the 50% loss modulus method/ $(229-140)/((215-136)/100) \approx 113/$ (see Figure 2 and 4).

The asphalt mixtures with polymer modified asphalt binders have different rheological properties when compared to conventional or oxidized binders, as can be seen from the numbers in curly brackets in Figure 4. The numbers express the ϵ_6 difference between the 50% loss modulus and the dissipated

energy concepts. With the mutual comparison of the ε_6 values difference, we therefore proved that the polymer modified binders absorb/dissipate more energy prior to fracture, even binders that are more stiff. In the other words, the commonly known principle of increased asphalt brittleness with increased stiffness is reversed in the case of polymer-modified binders. Here, asphalt binders modified with polymers show higher stiffness and better fatigue resistance at same time. The different internal structure of polymers may suggests this positive effect.

5. Variability of Fatigue Resistance in Pavement Design Methodology

The Californian flexible pavement design methodology incorporates the variability of resistance to fatigue in the M Value (Reliability Multiplier), while the French methodology calculates with a prediction interval of ε_6 value. The Czech Republic pavement design methodology employs a partial reliability factor γ_p (TP 170 2004; Monismith, Deacon, and Harvey 2000; De La Roche 2001). All of these selected design approaches are examples of stochastic approaches employed in pavement designs.

From these examples, a common prediction interval can be derived. The prediction interval does not completely account for variability in either of the aforementioned design methodologies. It is only a characteristic that mathematically describes a desired effect of variability in the prediction of values from regression. The prediction interval I of regression with reproducibility is utilized according to Equation 1 in order to present a variability in the portion to ε_6 as a superior fatigue characteristic used in French and Czech pavement design and in this paper. The value ($\varepsilon_{6, 5\%}$) is the minimum magnitude of strain derived from the fatigue line (Wöhler curve or S-N curve) at 10^6 cycles for a 5% probability of occurrence with reproducibility (Zak, Monismith, and Jarušková 2014):

$$\varepsilon_{6, 5\%} = 10 \exp \left[\log (\varepsilon_{6, 50\%}) - t_p \frac{s_{\log(\frac{\varepsilon}{N})}}{\sqrt{n}} \sqrt{n + 1 + \frac{(6 - \log(N))^2}{S_{\log(N)}^2}} - 1.65 * \frac{\sigma}{\sqrt{m}} \right] \quad (1)$$

where n is the number of measurements, $\overline{\log(N)}$ is the mean average of $\log(N)$, $s_{\log(\frac{\varepsilon}{N})}$ is the residual standard deviation in linear regression, $S_{\log(N)}$ is the standard deviation of the independent variable $\log(N)$, t_p is the coefficient of the t-distribution, σ is the standard deviation in log, m is the number of inter-laboratory tests and 1.65 is the value of the normal distribution for a 95% confidence level used by other

researchers studying reproducibility. Refer to Zak, Monismith, and Jarušková (2014). (Zak, Monismith, and Jarušková 2014) for the full description of Equation 1.

To get rid of the dependence of the position on the Wöhler curve; i.e., to compare the size of proportions lowering design values, it is necessary to express the values as a fraction of the original value. The proportionality coefficient can be expressed as follows:

$$\gamma = \frac{\epsilon_6}{\epsilon_{6, 5\%}} \tag{2}$$

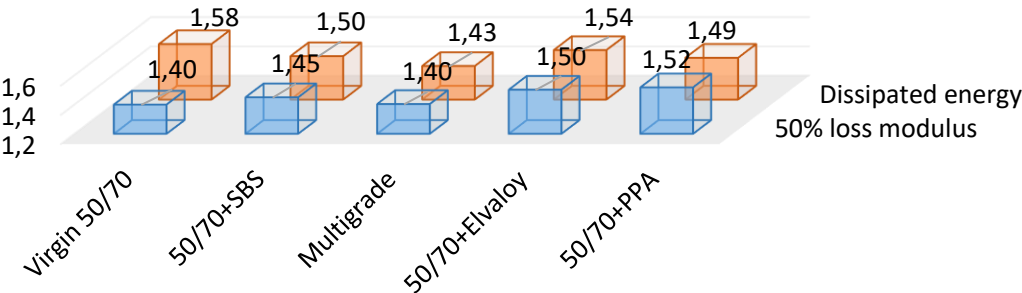


Figure 5. Test variability expressed as proportional coefficient γ .

6. Conclusion

This paper provides results from an asphalt mixture study of the effect of neat binder modifications on laboratory-simulated HMA fatigue resistance. The influence of polymer modifications on the asphalt mixtures resistance to fatigue was evaluated using two methodologies, 50_ loss modulus and dissipated energy concept.

The authors observed that asphalt mixtures with polymer modified asphalt binders have different rheological properties when compared to conventional or oxidized binders in terms of fatigue. Such phenomena can be observed using the dissipated energy concept. Polymer modified materials dissipate more energy prior to fracture than neat and oxidized binders, even those with higher stiffness and performance grade.

Results from a recently developed stochastic approach capable of accounting for fatigue resistance test variability and reproducibility in pavement design methodologies were also presented.

The authors demonstrated that the dissipated energy concept does not reduce fatigue resistance variability when compared to the commonly used 50% loss modulus concept. Despite this disappointment, dissipated energy remains a useful concept in fatigue investigations. The initial energy dissipated during each loading cycle captures effects not only of the imposed strain level but also of the dynamic mix properties. This is a good predictor of cycles of failure and thus would be a superior component of the deterioration model for asphalt mixtures containing polymer modified binders.

Acknowledgements:

Research reported in this paper was supported by COST CZ (LD) project of the Ministry of Education, youth and sports LD (No. LD15131).

7. References

- ASTM designation D7460-10. 2010. "Test Method for Determining Fatigue Failure of Compacted Asphalt Concrete Subjected to Repeated Flexural Bending." ASTM International. <http://www.astm.org/Standards/D7460.htm>.
- ČSN EN 12697-24+A1. 2007. "Bituminous Mixtures - Test Methods for Hot Mix Asphalt - Part 24: Resistance to Fatigue." Czech Office for Standards, Metrology and Testing.
- ČSN EN 13108-1. 2008. "Bituminous Mixtures - Material Specification - Part 1: Asphalt Concrete." Czech Office for Standards, Metrology and Testing.
- De La Roche, C. 2001. "Essai de Fatigue Sur Lex Enrobés Bitumineux. Résultats de L'expérience D'exactitude." *Revue Generale Des Routes (RGRA)*, no. 793 (March): 30–33.
- Fiedler, J, P Mondschein, and J Zak. 2013. "Notes on the Fatigue Properties of Asphalt Mixtures and the Pavement Design." In . Česká Budějovice: Sdružení pro výstavbu silnic.
- Freeme, Charles R., and Claude P. Marais. 1973. *Thin Bituminous Surfaces: Their Fatigue Behavior and Prediction*. National Institute for Road Research.
- Harvey, J. T., J. A. Deacon, A. A. Taybali, R. B. Leahy, and C. L. Monismith. 1997. "A Reiliability-Based Mix Design and Analysis for Mitigating Fatigue Distress." In . <http://trid.trb.org/view.aspx?id=501635>.
- Hopman, P.C., P.A.J.C. Kunst, and A. C. Pronk. 1989. "A Renewed Interpretation Method for Fatigue Measurement." In , 2:557–61. Madrid.
- Long, F. 2001. "Permanent Deformation of Asphalt Concrete Pavements" A Nonlinear Viscoelastic Approach to Mix Analyses and Design. University of California, Berkeley. <http://www.uctc.net/research/diss052.pdf>.
- Molenaar, A. 2007. "Prediction of Fatigue Cracking in Asphalt Pavements: Do We Follow the Right Approach?" *Transportation Research Record: Journal of the Transportation Research Board* 2001 (-1): 155–62. doi:10.3141/2001-17.
- Monismith, C. L. 2012. "Flexible Pavement Analysis and Design-A Half-Century of Achievement." In *Geotechnical Engineering State of the Art and Practice*, 187–220. American Society of Civil Engineers.
- Monismith, C.L, J. A. Deacon, and John Harvey. 2000. *WesTrack: Performance Models for Permanent Deformation and Fatigue*. Pavement research Center; Institute of Transportation Studies, University of California, Berkeley.
- Monismith, C.L, J. Harvey, B.W. Tsai, L. Fenella, and J. Signore. 2009. *Summary Report: The Phase 1 I-710 Freeway Rehabilitation Project: Initial Design (1999) to Performance after Five Years of Traffic (2009)*. University of California, Davis & Berkeley.
- Rowe, Geoffrey Michael, P. Blankenship, and T. Bennert. 2012. "Fatigue Assessment of Conventional and Highly Modified Asphalt Materials with ASTM and AASHTO Standard Specification." In *Four Point Bending - CRC Press Book*, 113–22. Davis, CA, USA.

- SHRP-A-404. 1994. Fatigue Response of Asphalt-Aggregate Mixes. Strategic Highway Research Program, National Research Council.
- Souliman, M.I., Waleed Zeiada, K. Kaloush, and M.S. Mamlouk. 2012. "Assessment of Different Flexure Fatigue Failure Analysis Methods to Estimate the Number of Cycles to Failure of Asphalt Mixtures." In *Four Point Bending - CRC Press Book*. Davis, CA, USA.
- Tangela, S.C.S. Rao, J. Craus, J. A. Deacon, and C.L. Monismith. 1990. Summary Report on Fatigue Response of Asphalt Mixtures. Strategic Highway Research Program, National Research Council.
- TP 170. 2004. "Navrhování Vozovek Pozemních Komunikací." Ministerstvo dopravy České republiky. <http://www.pjpk.cz/TP%20170.pdf>.
- Zak, J, and F Luxemburk. 2012. "Effect of Compaction and Winter Maintenance of Asphalt Mixtures on a Pavement Lifetime." In *GTZ Tuzla a GEO-EXPO 2012*, 965–72. Tuzla, Bosnia and Herzegovina: Faculty of Mining, Geology and Civil Engineering, University of Tuzla. doi:10.13140/RG.2.1.4455.4401.
- Zak, J, C. L. Monismith, and D Jarušková. 2014. "Consideration of Fatigue Resistance Tests Variability in Pavement Design Methodology." *International Journal of Pavement Engineering* 2014 (8): 1–6. doi:10.1080/10298436.2014.942858.
- Zak, J, J Valentin, and P Mondschein. 2013. "The Fatigue Behavior of Compacted Asphalt Mixtures Analysis-Contemporary Trends and Methods." *Road Review, Czech Road Society* 2013 (2): 31–34.

**2.4. Žák, J., Suda, J., Laboratory Design and Testing of Asphalt Mixtures
Dissipating Energy, 2019.**

Authors' contribution percentage:

50% Žák, J.,

50% Suda, J.

Laboratory Design and Testing of Asphalt Mixtures Dissipating Energy

Josef Zak^a, Jan Suda^b

^a Department of Construction Management and Economics, Faculty of Civil Engineering, Czech Technical University, Prague, Czech Republic

^b Department of Road Structures, Faculty of Civil Engineering, Czech Technical University, Prague, Czech Republic

Empirical methods of designing asphalt mixtures leave much room for improvement to fully utilize the potential of source materials. This approach has currently been replaced by a mechanistic-empirical approach, but only to a limited degree. In this regard, dissipating asphalt mixtures offer not only a new material, but a distinctly new approach to the design and grading of asphalt mixtures. These new dissipating asphalt mixtures have been developed for their greater resistance to the development of permanent deformations and cracks, as they dissipate the pressure from traffic and climatic influences to other forms of energy. Both conventional and innovative laboratory analyses of individual component properties are used for their development, including analyses of their mutual interactions within the asphalt mixture. This article presents the results as measured in a laboratory, including various dissipating asphalt mixtures comparison to conventionally produced mixtures.

1. Introduction

In essence, the development of an asphalt mixture is a multidisciplinary solution that must focus on the study of conditions to which this type of product is exposed (climatic impacts, traffic loading), as well as mechanical analyses considering their suitable use of asphalt mixtures dissipating energy within constructions, as well as their interaction with adjacent layers and the entire formation with the subgrade. The solution is further defined primarily by their development, composition of materials, mutual proportions, material structure and the chemical bonds between individual material-components used. Developing a material that meets these pre-defined criteria in a macro-scale and may also be effectively produced in the volumes required for the production of road infrastructure and further processed is equally important.

Currently, there is an effort on both a national and European level to innovate basic procedures regarding the design of flexible pavement. This is an effort searching for the most effective pavement in terms of lifespan, functionality and cost within the entire life cycle, including design, production, execution and pavement maintenance. The increase of road-transport volumes, expected increasing impact of pavement stress due to growing axle pressure, as along with new construction solutions for cargo vehicle tires, drives the effort to design cost-saving and quality pavement, as well as the need to innovate the basic construction materials of road construction.

An integral part of this process is the innovation of procedures regarding the characterization of these materials in order to address both the physical and mechanical essence of all basic processes and components affecting the behavior and overall transport-technology value of these pavements.

2. Methodology

From a certain perspective, dissipating asphalt mixtures are a new material, as well as a new approach to designing asphalt mixtures. Both conventional and innovative laboratory analyses of individual component properties, additives and admixtures, are used for the development and analysis of their mutual interactions, empirical and mechanical-physical properties.

New asphalt mixtures are developed with the goal of resisting the development of permanent deformation in the form of rut depth and cracks. The benefits of dissipating asphalt mixtures design is particularly seen as achieving maximum functional parameters of asphalt mixture source materials, including fillers, binders, additives and admixtures. This study also enhanced empirical (conventional) methodology of designing asphalt mixtures using mechanistic tests to achieve an optimal solution in monitored parameters. It was specifically found that the energy exerted by external powers (strain) was not stored

as deformation energy, but transformed, essentially dissipated to other forms of energy. Simultaneously, deformation is recoverable to the highest possible degree and the transition from a non-deformed to a deformed state is significantly lowered by internal viscosity resistances.

It is particularly important for the development of dissipating asphalt mixtures to use suitable equipment with the required parameters and a proper methodology for measuring and testing conditions to qualitatively ensure the best possible combinations of source materials. This approach allows design flexibility to meet the specific requirements regarding asphalt mixtures in pavement construction and operation conditions.

2.1. Methodology of design and evaluation

Eight asphalt binders from different producers offered in the were selected and evaluated for the development of the dissipating asphalt mixture (see Table 1). Six were polymer-modified asphalt binders, along with road asphalt, and an asphalt modified by crumb rubber with increased viscosity, produced by mixing road asphalt 50/70 with approximately 15% crumb rubber granulate in special mixing equipment annexed to the packing plant.

Gradation	Producer
50/70	1
45/80-65	2
45/80-75	1
45/80-75	3
45/80-75	2
45/80-85	1
25/55-80	4
CRMB 25/55-60 V	5

Table 1. Tested asphalt binders

The selected binders were evaluated both in view of their properties before and during aging and with consideration of their market price. The individual binders were evaluated using both empirical and functional tests, particularly emphasizing those changes caused over the course of asphalt binder aging. Short-term aging was simulated, covering changes occurring over the course of production, application

and compaction of the asphalt mixture, as well as long term aging intended to simulate the properties of the asphalt binders upon reaching the lifespan of the layer. Modified binder PmB 45/80-85 was selected from this research based on tested parameters. Comprehensive binders description can be found in [Dašek et al, 2018.].

The design and development of the dissipating asphalt mixture was performed for the wearing course [Žák et al. 2017] and base courses. However, this article extend this work and describes the design and evaluation of the asphalt mixture also for the base course.

The initial analyses were executed with three conventional (reference) mixtures for base courses - ACL 16S 50/70, ACL 22S 50/70 and ACL 22S PmB 25/55-65. The choice of type of the asphalt mixture with better dissipation energy arises from the evaluation of the reference mixtures, specifically from the evaluation of functional parameters. Coarse-grain versions better resist the development of permanent deformations [Žák et al. 2017]. Therefore, the ACL mixture with maximum grain $D = 22$ mm and qualitative class S was chosen on this basis. The aggregate structure of the individual mixtures was formed by crushed stone (granodiorite).

The subject of the project is not to mutually compare conventionally produced asphalt mixtures but rather to study the impact of the individual components of the mixtures on the resulting mechanical and physical properties. Thus to design a new mixture based on this knowledge, one with better energy dissipation.

It is not expected in these newly designed energy-dissipating asphalt mixtures that the material be cheaper in production costs compared with conventionally used materials, but that the new material will have significantly higher usability properties and better functional characteristics. This would decrease the overall life cycle costs of transport infrastructure reconstructions. The economic benefits of using such materials primarily lie with the maintenance providers and owners of transportation-infrastructure type constructions.

New asphalt mixtures are developed with the goal of maximizing the resistance of the asphalt layer and the entire formation (focused on wearing and base courses) against the development of permanent deformations (in the form of ruts) and faults caused by fatigue cracks (in form of cracks). It is important to select suitable measuring equipment with the required parameters, as well as the appropriate measuring methodology and testing conditions:

Resistance toward the development of permanent formations:

- Uniaxial shear test (50° C/60° C)

- Hamburg Wheel tracking test (50° C base course)

Fatigue resistance

- 4PB-PR (20°C)

Deformation parameters of asphalt mixtures:

- Stiffness modulus (the IT-CY method at 5° C, 15° C and 30° C)

3. Results and comparison

3.1. Optimization of asphalt mixtures

The choice of an asphalt mixture type with improved dissipation is based on an evaluation of the reference mixtures, specifically the evaluation of their mechanical parameters. Five versions of aggregate grading were created, to correspond to the grading curves according to the Czech national standard ČSN EN 13108-1. The aggregate comes from the same source as the aggregate for reference mixtures. Grading curves of the individual variants are shown in Figure 1.

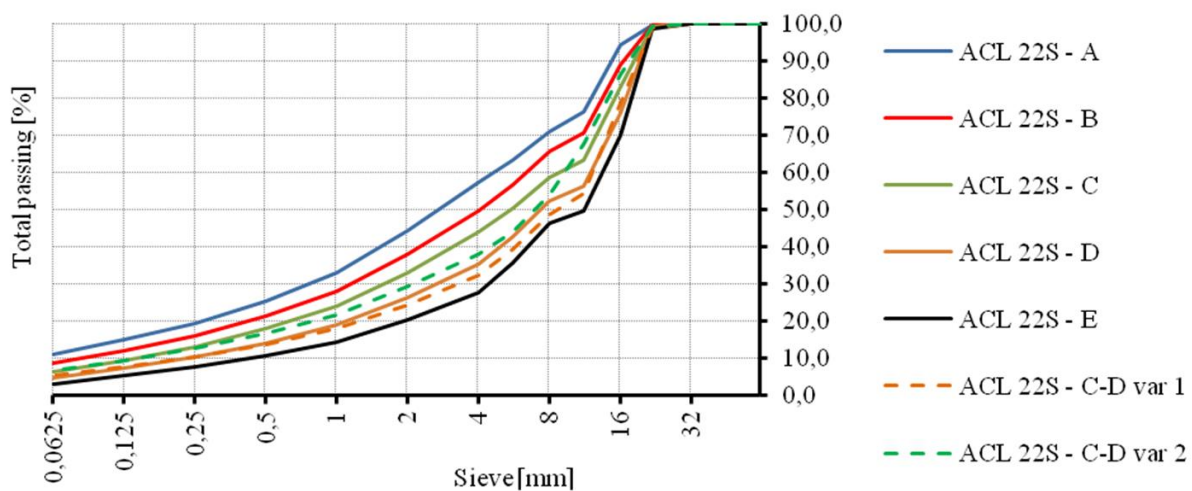


Figure 1. Coarseness of mixture composition ACL 22S - design

Basic volumetric parameters were measured for the mixtures produced, according to their respective technical specifications.

The individual asphalt mixture versions (A-D) were subsequently optimized to meet the requirements of the Czech national standard ČSN EN 13108-1. The parameters of the individual versions of mixtures designed are shown in Table 2.

ACL 22S PmB 45/80-85								
Version	A	B	C	C-D var 1	C-D var 2	D	E	ČSN EN 13108-1
Soluble binder content (% of weight)	4.1	4.1	4.1	4.2	4.5	4.2	4.2	min. 4.0
Void (%)	4.8	4.7	4.5	4.5	4.6	4.6	4.4	4.0-6.0
Aggregate air-void content (%)	14.6	14.5	14.2	14.6	15.2	14.6	14.4	
Soluble binder content (% of volume)	9.8	9.8	9.8	10.1	10.5	10.0	9.9	min. 9.2
Degree of air-void filled with asphalt (%)	67.1	67.4	68.7	69.1	69.4	68.2	69.1	

Table 2. Optimized version (A-E) of dissipating asphalt mixtures

The stiffness modulus was identified using cyclical stress in indirect tension. This parameter is an important deformation characteristic that is, along with the Poisson ratio, used for designing construction layers of pavements in the Czech Republic [J Zak et al. 2014]. The ability to dissipate greater stress impacts also grows with the increasing value of the stiffness modulus. In the case of the mixtures tested, temperatures of 5° C, 15° C and 30° C were chosen. This non-destructive test was performed on Marshall specimens on the UTM (Universal Testing Machine) in control-strain mode and defined straining pulses according to standard ČSN EN 12697- 26. The results are shown in Figure 2.

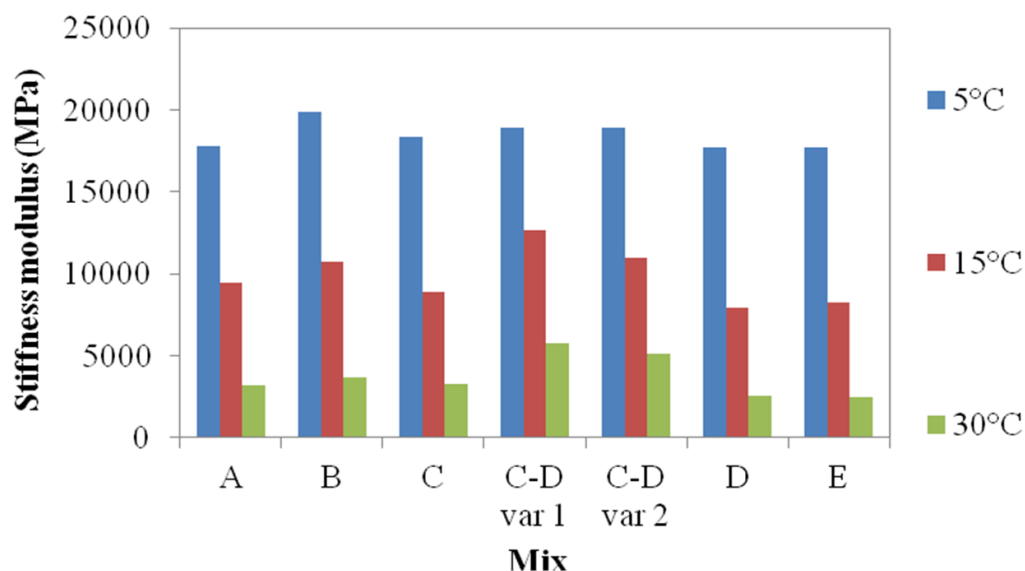


Figure 2. Stiffness modulus

All reference mixtures were tested for resistance against the development of permanent deformations according to Czech national standard ČSN EN 12697-22 on a Hamburg wheel tracking test in air

conditioned environment. This evaluated parameter defines the susceptibility of the asphalt mixture to permanent deformation, based on the depth of ruts formed caused by repeated pressure from a wheel at a defined temperature. The asphalt mixtures intended for testing were compacted in a lamellar compaction device. Above the specified parameters in the standard, the degree of compaction was required within the range of 99.0–101.0%. The test was performed at the temperature of 50° C and 60°C. The testing specimens were produced using the lamellar compaction device. The results are shown in Figure 3 and Table 2.

ACL 22S PmB 45/80-85		A	B	C	C-D var 1	C-D var 2	D	E	ČSN EN 13108-1 Requirements
Version									
Wheel driving test	WTS _{AIR} [%]	0.013	0.015	0.017	0.019	0.027	0.020	0.027	Are declared
	PRD _{AIR} [%]	1.0	1.5	1.4	1.3	1.6	1.5	1.4	Are declared

Table 2. Parameters of wheel tracking test

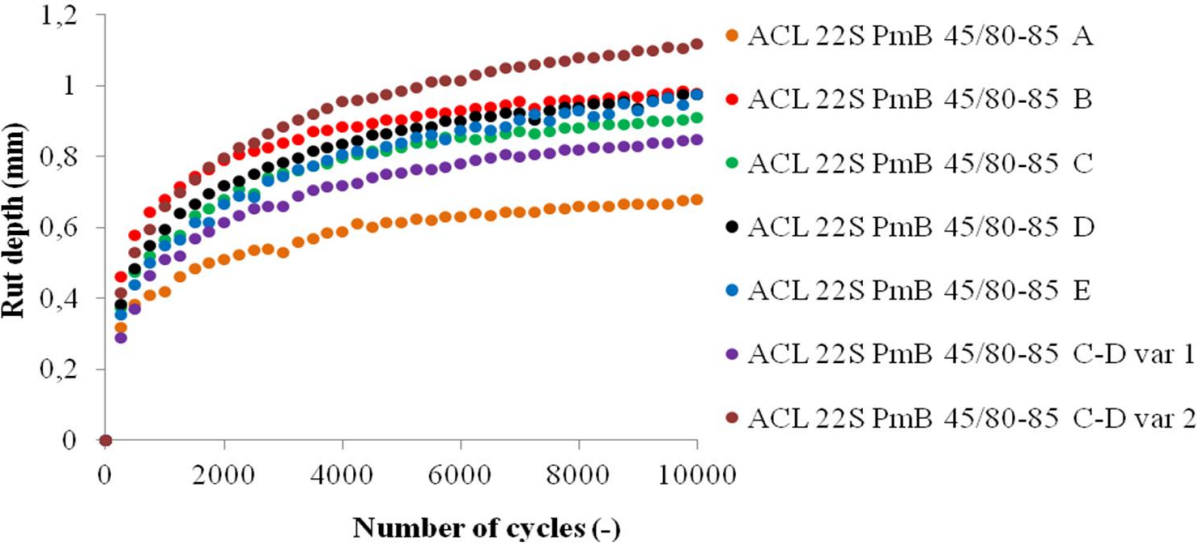


Figure 3. Record of development of permanent deformations in the wheel driving test

As is apparent from Table 2 and Figure 3, even with respect to the reference mixtures [Žák et al. 2017], the key comparison parameters of permanent deformations are not objectively better. Therefore, two additional mixtures (C-D) were designed at the same time, which combine the mixtures C and D in terms

of their grain and composition. As is apparent from Figure 3, the permanent deformation parameters improved.

Nonetheless, given the equipment and methodology used, these parameters are approaching a distinctive limit. In essence, all mixtures show very small permanent deformation, even after 10,000 cycles. Although mixture A came out best in terms of evaluating permanent deformations, it was excluded from further evaluation due to its large content of fine particles. In this regard, the Hamburg wheel tracking test is not able to distinguish the best asphalt mixture between superior asphalt mixtures. Among the results shown in Table 2 and Figures 2 and 3, versions C and C-D var 1 were further evaluated by monitoring their parameters of resistance against development of permanent deformations using the Uniaxial Shear Test and fatigue parameters. The 'dissipating asphalt mixture' for base courses would then be selected based on these two parameters.

3.2. Uniaxial shear test

The Uniaxial Shear Test (UST) is performed in standard laboratory equipment, Universal Testing Machine (UTM) with special assembly. In the case of this project, a Universal Testing Machine with a hydraulic unit was used.

Testing samples with a 150mm diameter were tested using a method of repeated creep following rest periods at two temperatures (50°C a 60°C). The test is done ate controlled stress mode. Both the the loading curve and deformation over the course of each cycle were measured. Mechanical parameters defining the sensitivity of the asphalt mixtures to permanent deformations were obtained through the evaluation of these cycles, the phase shifts between strain and resulting deformation, as well as the size of the elastic and plastic sheer strain. Examples of measured characteristics are included with the individual asphalt mixtures. The actual equipment and testing procedure are described in publication [Zak et al. 2016]. Utilization of in laboratory measured parameters and its relation to permanent deformation can be found in [Zak, Coleri, and Harvey 2018; Zak et al. 2017].



Figure 4. Universal Shear Tester

The parameters monitored that identify the resistance of asphalt mixtures against permanent deformations are those obtained from the UST. These include the shear modulus, accumulated permanent deformation regression coefficients, number of cycles to reach permanent shear strain, permanent shear strain at 5,000 and 10,000 cycles and increment of permanent shear strain. The testing bodies were produced using a gyratory compactor according to Czech national standard ČSN EN 12697-31 in the range of compaction 99.0-101.0%. The results are shown in Table 3 and Figure 4.

Shear parameters	ACL 22S – C		ACL 22S - C-D var 1	
	50° C	60° C	50° C	60° C
Shear modulus [MPa]	1,01E+05	7.08E+04	1.32E+05	7.76E+04
Regression of accumulated permanent deformation [-]				
parameter A	5.80E-03	5.63E-03	4.12E-03	4.62E-03
parameter B	8.21E-02	9.97E-02	9.47E-02	9.65E-02
Number of cycles to reach permanent shear strain [-]				
1% γ	3.25E+03	1.73E+02	9.45E+09	8.03E+08
3% γ	2.27E+07	2.01E+06	1.10E+14	6.15E+10
5% γ	4.26E+09	6.48E+08	8.56E+15	7.17E+12
Permanent shear strain				
at 5,000 cycles [m γ].	1.24E+01	1.49E+01	8.87E+00	1.19E+01
at 10,000 cycles [m γ].	1.29E+01	1.61E+01	9.24E+00	1.28E+01
Increment of permanent shear strain [m γ /10 ³]	9.10E-02	2.32E-01	7.49E-02	1.69E-01

Table 3. Shear parameters

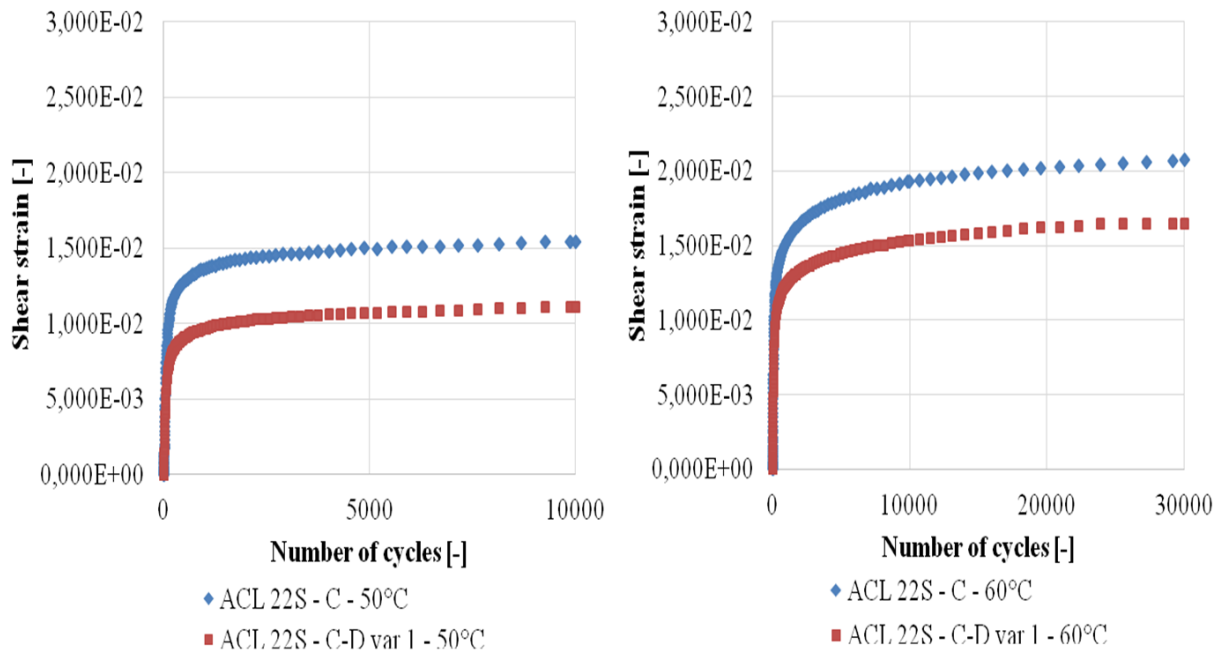


Figure 4. Accumulated shear strain (UST)

3.3. Fatigue

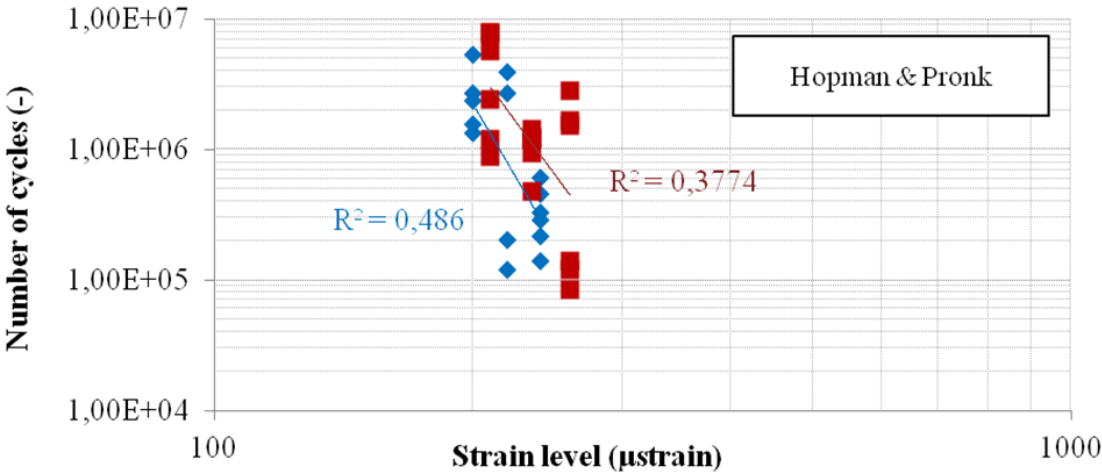
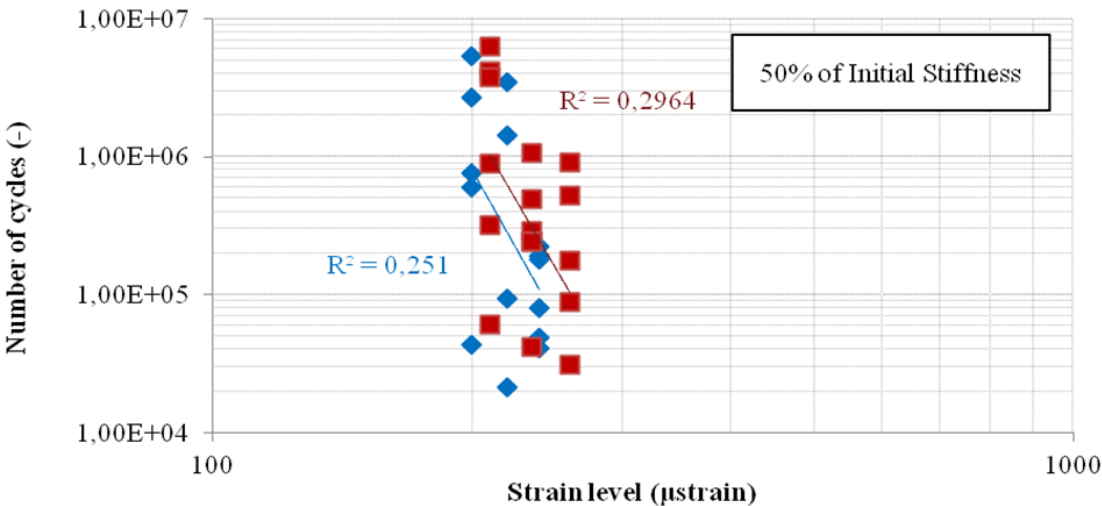
Fatigue is defined as the consequence of disruption of the internal structure of compacted asphalt mixture by repeated strain. It becomes apparent through a gradual decrease of the complex modulus in relation to the number of strain cycles. Therefore, it measures the lifespan of the asphalt mixture defined by the number of repeated strain cycles until the damage of the sample. In the case of a test in control strain mode, the disruption of the binding between strained particles of the material is registered as a decrease of loading resistances, where the loading resistance of the strained binding does not dissipate onto other binds.

The resistance of asphalt mixtures against deterioration is an important parameter of material that affects the life cycle of the pavement. The effect of the parameter characterizing resistance against fatigue is apparent from the established and valid design methodology for pavement construction, where it appears as an exponent of calculation relation, thus exponentially affecting the resulting value of the limited number of strain cycle repetitions. Therefore, the total value of fatigue parameters is significant both for the design and the life cycle of pavement construction.

The fatigue test is performed in the control strain mode on three levels in a manner ensuring that 50% decrease of the stiffness modulus occurring at the interval 10⁴-2.10⁶ cycles. The temperature is maintained at a constant value of 20±1° C. The frequency of strain was 30Hz according to Czech national standard ČSN EN 13108-20.

The testing samples were produced using a segmented compacting device with the compacting level ranging 99.0-101.0%. The specimens were subsequently cut to required testing bodies of defined sizes. The evaluation of fatigue parameters was conducted by multiple methods, specifically 50% decrease of the stiffness modulus according to Czech national standard ČSN EN 12697-24 and the dissipated energy ratio method (Hopman & Pronk) [Hopman et al. 1989, Žák et al. 2014, Boudabbous et al. 2013] and its modified method based on the proportional decrease of the complex modulus of stiffness - (Rowe) [Maggiore et al. 2014, Rowe et al. 1996, Rowe et al. 2000].

These two methods are based on the same idea of dividing the results of the fatigue tests performed in the mode of managed strain in the form of a ratio of the dissipated energy into three phases and defining the values of the cycles (N1) on the border of phase II and III as material fatigue resistance. This has been amended by simple regression analysis to obtain not subjective resistances (N1 values) of all test results [Zak, Valentin, a Mondschein 2013]. The results are shown in Figures 5 and 6.



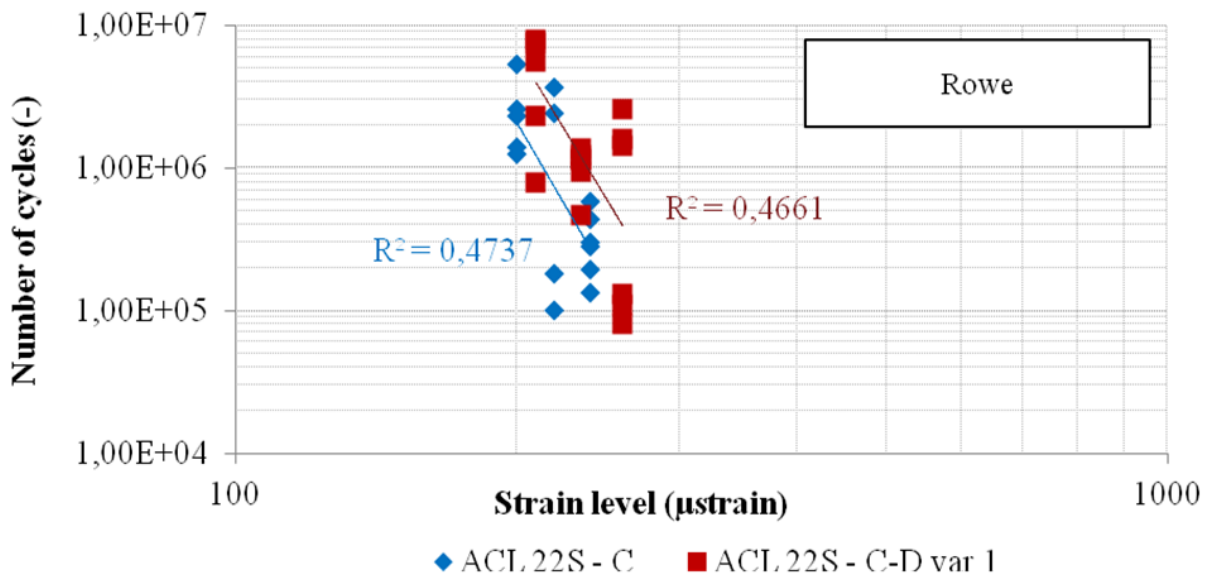


Figure 6. Evaluation of fatigue resistance

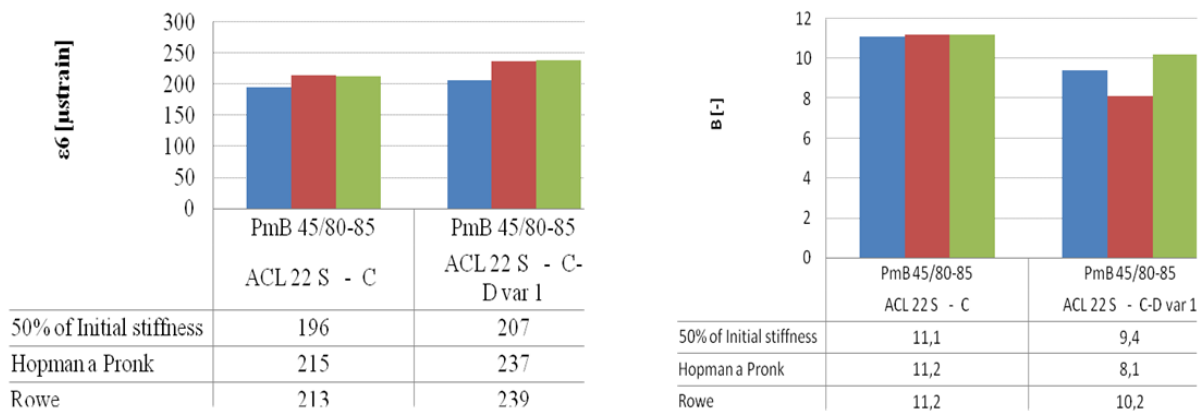


Figure 7. Fatigue parameters based on the Wöhler Curve

Figure 6 indicates the comparison of the individual methods at strain level corresponding to 10^6 cycles based on fatigue curve [Žák et al. 2014]. This proves the hypothesis that fatigue resistance of asphalt mixtures established through the method of energy dissipation is higher than the resistance established through the method of a 50% decrease of stiffness modulus. This phenomenon is more particularly apparent in modified asphalt binders.

3.4. Schematic comparison

The subject of this project is not to compare conventionally produced asphalt mixtures to one another, but to study the impacts of the individual components of the mixtures on the resulting mechanical and physical properties and, on this basis, to design a new mixture with improved energy dissipation. A further goal is

to broaden the options for maximizing the functional properties of asphalt mixtures, using more precise processes in evaluation and more precise testing procedures with greater distinguishing capabilities.

The parameters monitored are verified by comparison with conventionally produced mixtures. This comparison provides both information about whether the dissipating mixture was optimally designed, as well as an insight into the impact of the source material on the resulting parameters of the asphalt mixtures.

Figure 4 and Table 3 show the comparison of basic volumetric and grading properties. Figure 6 indicates the comparison of functional parameters of the newly designed dissipating asphalt mixture ACL 22S - C-D var 1 with reference mixtures.

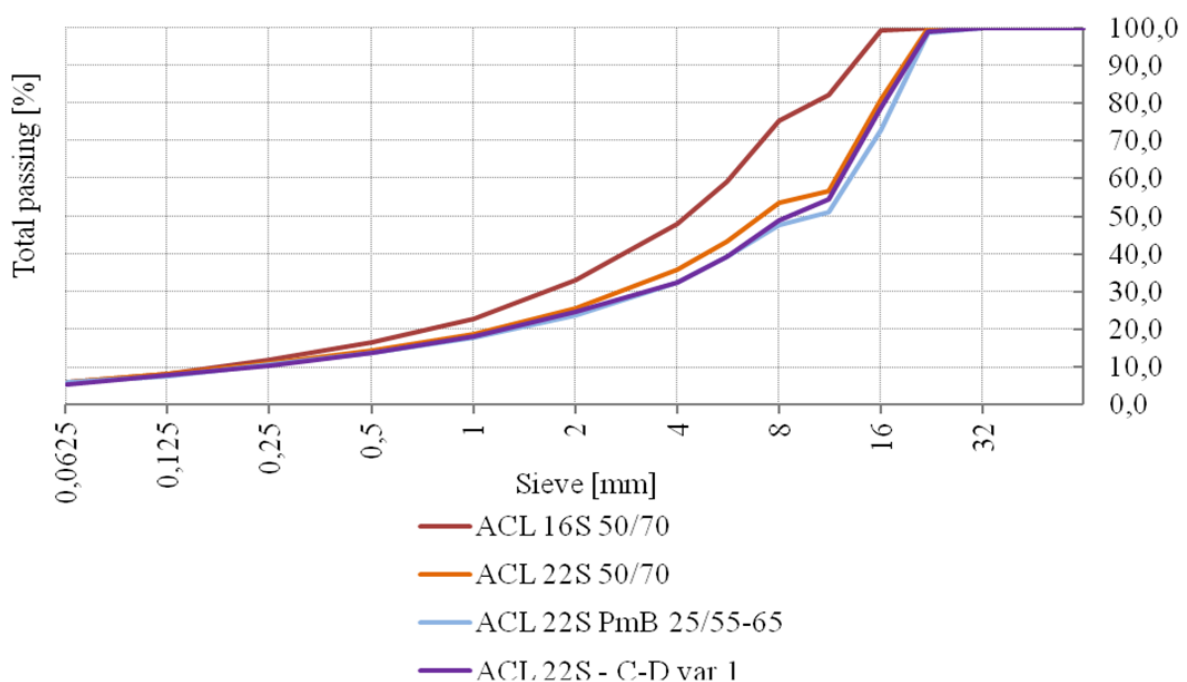
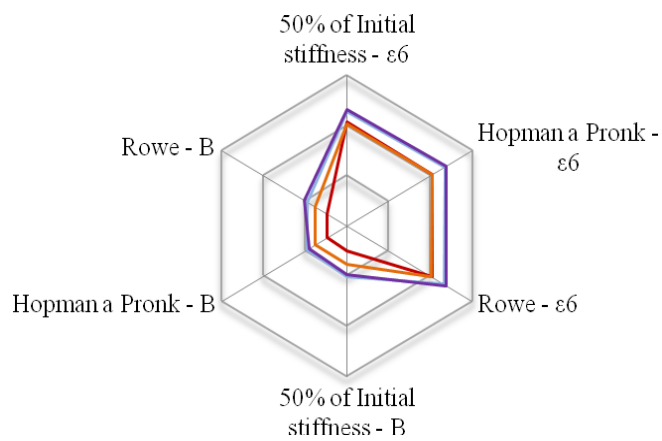
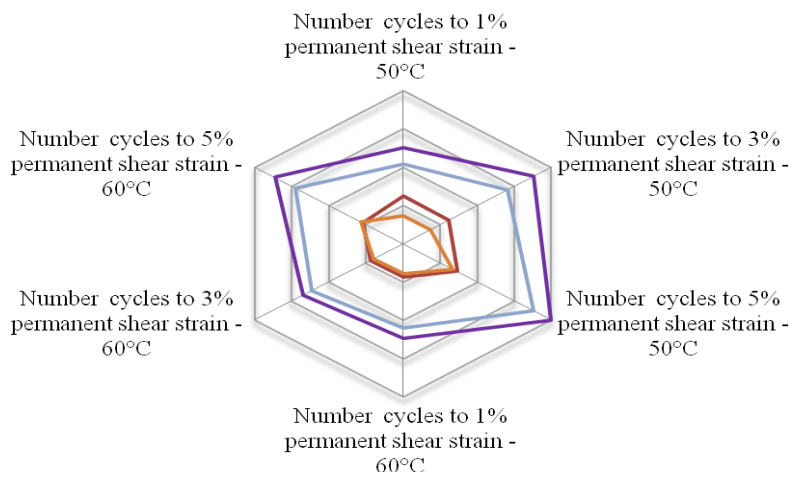
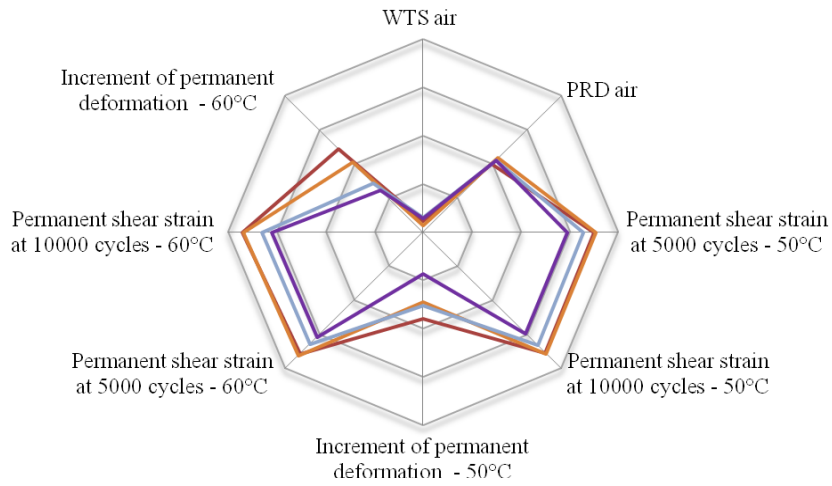


Figure 5. Grain composition of asphalt mixtures

Mixture		ACL 16S 50/70	ACL 22S 50/70	ACL 22S PmB 25/55-65	ACL 22S - C-D var 1 PmB 45/80-85
Binding					
Air void	[%]	3.1	4.6	3.4	4.5
Soluble binder content	[%]	5.3	4.3	4.0	4.2
Aggregate air-void content	[%]	15.6	14.8	12.9	14.6
Binder content in the mixture	[volume %]	12.5	10.2	9.4	10.1
Degree of air-void filled with asphalt	[%]	80.0	68.8	73.2	69.1

Table 5. Comparison – volumetric parameters of asphalt mixtures



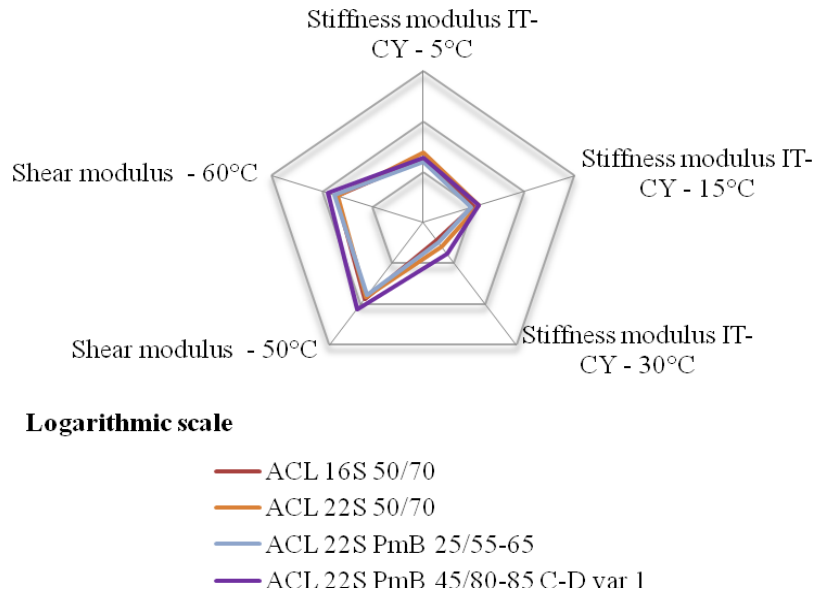


Figure 6. Schematic comparison of the designed dissipating asphalt mixture and reference mixtures

As is clearly apparent from the above results, compared to other evaluated reference mixtures, the mixture identified as ACL 22S PmB 45/85-80 - C-D var 1 shows qualitatively very good resistance against permanent deformations and fatigue resistance. The above methodology of designing a mixture with both empirical and mechanical tests enabled designing a qualitatively higher-performance asphalt mixture from the perspective of the monitored parameters, while also maximizing parameters within the used source materials regarding permanent deformation and fatigue cycles. The aspect of comparing studied mixtures within optimization using standardized tests (Wheel tracking test and the Uniaxial shear test) must be also highlighted.

4. Conclusions

This article proves the possibilities for maximizing the functional properties of asphalt mixtures by using more precise evaluating and testing procedures with higher differentiation capabilities.

The benefits of the functional design of dissipating asphalt mixtures can be seen particularly in attaining maximum functional parameters of asphalt mixtures with regard to the source materials used - fillers, binders, additives and admixtures. This research also developed unique combination of mechanical and empirical test methods for asphalt mixture design to reach optimal designs within the parameters monitored. Using such procedures enabled the design of a mixture with a significantly greater resistance against permanent deformations at the same time with keeping appropriate values of other properties.

The disadvantages of developing dissipating asphalt mixtures in regular industry application may be particularly characterized as somewhat higher requirements regarding laboratory equipment and testing devices, as well as the actual time requirements and testing.

4.1. Acknowledgments

This paper was elaborated within the research project No. FV10526 in the program TRIO of the Ministry of Industry and Trade of the Czech Republic.

5. References

- Boudabbous M., Millien A., Petit C., Neji J. 2013. Energy approach for the fatigue of thermoviscoelastic materials: Application to asphalt materials in pavement surface layers. In *International Journal of Fatigue*, Volume 47, Pages 308-318, ISSN 0142-1123.
- Dašek O., Coufalík, P., Koudelka T., Hýzl P., Žák J., Suda J., Špaček P., Hegr Z. 2018. Comparison of asphalt binders properties, submitted in *Silniční obzor*, ISSN 0322-7154.
- Hopman P. C., Kunst P. A. J. C., Pronk A. C. 1989. A Renewed Interpretation Method for Fatigue Measurement. presented on 4th Eurobitume Symposium, Madrid, 1989, 2, 557–561.
- Maggiore C., Airey G., Marsac P. 2014. A dissipated energy comparison to evaluate fatigue resistance using 2-point bending. *Journal of Traffic and Transportation Engineering (English Edition)*, Volume 1, Issue 1, February 2014, 49-54, ISSN 2095-7564.
- Rowe G. M. 1996. Application of the dissipated energy concept to fatigue cracking in asphalt pavements.
- Rowe G.M.; Bouldin M. G. 2000. Improved techniques to evaluate the fatigue resistance of asphaltic mixtures, 2nd Eurasphalt & Eurobitume Congress Barcelona, pp. 754-763.
- Zak J., C. L. Monismith, and D. Jarušková. 2014. Consideration of Fatigue Resistance Tests Variability in Pavement Design Methodology. *International Journal of Pavement Engineering*, vol. 2014, no. 8, pp. 1–6.
- Zak J., Suda J., Mondschein P., Vacin O., Stoklasek S. 2015. Asphalt Binder Modification Technologies and Its Influence on Mixture Durability with Regard to Fatigue Resistance. presented on 3rd Annual international Conference on Architecture and Civil Engineering, Singapore.
- Zak, J., Suda, J., Dasek, O. and Spacek, P. 2017. Asphalt Mixtures that Dissipate Energy. Athens: ATINER'S Conference Paper Series, No: CIV2017-2269.
- Zak, J., Stastna, J., Vavricka, J., Milackova, K., Kasek, L. and Zanzotto, L.. 2014. „Poisson's Ratio of Hot Asphalt Mixtures Determined by Relaxation and Small Amplitude Oscillation Tests". *Journal of Testing and Evaluation* 43 (2). <https://doi.org/DOI: 10.1520/JTE20130325>.
- Zak, J, E Coleri, and J. T. Harvey. 2018. „Incremental Rutting Simulation with Asphalt Mixture Shear Properties". In *Solving Pavement and Construction Materials Problems with Innovative and Cutting-edge Technologies*, 13–24. Hangzhou, China: Springer, Cham. https://doi.org/10.1007/978-3-319-95792-0_2.
- Zak, J, E Coleri, J. Stastna, and J. T. Harvey. 2017. „Accumulated Equilibrium Compliance as a Rutting Susceptibility Parameter". Submitted to *Sustainable Civil Engineering Journal*.
- Zak, J., C. L. Monismith, E Coleri, a J. T. Harvey. 2016. „Uniaxial Shear Tester - Test Method to Determine Shear Properties of Asphalt Mixtures". *Association of Asphalt Paving Technologists AAPT Journal* 85.
- Zak, J., J Valentin, P Mondschein. 2013. „Analýza únavového chování asfaltových hutněných směsí – současné trendy a metody". *Silniční obzor, Česká silniční společnost* 2013 (2): 31–34.

2.5. Žák, J., Coleri, E., Harvey, J., Incremental rutting prediction with asphalt mixture shear properties, 2018.

Authors' contribution percentage:

80% Žák, J.,

10% Coleri, E.,

10% Harvey, J.

Incremental rutting prediction with asphalt mixture shear properties

Josef Zaka, Erdem Colerib, John Harveyc

a CTU in Prague, Faculty of Civil Engineering, Thakurova 7, Prague, Czech Republic. E-mail: josef.zak@fsv.cvut.cz.

b Oregon State University, School of Civil and Construction Engineering, 101 Kearney Hall, Corvallis, OR, 97331, USA.

c *University of California Pavement Research Center, Department of Civil and Environmental Engineering, University of California, Davis, Davis, CA, 95616, USA.*

It is a purpose of the article to present the correlation between two devices developed to measure shear properties of asphalt mixtures. The shear properties are measured by well-known Superpave Shear Tester and developed Uniaxial Shear Tester. The material characteristics are determined from two test methodologies. Shear small amplitude oscillation test, known also as a frequency sweep shear test and repeated shear tests are utilized. The properties, characterizing the complex moduli, are determined with the use of sigmoidal function used in Mechanistic Empirical Pavement Design Guide (Hallin 2004). The Gamma function (Deacon et al. 2002) is used to determine the properties from the repetitive shear tests. The CalME program is utilized to perform the incremental recursive simulations under three selected climate conditions, two levels of traffic loading and two pavement structures. On the basis of simulated data comparison was found the optimal correlation coefficient for UST device. Calculated p-value of Welch-modified two sample t-test for the distributions of predicted rutting from UST and SST test result suggests that surface rutting predicted by using UST and SST test results are statistically equal with high p-values. Thus, the data from the proposed UST test equipment can be used for mechanistic-empirical (ME) pavement design and will provide rutting predictions that are statistically equal to the predictions for SST. The predicted rut depth was also found to be well correlated with accumulated equilibrium compliance.

1. Introduction

The increasing amount of heavy truck traffic together with increasing axle weights started to increase the demand for pavement structures with higher performance. Especially the heavy truck loading is a cause of pavement deterioration considering the pavement rutting. Flexible pavement permanent deformations in form of rutting reduce the quality of transportation and form safety risks. Surface rutting prevents the water from draining out of the pavement surface, standing water reduces the friction between pavement surface and the wheel, thus prolongs the breaking distance and enhances the risk of aquaplaning. Particularly on motorways and expressways, ruts can cause loss of driver's control over a vehicle at higher speeds during the overtaking. Thus the engineer's objective is to reduce permanent deformation by better predicting and monitoring the pavement rutting and taking the appropriate timely actions, such as reconstruction or rehabilitation, if needed.

Nowadays, an engineer has the option to choose from different test methodologies that suggest the link between the laboratory measured properties and field performance in regard of rutting (Von Quintus et al. 2012). The herein presented study is dealing with those test methods that has been used to develop transfer functions, and their effectiveness has been proven over the years of use by numerous researchers.

The permanent deformation response of asphalt mixtures was broadly studied as part of SHRP and reported in (Monismith et al. 1994). One of the research outcomes was the development of the Superpave Shear Tester (SST). The performance models, also referred as transfer functions, were further developed as part of WesTrack project (Monismith, Deacon, and Harvey 2000). Further the Superpave Shear Tester became a tool for mix design and The Repeated Shear Test at Constant Height (RSST-CH) is judged to be preferred method for analyzing the permanent deformations of asphalt mixtures (Harvey et al. 2002).

In the NCHRP 719 report, (Von Quintus et al. 2012), summarized transfer functions and recalibrated them using a broad database composed of full-scale test sections and results from Heavy Vehicle Simulators. The WesTrack transfer function was proved to be correlating well with asphalt mixtures' in situ rutting performance and implemented into MEPDG design program.

The Uniaxial Shear Tester was developed as part of the cooperation between University of California Pavement Research Center and Czech Technical University in Prague. The aim of the research was to develop a testing device that would allow to perform shear test in Universal Testing Machines (UTM), known also as Nottingham Asphalt Testers (NAT), so that the laboratories equipped with such a test device will be able to measure shear properties of asphalt mixtures (Zak, Monismith, et al. 2015). At the same time an innovative approach was proposed to calculate the accumulated equilibrium compliance as a linear viscoelastic parameter characterizing the long-life mixture rutting performance (Zak, Coleri, et al. 2015).

The aim of this study is to predict pavement rutting performance using CalME software (an ME analysis and design program for new flexible pavements and rehabilitation) and asphalt mixture shear properties measured by SST and UST test methods. The goal is to assess whether the properties measured by these test methods are able to simulate statistically equal rut depth predictions through the use of WesTrack transfer functions and a shear based incremental-recursive procedure.

It is a purpose of the article to present these correlations between two devices developed to measure shear properties of asphalt mixtures. Further the article proves that the data from the UST test equipment can be used for mechanistic-empirical (ME) pavement design and will provide rutting predictions that are statistically equal to the predictions for SST. The predicted rut depth was also found to be well correlated with accumulated equilibrium compliance.

2. Experiments

2.1. Material specification

The simulations were performed with 3 asphalt mixtures. To make easier the orientation each asphalt mixture was denoted with number. Hot mix #1 contains 4.8% neat asphalt binder PG64-10 and 25% reclaimed asphalt, the nominal maximum aggregate size was 3/4". The mixture was manufactured in the asphalt plant and small batches were taken from the construction site. From the mixture were prepared cylindrical specimens in Gyrotory compactor, preferably was produced cylinder 135mm high and 150mm in diameter. The specimen was cut from the cylinder by double blade saw to obtain parallel sides. Further was the testing procedure in accordance with (AASHTO T 320-07 2011) in case of SST. The description of sample preparation for testing

in UST can be found in (Zak, Monismith, et al. 2016). Mix #2 nominal maximum aggregate size is also 3/4", it contains 15% of reclaimed asphalt and most importantly high polymer modified asphalt binder PG64-28. Batches of mix #2 were also taken from the construction site. Blocks of Mix #3 were cut from the UCPRC, Davis test section, from the blocks were drilled and cut the cylindrical samples. Then the samples were prepared as mentioned above. The mix #3 is 1/2in. gap-graded rubberized hot-mix, it contains 7% asphalt binder PG64-10 without any reclaimed asphalt. The grading of aggregates is presented in the Table 1.

2.2. Determination of properties from laboratory measured data

To obtain complete characteristics for rut depth predictions described in the following paragraphs were performed two tests. First the small amplitude oscillation tests were performed, known also as the frequency sweep shear tests. Data of the complex shear moduli at temperature at 3, 15, 30, 45 and 60°C were selected and a data fit was performed to the measured frequencies in the range from 0.01Hz to 10Hz. The dynamic moduli and their dependence on temperature and test frequency are described in form of sigmoidal function described by equation 1. The equation 1 defines the master curve as was presented in mechanistic-pavement design guide (MEPDG) (Hallin 2004) where T_r , reduced time of loading at the reference temperature is described as presented in equation 2 ("CalME Manual" 2011; Hallin 2004).

$$\log(E^*) = \delta + \gamma \frac{\alpha}{1 + \exp [\beta + \gamma * \log(T_r)]} \quad (1)$$

Where E is the tensile modulus in MPa and α, β, γ , and δ are the determined constants. The tensile modulus is from measured complex shear modulus converted through the well-known relation from elastic theory, $E=2G*(1+v)$, where G is a measured shear modulus and v is a Poisson's ratio.

$$T_r = lt * \left(\frac{visc_{ref}}{visc} \right)^{aT} \quad (2)$$

Here lt is a loading time, $visc_{ref}$ is a binder viscosity at reference temperature, $visc$ is a binder viscosity at the present temperature and aT is a shift factor. Model parameters were determined

in excel, when the Residual Sum of Squares (RSS) fit was performed using the solver. The measured properties were derived from five replicates.

Secondly the Repeated Shear Tests (RST) were performed. Prolong version of standard repeated shear test was performed when all the samples were loaded with 30 000 of repeated cycles. RST were run always on five replicates at 50°C. Method developed by (Deacon et al. 2002) was utilized to predict rutting of the asphalt layer. The laboratory data were fitted using the Gamma function:

$$y_p = A + \alpha * \left[1 - \exp\left(\frac{-\ln(N)}{\gamma}\right) * \left(1 + \frac{\ln(N)}{\gamma}\right) \right] * \exp\left(\frac{\beta + \tau}{\tau_{ref}}\right) \quad (3)$$

Where N is a number of cycles, A, α , β , γ and δ are model parameters, τ is a shear stress, τ_{ref} is a reference shear stress. The final rut depth increment was calculated from the following equation ("CalME Manual" 2011; Deacon et al. 2002):

$$rd_i = K * h_i * y_p \quad (4)$$

Here rd_i is rut depth increment, K is a calibration factor and y_p is a plastic shear strain from equation 3. The models parameters were obtained performing the RSS in excel, when the optimum value was found with the help of solver. For the selected materials the measured properties reach its steady state trend in between first 100 to 300 cycles during Uniaxial Repeated Shear Test (URST) (Zak, Monismith, et al. 2016). As the test procedure is compound from 30 000 cycles, the performed RSS analysis tends to neglect the first loadings. In this regard a weight function was substituted into regression to give more weight in RSS to first set of 300 cycles. The weighting function (equation 5) with parameters a=6 and b=-0.01 was used. The repeated shear tests were performed always with five replicates.

$$Weight = \exp [a + b * N * \ln(N)] \quad (5)$$

3. Incremental recursive simulation

3.1. Specification of pavements and environmental conditions

The factorial of rut depths with 3 climate regions was run in CalME. The Inland Valley, Low Mountain and High Desert climate was chosen as a set expressing broad range of temperatures. Two traffic levels were selected. First denoted as TI10 where the pavement was loaded with 390,000 cycles in first year. The second traffic level was chosen to be TI 14 with 6,250,000 axles in pavement first year in service. The growth rate was selected to be 5% annually for both traffic levels. To bear such a loading were selected two pavement structures. The pavement structure was selected in the view of minimization of other distresses except the rutting. So the thick asphalt mixture layer on the thick unbound stiff aggregate base was selected. Selected pavement structures are in FIG. 1.

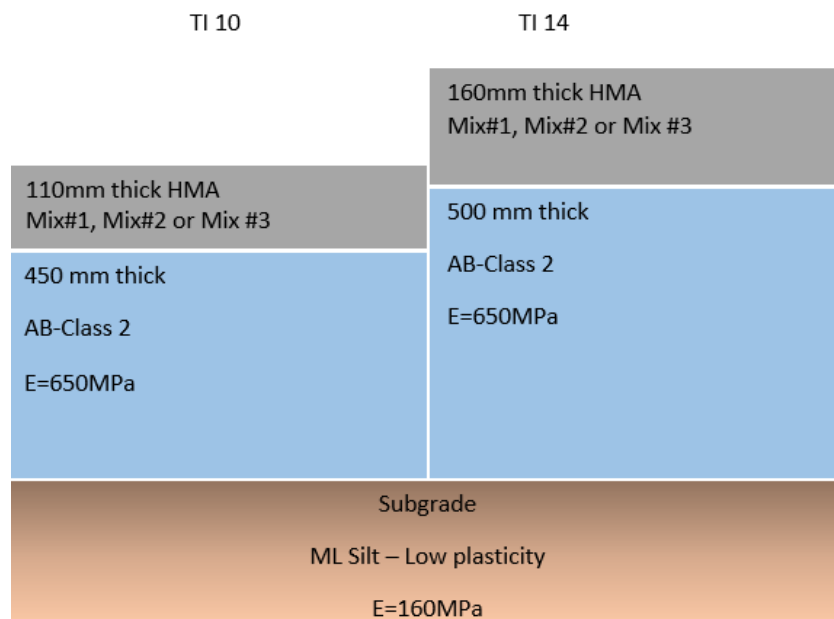


Figure 1. Illustration of selected pavement structures

3.2. Incremental recursive simulation

In this approach, the pavement is assumed to behave as a multilayer elastic system. The idealization of a specific asphalt pavement permanent response was presented in (Deacon et al. 2002). The principle is based on the calculation of rut depth estimate developed with traffic

at depth of 50mm below the outside edge of tire. The permanent shear strain in the asphalt layers is assumed to accumulate according to the principle relating the accumulated elastic shear strain measured in laboratory to permanent strain in pavement developed in (Deacon et al. 2002). The computer program known as CalME has been used to perform the predictions (Ullidtz et al. 2010).

3.3. Uniaxial Shear Tester calibration

The term K is a parameter that relates RD to plastic strain. The K parameter was first used during the WesTrack project (Monismith, Deacon, and Harvey 2000). Parameter K ranges from about 5.5 for a 150-mm layer to 10 for a 305-mm thick asphalt concrete layer (Deacon et al. 2002). Based on correlation between predicted RD was calculated parameter that relates the shear properties measured by UST to predicted plastic strain in pavements. The RSS was computed for each rut depth predictions at every condition and from these the average RSS was computed. Based on the RSS value minimization was found that the optimal KUST parameter should be selected equal to 0.63 of its K equivalent ($KUST = K \cdot 0.63$).

The numerically predicted rutting occurred during first 14 days was more than 50% of total rutting after 40 years in some cases. The initial rutting depends highly on the A parameter of model presented in equation 3. However the A parameter can be selected widely if the other model parameters are changed accordingly without a significant effect on total RSS between model and experimentally measured data. In view of this the rutting predicted for first 14 days was omitted. As the reference point was used the first calculated point. This trimming neglected rutting in first 0.002% of total calculated pavement lifetime.

If the correlation coefficient KUST was selected equal to 0.63 of its K equivalent and first 14 days of rutting was omitted then the predicted rutting is as presented in FIG. 2 and 3. The typical trend of calculated rut depths was selected for two climate conditions, High Desert and Low Mountain. As can be seen from both figures the predicted rutting correlates well.

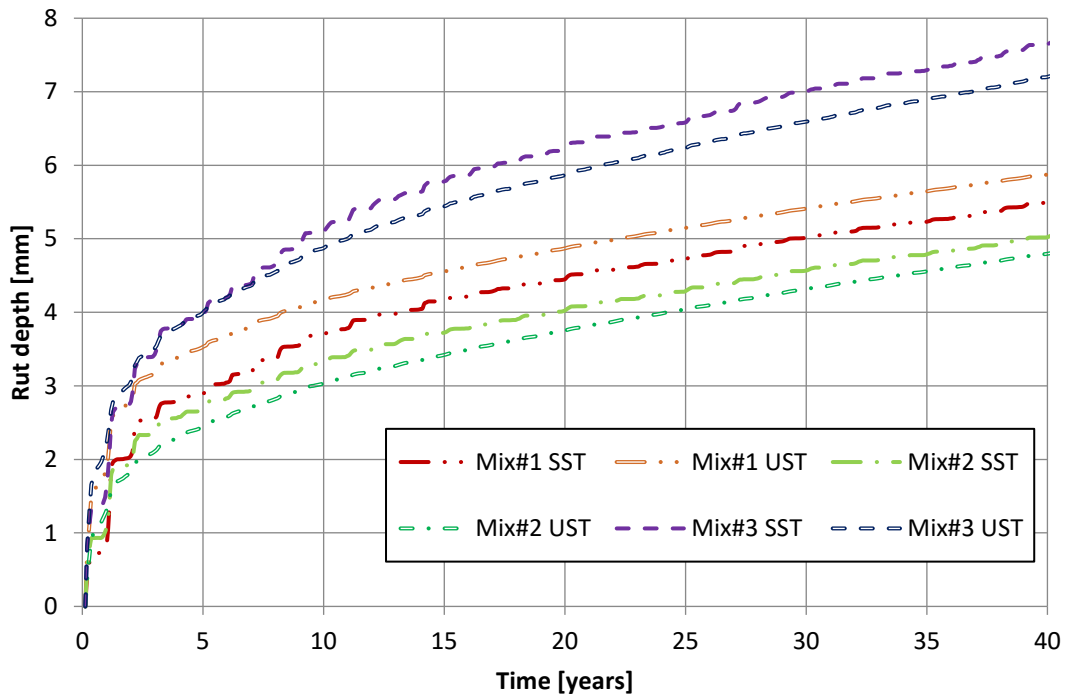


Figure 2. Rut depth prediction, TI 14, High Desert climate

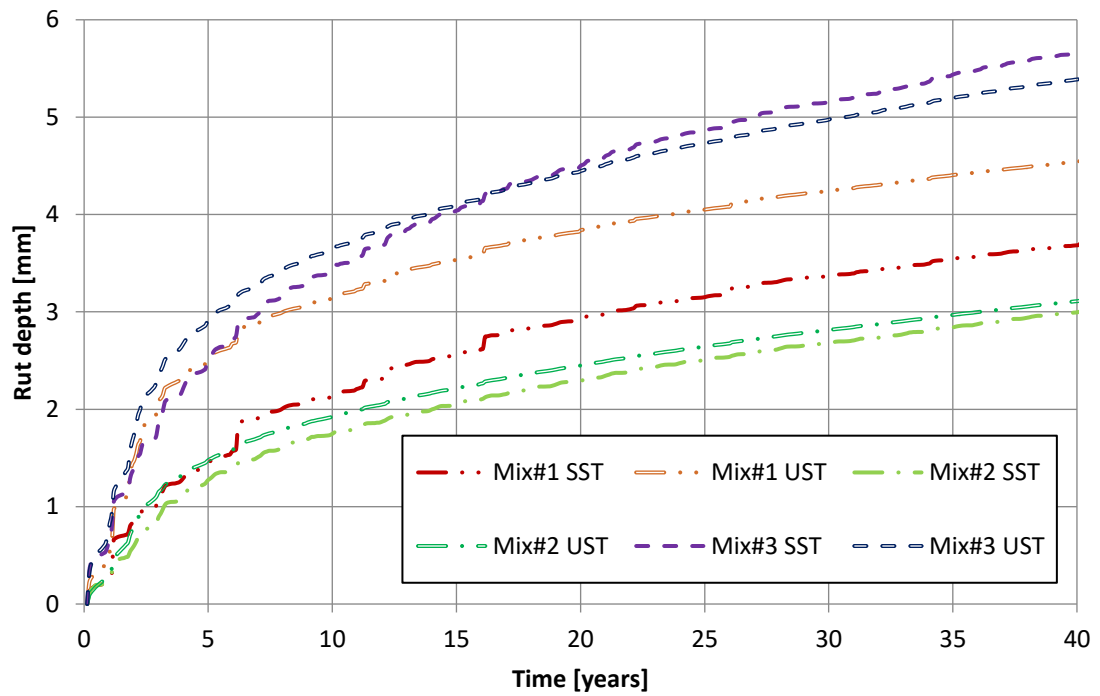


Figure 3. Rut depth prediction, TI 10, Low Mountain climate

3.4. Welch-modified two sample t-test

In order to determine the statistical significance of the CalME predicted rut depth differences for UST and SST results, Welch-modified two sample t-test (Insightful 2001) is used. This statistical test is recommended to be used for evaluating small datasets (Ruxton 2006) and assumes unequal dataset variances. F_1 and F_2 are two distributions for predicted rut depths (from UST and SST test results) at 10th, 20th, and 40th years for the climate regions and traffic levels of this study, the possible hypotheses and alternatives concerning these distributions are:

$$H_0: F_1(x) = F_2(x)$$

$$H_A: F_1(x) \neq F_2(x)$$

(6)

Decision rule: Reject H_0 if p-value < 0.10; Fail to reject H_0 if p-value \geq 0.10

Calculated p-value for the distributions of predicted rutting from UST and SST test results for years 10, 20, and 40 are 0.70, 0.95, and 0.91, respectively. This result suggests that surface rutting predicted by using UST and SST test results are statistically equal with high p-values. Thus, the data from the proposed UST test equipment can be used for mechanistic-empirical (ME) pavement design and will provide rutting predictions that are statistically equal to the predictions for SST.

Provided test results proves the correlation of incremental rutting simulation over 40 years. Which is more than the flexible pavement (wearing course especially) would last in real where the design period of the flexible pavements range from 20 to 30 years at best.

4. Correlation between accumulated equilibrium compliance and predicted rut depth

The procedure describing the calculation of Accumulated Equilibrium Compliance (AEC), J_e , acc, was proposed in (Zak, Coleri, et al. 2016). The accumulated creep compliance is calculated with the help of linear viscoelastic theory. The arbitrary rheological model can be used to calculate the retardation spectra. In view of the generally known principles that long-time

processes are revealed in detail in the retardation spectrum and as the equilibrium compliance is obtained by integration over a discrete retardation spectrum it is suggest that such a material parameter express the long-life asphalt mixture performance regard to permanent deformation potential.

In this study was used 4-unit standard Kelvin-Voigt model, as was proposed in (Zak, Coleri, et al. 2015). The interval fitting procedure was utilized and the AECs were calculated for each asphalt mixture. The AEC values can be found in Table 2 in the appendix. If the linear regression between AEC and predicted rut depths is performed, then the correlation coefficient between these two variables may be expressed. The calculated correlation coefficients are listed in the Table 3 in the appendix. The value represents correlation between six determined AECs from repeated shear tests in laboratory and six predicted rut depths at selected pavement during service period, loadings and climate conditions. The dependence on these conditions is presented in the FIG. 4.

The average correlation coefficient from the selected climate conditions, pavement structures and loadings after 10years in service is -0.81. Consequently the correlation coefficient is equal to -0.81 after 20 years and -0.79 after 40 years in service. The negative correlation coefficient is evident, the higher AEC means less rutting potential. The overall average correlation coefficient is -0.8. Thus from the results of simulated rut depths and determined ACE may be concluded that the AEC is a suitable criterion for the asphalt mixture permanent deformation susceptibility.

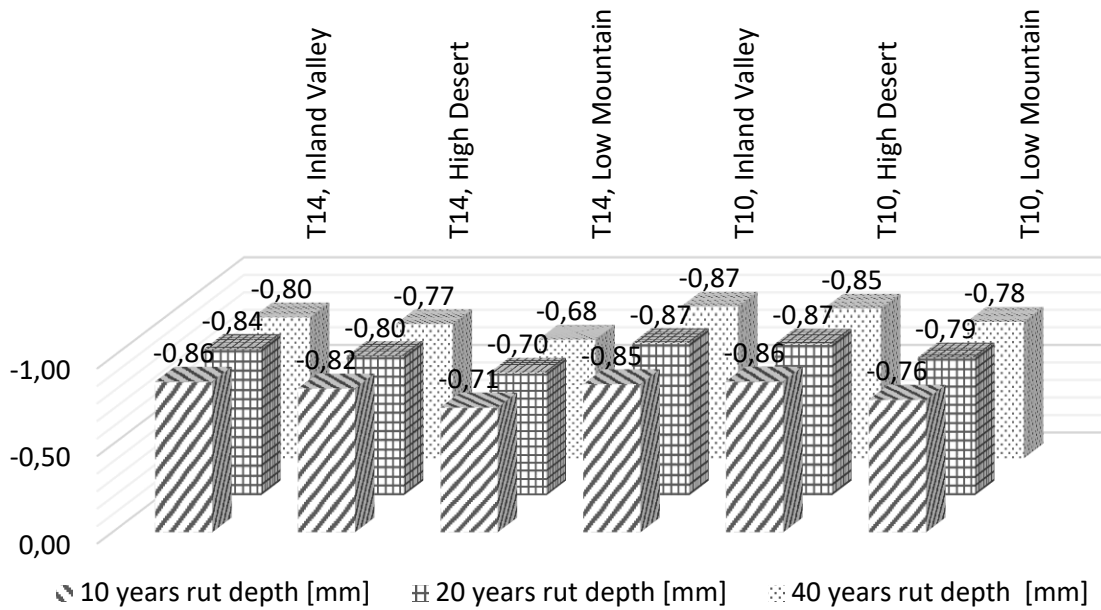


Figure 4. Correlation between accumulated equilibrium compliance and simulated rut depth.

5. Conclusions

It was purpose of this paper to compare the ability to determine the shear properties of newly developed UST device to currently used SST device through the pavement rutting predictions.

The incremental rutting predictions in CalME program were utilized for this purpose and the rut depth predictions were simulated for three asphalt mixtures in three climate conditions and with two selected traffic loading.

It can be concluded that the trends of predicted rut depths from properties determined from tests performed with UST and SST correlate well.

Calculated p-value for the distributions of predicted rutting from UST and SST test results for years 10, 20, and 40 suggests that surface rutting predicted by using UST and SST test results are statistically equal with high p-values. Consequently, the data from the developed UST test equipment can be used for mechanistic-empirical (ME) pavement design and will provide rutting predictions that are statistically equal to the predictions for SST.

It was found that the predicted rut depths correlate well also with the linear viscoelastic parameter, determined from repeated shear tests, the accumulated equilibrium compliance. Thus the computed accumulated equilibrium compliance is a suitable criterion for the assessment of the asphalt mixture susceptibility to permanent deformations.

Acknowledgments

The work reported here was supported by the project No. FV10526 in the program TRIO of the Ministry of Industry and Trade of the Czech Republic and also supported by both United States and Czech Republic governments through J. William Fulbright Commission.

6. References

- AASHTO T 320-07. 2011. "Standard Method of Test for Determining the Permanent Shear Strain and Stiffness of Asphalt Mixtures Using the Superpave Shear Tester (SST)." American Association of State Highway and Transportation Officials.
- "CalME Manual." 2011. University of California, Berkeley.
- Deacon, John, John Harvey, Irwin Guada, Lorina Popescu, and Carl Monismith. 2002. "Analytically Based Approach to Rutting Prediction." *Transportation Research Record: Journal of the Transportation Research Board* 1806 (-1): 9–18. doi:10.3141/1806-02.
- Hallin, John P. 2004. NCHRP 1-37A Guide for Mechanistic-Empirical Design. National Cooperative Highway Research Program. <http://apps.trb.org/cmsfeed/TRBNetProjectDisplay.asp?ProjectID=218>.
- Harvey, J., I. Guada, C. Monismith, M. Bejarano, and F. Long. 2002. "Repeated Simple Shear Test for Mix Design: A Summary of Recent Field and Accelerated Pavement Test Experience in California." In . Copenhagen, Denmark.
- Insightful. 2001. "S-Plus 6 for Windows User's Guide." Insightful Corporation, Seattle, Washington.
- Monismith, C.L., J. A. Deacon, and John Harvey. 2000. *WesTrack: Performance Models for Permanent Deformation and Fatigue*. Pavement research Center; Institute of Transportation Studies, University of California, Berkeley.
- Monismith, C. L., R. G. Hicks, F. N. Finn, J. Sousa, J. Harvey, S. Weissman, J. Deacon, J. Coplantz, and G. Paulsen. 1994. "Permanent Deformation Response of Asphalt Aggregate Mixes," August, 1–437.
- Ruxton, G.D. 2006. "The Unequal Variance T-Test Is an Underused Alternative to Student's T-Test and the Mann–Whitney U Test." *Behavioral Ecology*. doi:10.1093/beheco/ark016.
- Ullidtz, Per, J. T. Harvey, Imad Basheer, David Jones, Rongzong Wu, Jeremy Lea, and Qing Lu. 2010. "CalME, a Mechanistic-Empirical Program to Analyze and Design Flexible Pavement Rehabilitation." *Transportation Research Record: Journal of the Transportation Research Board* 2010 (2153): 143–52. doi:10.3141/2153-16.
- Von Quintus, H., Jagannath M., Bonaquist R., Ch.W. Schwartz, and Regis L. Carvalho. 2012. *Calibration of Rutting Models for Structural and Mix Design*. Washington, D.C.: Transportation Research Board - National Research Council.

- Zak, J, E Coleri, J. Stastna, and J. T. Harvey. 2017. "Accumulated Equilibrium Compliance as a Rutting Susceptibility Parameter." Submitted to Road Materials and Pavement Design Journal.
- Zak, J, J Stastna, L Zanzotto, and D MacLeod. 2013. "Laboratory Testing of Paving Mixes – Dynamic Material Functions and Wheel Tracking Tests." International Journal of Pavement Research and Technology, 3, , no. 6: 147–54. doi:10.6135/ijprt.org.tw/2013.6(3).147.
- Zak, J., C. L. Monismith, E Coleri, a J. T. Harvey. 2016. „Uniaxial Shear Tester - Test Method to Determine Shear Properties of Asphalt Mixtures". Road Materials and Pavement Design Journal, 87–103. doi:10.1080/14680629.2016.1266747.

TABLES

Mixture type / Sieve size:	3/4" (19m m)	1/2" (12.5 mm)	3/8" (9.5 mm)	No. 4 (4.75 mm)	No. 8 (2.36 mm)	No. 16 (1.18 mm)	No. 30 (600 μm)	No. 50 (300 μm)	No. 100 (150μ m)	No. 200 (75μ m)	RA P
Mix#1 3/4" HMA PG 64-10	100	78	63	45	32	27	19	15	10	5	25
Mix#2 3/4" HMA PG64-28PM	100	88	76	48	34	27	20	14	8	5	15
Mix#3 1/2" RHMA- G PG 64-10	100	98	83	40	23	-	12	-	-	5	-

Table 1. Asphalt mixture grading

Designation	Frequency sweep								
	d	b	g	aT	A	VTS	Eref	tref	a
Mix#1_SST_3I4 HMA PG 64-10	1.699	1.139	0.783	0.719	9.631	-3.505	1316.472	30	2.483
Mix#2_SST_3I4 HMA PG 64-28PM	1.699	1.903	0.439	1.485	9.631	-3.505	479.100	30	3.937
Mix#3_SST_R-HMA-G	1.699	1.444	0.394	0.809	9.631	-3.505	961.776	30	3.937
Mix#1_UST_3I4 HMA PG 64-10	1.000	0.328	0.149	0.945	9.631	-3.505	351.863	30	3.182
Mix#2_UST_3I4 HMA PG 64-28PM	1.000	0.478	0.160	0.956	9.631	-3.505	278.045	30	3.182
Mix#3_UST_R-HMA-G	1.000	0.488	0.116	1.032	9.631	-3.505	235.455	30	3.182
-	Repeated Shear						Accumulated equilibrium compliance, J_e , acc [1/Pa]:		
	A	a	tref	b	g	d			
Mix#1_SST_3I4 HMA PG 64-10	1.401	2.639	0.100	0.000	3.346	1.000	1.53E+11		
Mix#2_SST_3I4 HMA PG 64-28PM	1.458	1.749	0.100	0.000	2.920	1.000	2.39E+11		
Mix#3_SST_R-HMA-G	0.550	4.980	0.100	0.000	5.090	1.000	1.58E+11		
Mix#1_UST_3I4 HMA PG 64-10	0.525	3.390	0.100	0.000	1.504	1.000	1.75E+11		
Mix#2_UST_3I4 HMA PG 64-28PM	0.556	1.895	0.100	0.000	2.178	1.000	2.97E+11		
Mix#3_UST_R-HMA-G	0.125	3.772	0.100	0.000	2.780	1.000	1.20E+11		

Table 2. Used material parameters

Conditions:	T14, Inland Valley						Rut depth and ACE correlation
Asphalt mixture and used test device	Mix#1 SST	Mix#1 UST	Mix#2 SST	Mix#2 UST	Mix#3 SST	Mix#3 UST	
Rutting after 10 years [mm]	4.54	4.53	3.85	3.23	5.86	5.22	-0.86
Rutting after 20 years [mm]	5.54	5.34	4.60	4.00	7.17	6.26	-0.84
Rutting after 40 years [mm]	6.70	6.37	5.64	5.08	8.74	7.62	-0.80
Conditions:	T14, High Desert						
Rutting after 10 years [mm]	3.71	4.17	3.32	3.04	5.13	4.89	-0.82
Rutting after 20 years [mm]	4.48	4.88	4.05	3.76	6.26	5.89	-0.80
Rutting after 40 years [mm]	5.50	5.88	5.03	4.80	7.66	7.21	-0.77
Conditions:	T14, Low Mountain						
Rutting after 10 years [mm]	3.05	3.58	3.05	2.97	4.32	4.44	-0.71
Rutting after 20 years [mm]	3.84	4.31	3.83	3.71	5.43	5.41	-0.70
Rutting after 40 years [mm]	4.89	5.34	4.94	4.77	6.78	6.68	-0.68
Conditions:	T10, Inland Valley						
Rutting after 10 years [mm]	2.27	3.08	1.52	1.60	3.19	3.38	-0.85
Rutting after 20 years [mm]	3.05	3.73	1.97	2.04	4.16	4.14	-0.87
Rutting after 40 years [mm]	3.80	4.39	2.49	2.58	5.23	5.02	-0.87
Conditions:	T10, High Desert						
Rutting after 10 years [mm]	3.18	4.12	2.50	2.27	4.12	4.16	-0.86
Rutting after 20 years [mm]	3.90	4.75	3.10	2.80	5.20	4.98	-0.87
Rutting after 40 years [mm]	4.74	5.51	3.82	3.51	6.44	5.97	-0.85
Conditions:	T10, Low Mountain						
Rutting after 10 years [mm]	2.16	3.16	1.76	1.93	3.45	3.65	-0.76
Rutting after 20 years [mm]	2.93	3.84	2.30	2.45	4.51	4.45	-0.79
Rutting after 40 years [mm]	3.69	4.54	3.00	3.11	5.66	5.39	-0.78

Table 3. Calculated rut depths and correlation with accumulated equilibrium compliance

2.6. Žák, J., Shear accumulated equilibrium compliance as permanent deformation susceptibility parameter, 2020.

Authors' contribution percentage:

100% Žák, J.,

Shear Accumulated Equilibrium Compliance as Permanent Deformation Susceptibility Parameter

Josef Zak^a,

^a CTU in Prague, Faculty of Civil Engineering, Department of Construction Management and Economics, Thakurova 7, Prague, Czech Republic. E-mail: josef.zak@fsv.cvut.cz

Acknowledgement:

The work reported here was supported by both United States and Czech Republic governments through J. William Fulbright Commission.

Abstract:

Described procedure summarizes the derivation of accumulated creep compliance in the sequence of the creep and recovery cycles that can be easily fitted to experimentally measured data. The local minima in each measured cycle after the recovery were selected and combined into a set that characterized the irreversible deformation of the specimen during the test. Further, the interval fitting procedure was utilized. The estimation of the discrete retardation spectrum from the used 4-modes standard Kelvin-Voigt model was discussed and the accumulated compliance calculated. It was proved that the accumulated compliance may be used as the pavement rutting criterion (expressing the performance of asphalt in terms of its susceptibility to permanent deformations). The proposed theory was demonstrated on experimentally measured asphalt properties in the two test devices. Repeated Shear tests were performed in the Superpave Shear Tester and the Uniaxial Shear Tester. It was found that the accumulated equilibrium compliance correlates with the asphalt mix rutting parameters. As it is presented and in the view of the general principles showing that long-time processes are revealed in more detail in the retardation spectrum, the use of the accumulated equilibrium compliance can be useful as a criterion for the long life rutting potential.

Keywords: Asphalt pavement deformation; shear properties, Superpave Shear Tester, Uniaxial Shear Tester, linear viscoelastic simulation, retardation spectrum, accumulated equilibrium compliance

1. Introduction

The aim of this contribution is to present a procedure for the calculation of the linear viscoelastic parameter, retardation spectrum area, associated with the equilibrium compliance, as a characteristics describing the long-standing asphalt mixture rutting capability determined from the laboratory measured shear properties. Such a parameter characterizing the rutting susceptibility, as a one value parameter, can be easily used by the asphalt paving community. Based on the pavement Finite Element Analysis [1] and a literature review (Harvey et al., 2002; Harvey et al., 2001; Monismith et al., 1994; Von Quintus et al., 2012), the shear properties of asphalt mixtures are judged to be crucial for the asphalt mixture susceptibility to permanent deformation. Thus, the herein described procedure uses the laboratory measured shear characteristics of asphalt mixtures.

The asphalt mixture is a material that exhibits both the rate-dependent viscoelastic and viscoplastic behavior and the rutting is directly related to the rate-dependent behavior (Underwood et al., 2011). The usefulness of the linear viscoelasticity in the study of thermo-mechanical behavior of asphalt mixture has also been proven by others (Alavi & Monismith, 1994; Zou et al., 2010).

Repetitive stress is frequently used as the primary testing method in the studies of material behavior. Although large deformations certainly occur in these tests (material exhibits nonlinear behavior), the linear viscoelastic properties of the studied materials have an important impact on their behavior in the nonlinear viscoelastic domain (Zak et al., 2013).

Tsai, in his work (Tsai et al. 2004), reported on the use of the Genetic Algorithm solving nonlinear optimization problems for the fitting of the bitumen complex shear modulus. Part of the presented contribution is also aimed at the calculation of the discrete relaxation spectrum of the binder. Relaxation spectra were studied in [11], where the binder relaxation spectrum is reported to correlate with the asphalt mixture fatigue properties and the bitumen shear susceptibility, i.e. the viscosity.

In Tsai's studies, the relaxation spectrum was determined from the small amplitude oscillation measurements, [12]. The approach presented in our contribution used the retardation spectrum from the repeated creep and recovery tests. Several representative examples are discussed below.

2. Material properties

2.1. Specimen preparation and material specification

Asphalt test specimens were prepared from five different mixes. Details of each mix are shown below:

- Mix 1: 3/4 in. with 4.8 percent PG64-10 asphalt binder, 25% recycled asphalt (RAP) and 0.9 percent hydrated lime anti-strip additive. This mix was plant produced and sampled during the paving process
- Mix2: 3/4 in. with 5 percent PG64-28PM modified asphalt binder, 15 percent RAP and 0.9 percent hydrated lime anti-strip additive. This mix was plant produced and sampled during the paving process
- Mix 3: 1/2 in. gap-graded rubberized asphalt (RHMA-G), with 7 percent PG64-10 asphalt binder and 4 percent air void content. Specimens from this mix were cut from the UCPRC test track.
- Mix 4: ACO 11+ 50/70 with 5.6 percent 50/70 penetration grade asphalt binder. Air void content was 3.5 percent and mix design was performed in accordance with (EN 13108-1, 2008).
- Mix 5: Same mix as mix 2 except specimens were prepared with a targeted 96 percent degree of compaction. Actual specimens had an average air void content of 7.6 percent.

The testing matrix was designed so that the validation of the measured asphalt mixture properties would be done over a broad range of mixture properties. Thus, it covers:

- Laboratory prepared mixes and asphalt plant produced material.
- Samples taken from the pavement and samples prepared in the laboratory.
- Polymer modified, rubberized, and conventional binders.
- Mix designs according to European and Caltrans (California, United States) material specifications.
- Well compacted and poorly compacted mixtures.
- A variety of aggregate sources.

The Repeated Simple Shear Test at Constant Height was performed in accordance with [14] in the case of the Superpave Shear Tester (SST). The Uniaxial Repeated Shear Test was done in accordance with the procedure presented in [15].

3. Experiments

Numerical simulations of two experiments are taken into consideration in this paper. The Repeated Simple Shear Test at Constant Height (RSST-CH) as one of the most common tests run by the Superpave Shear Tester is used to measure the shear properties of selected asphalt mixtures. The specimen is subjected to a shear load in a horizontal direction while the specimen's height is maintained through the application of a vertical load. The repeated shear load consisted of 0.1s creep followed by a 0.6s recovery period. The haversine horizontal load differs from its vertical equivalent loading in its amplitude.

The other test method is the Repeated Uniaxial Shear Test (RUST) performed with the Uniaxial Shear Tester (UST). A brief description of loading is provided in this paragraph. More information about UST can be found in [15], [16]. The RUST test is performed in a steel cylinder ensuring the lateral compaction of the tested material during the test. The shear load is applied through the steel insert that is pushed down through the specimen exciting the shear load in the tested material. The loading diagram is similar to the RSST-CH test. The specimen was subjected to thirty thousand cycles consisted of 0.1s of shear creep followed by 0.6s recovery at a constant temperature while the strain is determined from the steel insert deflection. The test temperature should be selected appropriate to the pavement construction condition. In our case, all the specimens were tested at 50°C in RSST-CH and RUST, and both tests were performed in the stress controlled mode. The applied stress was equal to 100kPa.

4. Linear viscoelastic simulation

If we assume that the load is expressed as the Heaviside step function and the time of creep has a length a . the whole cycle has length b (*i.e the time of recovery is $b-a$*), then the loading may be written as:

$$\tau(t') = \tau_0 \sum_{n=0}^{n=i} [H(t' - n * b) - H(t' - a - n * b)] \quad (1)$$

where τ_0 is the stress amplitude, H is the Heaviside step function [17] and n is an integer from 0 to $i=30000$, in our case.

For the purpose of the linear viscoelastic simulation, the constitutive equation [17] may be used:

$$\gamma(t) = \int_{-\infty}^t J(t-t') * \bar{\tau}(t') dt' \quad (2)$$

where J is the compliance function, $\gamma(t)$ is the deformation, and $\bar{\tau}(t')$ is the time derivative of stress. In a view of the causality principle, equation 2 may be written as:

$$\gamma(t) = \int_{-\infty}^{\infty} H(t-t') J(t-t') \bar{\tau}(t') dt' \quad (3)$$

The differentiation of (1) yields:

$$\frac{d\tau(t')}{dt'} = \tau_0 \sum_{n=0}^{n=i} [\delta(t' - n * b) - \delta(t' - a - n * b)] \quad (4)$$

where δ is the Dirac delta function. Subsequently, substituting equation 4 into 3 we obtain:

$$\gamma_{acc}(t) = \tau_0 \sum_{n=0}^{n=i} [H(t-nb)J(t-nb) - H(t-a-nb)J(t-a-nb)] \quad (5)$$

The response to the repeated shear stress is now determined by the form of the shear compliance function that is determined (in the linear viscoelasticity) by the retardation spectrum of the studied material. The retardation spectra of the studied materials were calculated by using the standard B-parameter Kelvin-Voigt model was used [17] where B is the number of parameters in the standard Kelvin-Voigt model proportional to the number of Kelvin modes m ($A=2m+1$).

$$J(t) = J_g + \sum_{a=1}^{a=m} J_a \left[1 - \exp\left(-\frac{t}{\tau_{v,a}}\right) \right] \quad (6)$$

where J_g is the instantaneous (glassy) compliance, J_a is the compliance of a -th Kelvin-Voigt mode and $\tau_{v,a}$ is the retardation time. The final accumulated strain can be written as a function of time by substituting equation 6 into equation 5, as follows:

$$\gamma_{acc}(t) = \tau_0 \sum_{n=0}^{n=i} \left[H(t - nb) \left\{ J_g + \sum_{a=1}^{a=m} J_a \left\langle 1 - \exp\left(-\frac{(t - nb)}{\tau_{v,a}}\right) \right\rangle \right\} - H(t - a - nb) \left\{ J_g + \sum_{a=1}^{a=m} J_a \left\langle 1 - \exp\left(-\frac{t - a - nb}{\tau_{v,a}}\right) \right\rangle \right\} \right] \quad (7)$$

The operation of obtaining the accumulated creep compliance entails the summation of 30 000 creep and recovery cycles. The first 65 cycles of strain derived from the Repeated Shear test and its approximation are presented in Figure 2.

The aim of the above presented approach is to obtain a function that will be suitable for the approximation of the experimental data from the Repeated Shear tests. The fitting procedure finds a set of model parameters pursuant to the least-squares fit of experimental data. The fitting concept of equation 7 to experimentally measured data, with 30 000 creep and relaxation cycles, results in high computation time even for the 4-mode Kelvin-Voigt model. Therefore, extensive effort was made to simplify equation 7 for the fitting purposes as is discussed below.

The purpose of this paper is not to compare various viscoelastic models, which might be found in other publications, but rather present the procedure to calculate accumulated equilibrium compliance for repeated creep tests, present sample data, calculated results and suggest the possible use of the accumulated equilibrium compliance.

A general assumption can be made: the rutting is caused primarily by the accumulation of permanent (irreversible) strain in the pavement structure. If the test procedure captures the in situ repetitive loading of the examined material, then the laboratory measured irreversible strain may be related (equivalent) to the rutting phenomenon in pavements. In the sense of accumulated compliance, such an assumption may be exploited and the local minima of accumulated compliance, may be taken into further analysis. Such a data selection expresses the irreversible part of the deformation during the Repeated Shear test and will be referred to as the bottom envelope.

Then, if one only wants to calculate the accumulated permanent strain, i.e. the last point of each creep and recovery cycle, the calculation can be performed at time $t=k*b$, where k is a non-negative integer ($k=0, 1, 2, 3, \dots$). This yields equation 5 as:

$$\gamma_{acc,min}(kb) = \tau_0 \sum_{n=0}^{k=i} [H\{b(k-n)\}J\{b(k-n)\} - H\{b(k-n)-a\}J\{b(k-n)-a\}] \quad (8)$$

Again, if $k-n=l$, then l is a non-negative integer and:

$$\gamma_{acc,min}(l) = \tau_0 \sum_{l=0}^{l=i} [H(bl)J(bl) - H(bl-a)J(bl-a)]$$

$$H(bl) = \begin{cases} 1, & l > 0 \\ 0, & l = 0 \end{cases} \quad \text{and} \quad H(bl-a) = \begin{cases} 1, & l > 0 \\ 0, & l = 0 \end{cases} \quad (9)$$

Hence, the “discrete” accumulated compliance may be expressed as:

$$\gamma_{acc,min}(l) = \tau_0 \sum_{l=1}^{l=i} [J(bl) - J(bl-a)] \quad (10)$$

The calculation of local maxima may be found with the application of the above described operations for $t=k*b+a$, in equation (5), resulting in:

$$\gamma_{acc,max}(l) = \tau_0 \sum_{l=1}^{l=i} [J(bl) - J(bl-a)] \quad (11)$$

The usefulness of equations 10, and 11 is not only in the simple calculation of the local minima of accumulated compliance, but it also allows the interval calculation. In other words, not all the previous minima need to be expressed if one wants to calculate the values of interest in the desired cycle.

The procedure of fitting the rheological model to the measured accumulated compliance may involve the calculation of several intervals and their mutual completion. Two intervals were used in this study. In our case, the exponential interval with the exponent P was selected.

We can express the accumulated compliance in the form of a matrix in a time domain by the following equation.

$$\gamma_{acc,max}[x; y] = \mathbb{A} = \left[b * n^P; \tau_0 \sum_{l=1}^{l=n^P} [J(bl) - J(bl - a)] \right] \text{ for } n \in \mathbb{Z}^+ \subseteq \langle 1; IL \rangle \quad (12)$$

where \mathbb{A} is a IL -by-2 matrix, the first column expresses the position in time, while the second column contains the calculated value of accumulated compliance. Further, IL is the interval length, n is a positive integer from 1 to IL and P is a parameter of the exponential interval. The intervals and \mathbb{A} matrices may be calculated separately with different P parameters and interval lengths, IL , and appended one to the other. Let the experimentally measured data, values from the bottom envelope and their dependence on time, be listed in a matrix denoted as \mathbb{M} . The final fitting procedure contains the search for the rheological model parameters providing the best fit of \mathbb{A} to \mathbb{M} . The well-known least squares approximation method was found to be appropriate for such a purpose.

In view of computing time, the use of the minimum adequate number of the rheological model parameters and the generation of minimum data points should be kept on mind. For the approximation of the data obtained from both Repeated Shear tests, RSST-CH and URST, the four unit standard Kelvin-Voigh model was found to be sufficient to use and the two approximation intervals were generated. The first interval exponent, P , was equal to 3 and the variables, n , were generated in the interval of up to 22. The second interval exponent was 4 and n -s were up to 13. With the selection of these parameters, the approximation procedure took up to 30 seconds of computing time. An example of a typical fit may be seen in Figure 3.

It was found that such a system was overdetermined and that the range of retardation times or the range of compliance magnitudes needed to be limited. At the beginning, nothing was known about the magnitudes of J_a and $\tau_{v,a}$, thus a broad range [10 to 10^4] was specified for each $\tau_{v,a}$ in the case of RSST-CH and a range [4 to 10^4] in the case of URST. The starting magnitudes of J_a were set, evenly distributed in a range of [$1 \cdot 10^7$ to $4 \cdot 10^7$]. The starting magnitude of the instantaneous compliance was selected equal to $2 \cdot 10^7$.

These magnitudes were found to be appropriate for all analyzed experiments in both tests. Sure, if a narrow parameter range is specified, the approximation procedure will lead to a local optimum. Thus, it is recommended to check the fit of the computed function to experimental data in the plot as well. All the computed parameters are listed in table 1 in the Appendix.

From the proposed model, the retardation spectrum can be easily found from experimental data. The standard Kelvin-Voigt model has a discrete retardation spectrum where $\tau_{v,a}$ are retardation times and J_a are the corresponding weights (partial compliances) [17].

The integration of the retardation spectrum, together with the instantaneous compliance, determines the equilibrium compliance [12], [17]:

$$J_e = \int_{-\infty}^{\infty} L d \ln \tau_v + J_g \quad (13)$$

where L is the retardation spectrum and J_e is the equilibrium compliance.

As the m -unit standard Kelvin-Voigt model was used, J_g is ordinarily negligible in comparison with the integral, thus the equilibrium compliance can be expressed from the discrete retardation spectrum using a numerical integration. If the above mentioned is taken into account, Simpson's rule may be applied and equation 13 may be expressed as follows:

$$J_{e, acc} = \sum_{a=1}^m \frac{J_a + J_{a+1}}{2} * (\tau_{a,v} - \tau_{a+1, v}) \quad (14)$$

where $J_{e, acc}$ is our desired accumulated equilibrium compliance. The plot of the retardation spectrum can be seen in the following Figure 4; experience has shown that the logarithmic time scale is convenient. The gray area under the spectrum is the accumulated equilibrium compliance.

4.1. Discussion of equilibrium compliance determined for selected asphalt mixtures

Considering that the long-time processes are revealed in more detail in the retardation spectrum, one can link those to the rutting potential. The accumulated equilibrium compliance was calculated for both RUST and

RSST-CH, the correlation of both can be seen in Figure 5a. The correlation coefficient was equal to 0.89. From this, one can conclude that both tests are able to determine equivalent parameters of the shear for asphalt mixtures when the accumulated equilibrium compliance is considered. The correlation of other properties was discussed in [16].

It was found during the WesTrack project [18], that cycles to the 5% of permanent shear strain (5%PSS) criterion related to the laboratory measured properties as far as the material rutting is considered. The appropriate correlations are shown in Figures 5b and 5c. Figure 5b depicts the correlation of 5%PSS to the accumulated equilibrium compliance derived from URST, while the correlation of 5%PSS to the accumulated equilibrium compliance is expressed in figure 5c. The correlation coefficient was equal to 0.98 and 0.94, respectively. Statistically speaking, both correlations are very good.

Asphalt mixture #2 performed best in the view of asphalt mixture's susceptibility to permanent deformations. Mix #2 was the only material with a polymer modified asphalt binder. The Repeated Shear test of the asphalt mixture may be, to a certain extent, less severe than the Multiple Stress Creep and Recovery test (MSCR) for asphalt binders. When the MSCR test is capable of better capturing the recovery ability of the asphalt binder, it is considered to be a superior surrogate of the PG specification in comparison with the resistance of binder to permanent deformations. The proposed principle of the accumulated equilibrium compliance as a criterion seems to be capturing the same principles in the domain of asphalt mixtures, as can also be seen from the noticeable gap between polymer modified and all the tested mixtures with neat or rubberized binders.

Many correlations of the characteristics of the Repeated Shear test may be presented in this paper, but, in view of the limited paper extent, the reader is asked also to refer to [15], [16], [19], where the other correlations are obvious.

Usually to obtain cycles to 5%PSS, the trend of the PSS needs to be extrapolated. Thus the value is dependent on the extrapolation process (selected function, regression analysis and selected range) The presented process of accumulated equilibrium compliance derive long-time performance from the whole experimental data set, without need of extrapolation.

All of the presented information suggest that the accumulated equilibrium compliance may be a useful criterion assessing the performance of asphalt mixture in rutting.

5. Conclusions

Various models of the complex modulus and the Time-Temperature Superposition principle were used for the study of asphalt binders. Relatively little has been done to apply the linear viscoelastic theory to the Repeated Shear test and its relationship to the asphalt pavement design.

The herein described procedure summarizes the development of accumulated compliance function in such a form that can be easily fitted to experimentally measured data. The local minima of the recovery part of this function, in each measured cycle, were selected and combined into a set of data that is referred to as the bottom envelope. The numerical method for the description of the equivalent discrete values of local minima was described with the use of the linear viscoelastic theory. Furthermore, the interval fitting procedure was utilized in order to reduce the computation time.

The 4-unit standard Kelvin-Voigt model was used in this contribution. The accumulated equilibrium compliance was calculated from discrete retardation spectrum of the model. The procedure is not limited only to such a model, and rheological models with arbitrary spectra may be also taken into consideration. All in all, the programmed script is capable to find the retardation spectrum and accumulated equilibrium compliance from both the Repeated Shear tests in up to 30 seconds of computation time.

It was found that the computed accumulated equilibrium compliance is a suitable criterion for the assessment of the susceptibility of asphalt mixture to permanent deformations. In view of the generally known principles that long-time processes are revealed in detail in the retardation spectrum, it is possible to use the link of the accumulated equilibrium compliance to the rutting potential.

To prove the above noted findings, two UST and SST test devices were utilized. It was found that the accumulated equilibrium compliance correlates with the rutting parameter cycles of asphalt mixture to the 5% of permanent shear strain. At the same time, it was proven that both test devices, the established SST and the newly developed UST, were capable to determine the equivalent asphalt shear properties of mixture specified there in the form of retardation spectra and the accumulated equilibrium compliance.

On the basis of experimental data and the derived retardation spectra, it was demonstrated that the instantaneous (glassy) compliance is negligible in the calculation of the accumulated equilibrium compliance.

The presented innovative principle of the accumulated equilibrium compliance can stimulate the discussion about the implementation of such a criterion as a one value parameter expressing the long-life rutting performance of asphalt mixture in the professional community.

6. References:

- D. B. McLean, Permanent deformation characteristics of asphalt concrete. PhD Thesis, University of California, Berkeley, 1974.
- J. Harvey, I. Guada, C. Monismith, M. Bejarano, and F. Long, "Repeated Simple Shear test for Mix Design: A Summary of Recent Field and Accelerated Pavement Test Experience in California," presented at the Ninth International Conference on Asphalt Pavements, Copenhagen, Denmark, 2002.
- J. Harvey, S. Weissman, F. Long, and C. Monismith, "Tests to evaluate the stiffness and permanent deformation characteristics of asphalt/binder-aggregate mixes, and their use in mix design and analysis," presented at the Association of Asphalt Paving Technologists Technical Sessions, 2001, Clearwater Beach, Florida, USA, 2001, vol. 70, pp. 576–604.
- C. L. Monismith et al., "Permanent Deformation Response of Asphalt Aggregate Mixes," pp. 1–437, Aug. 1994.
- H. Von Quintus, J. Mallela, R. Bonaquist, C. W. Schwartz, and R. L. Carvalho, Calibration of Rutting models for structural and Mix Design. Washington, D.C.: Transportation Research Board - National Research Council, 2012.
- B. S. Underwood, T. Yun, and Y. R. Kim, "Experimental Investigations of the Viscoelastic and Damage Behaviors of Hot-Mix Asphalt in Compression," *Journal of Materials in Civil Engineering*, vol. 23, no. 4, pp. 459–466, Apr. 2011.
- S. H. Alavi and C. L. Monismith, "Time and Temperature Dependent Properties of Asphalt Concrete Mixes Tested as Hollow Cylinders and Subjected to Dynamic Axial and Shear Loads," in *Journal of the Association of Asphalt Paving Technologists*, 1994, vol. 63.
- G. Zou, X. Zhang, J. Xu, and F. Chi, "Morphology of Asphalt Mixture Rheological Master Curves," *Journal of Materials in Civil Engineering*, vol. 22, no. 8, pp. 806–810, 2010.
- J. Zak, J. Stastna, L. Zanzotto, and D. MacLeod, "Laboratory Testing of Paving Mixes – Dynamic Material Functions and Wheel Tracking Tests," *International Journal of Pavement Research and Technology*, no. 6, pp. 147–154, 2013.
- B.-W. Tsai, V. Kannekanti, and J. Harvey, "Application of Genetic Algorithm in Asphalt Pavement Design," *Transportation Research Record: Journal of the Transportation Research Board*, vol. 1891, no. 1, pp. 112–120, Jan. 2004.
- B.-W. Tsai and C. L. Monismith, "Influence of Asphalt Binder Properties on the Fatigue Performance of Asphalt Concrete Pavements (With Discussion)," in *Journal of the Association of Asphalt Paving Technologists*, 2005, vol. 74.
- J. D. Ferry, *Viscoelastic Properties of Polymers*, 3rd ed. John Wiley & Sons, Inc., 1970.
- ČSN EN 13108-1, "Bituminous mixtures - Material specification - Part 1: Asphalt Concrete." Czech Office for Standards, Metrology and Testing, 2008.
- AASHTO T 320-07, "Standard Method of Test for Determining the Permanent Shear Strain and Stiffness of Asphalt Mixtures Using the Superpave Shear Tester (SST)." American Association of State Highway and Transportation Officials, 2011.
- J. Zak, C. L. Monismith, E. Coleri, and J. T. Harvey, "Uniaxial Shear Tester - Test Method to Determine Shear Properties of Asphalt Mixtures," *Road Materials and Pavement Design Journal*, pp. 87–103, 2016.
- J. Zak, E. Coleri, and J. T. Harvey, "Incremental Rutting Simulation with Asphalt Mixture Shear Properties," in *Solving Pavement and Construction Materials Problems with Innovative and Cutting-edge Technologies*, Hangzhou, China, 2018, pp. 13–24.

- N. W. Tschoegl, *The Phenomenological Theory of Linear Viscoelastic Behavior: An Introduction*. Berlin, Germany: Springer-Verlag, 1989.
- C. L. Monismith, J. A. Deacon, and J. Harvey, *WesTrack: Performance Models for Permanent Deformation and Fatigue*. Pavement research Center; Institute of Transportation Studies, University of California, Berkeley, 2000.
- J. Zak, J. Suda, and P. Ryjacek, "Polymer Modification Technologies and its Fatigue resistance in Pavement Structures," in *Innovative and Sustainable Solutions in Asphalt Pavements*, Shangdong, Peoples R. China, 2016, pp. 11–18.

Figures and tables:

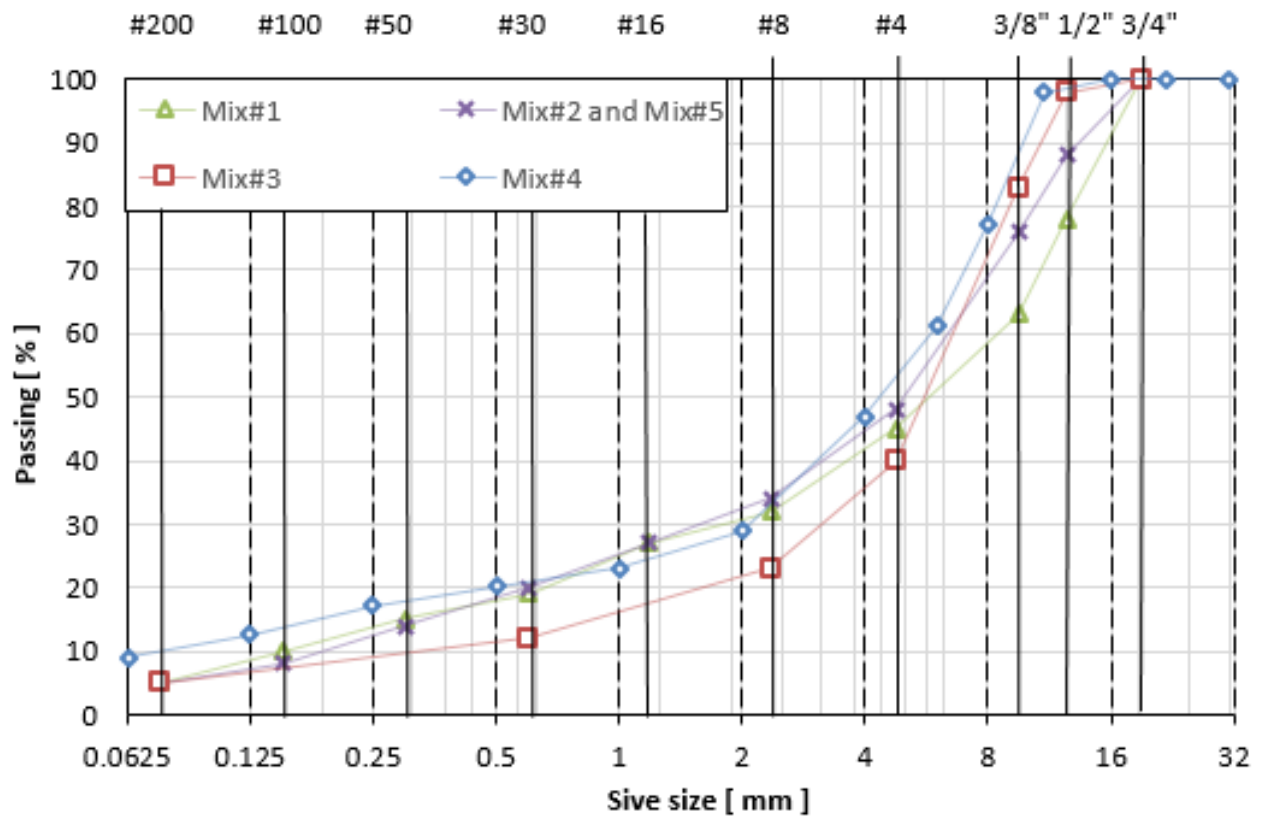


Figure 1. Asphalt mixture grading curve

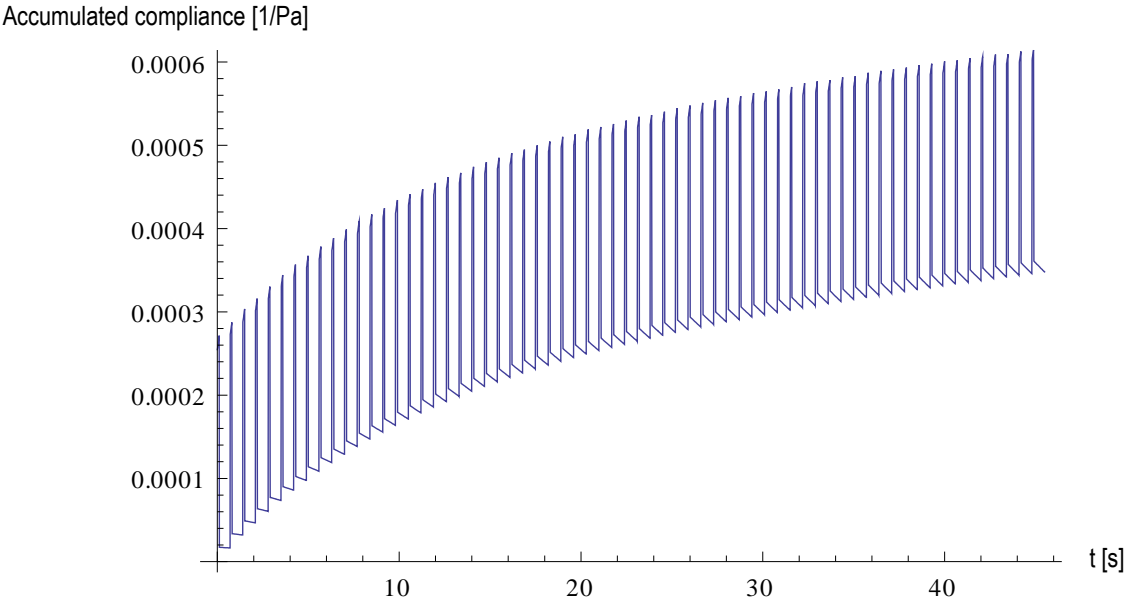


Figure 2. Simulation of repeated shear test first full 65 cycles Mix#1 3/4" HMA PG64-10

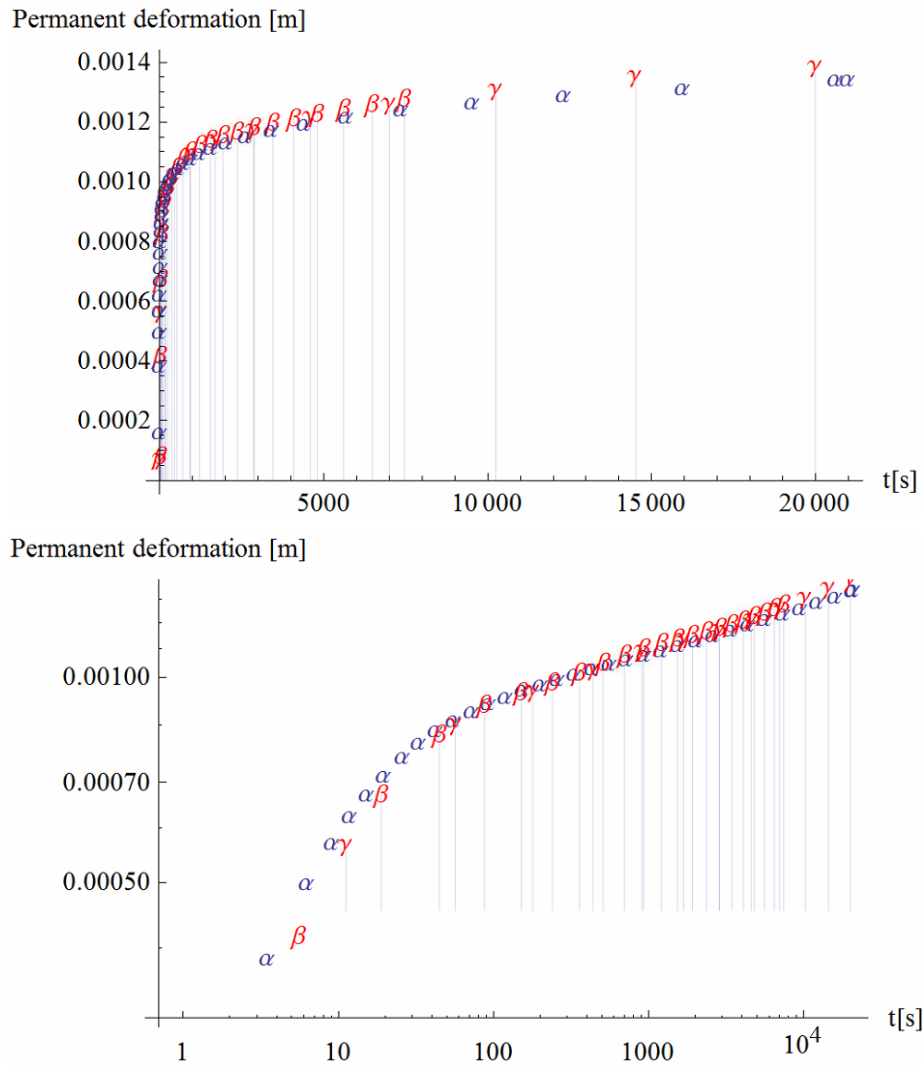


Figure 3. Fit of discrete accumulated compliance to local minima of measured data with two calculated intervals RUST (blue alfa points-experimental data, red points-simulated data, beta - first interval, gamma - second interval), Mix#1 3/4" HMA PG64-10

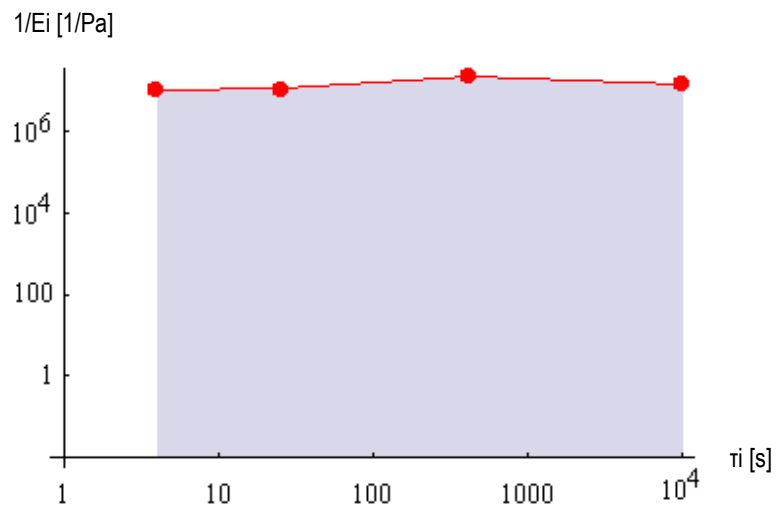


Figure 4. 4-Unit standard Kelvin-Voigt discrete retardation spectrum of Mix#1 3/4" HMA PG64-10

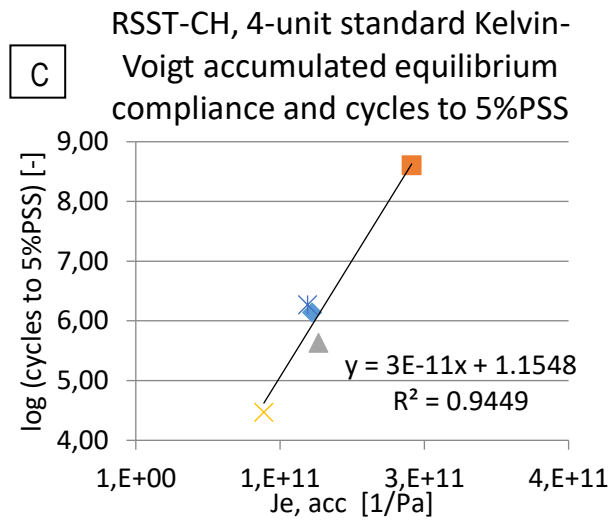
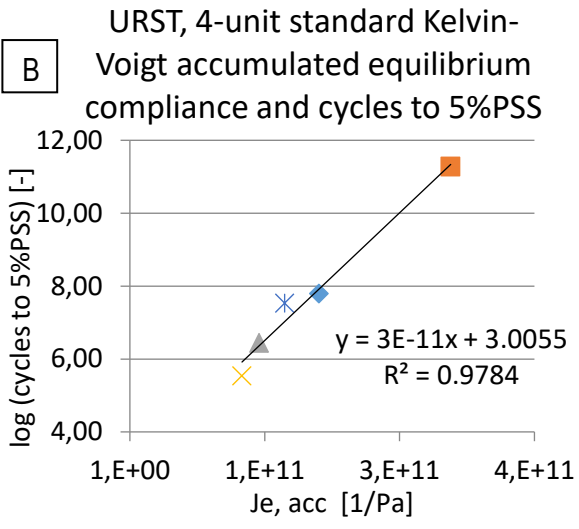
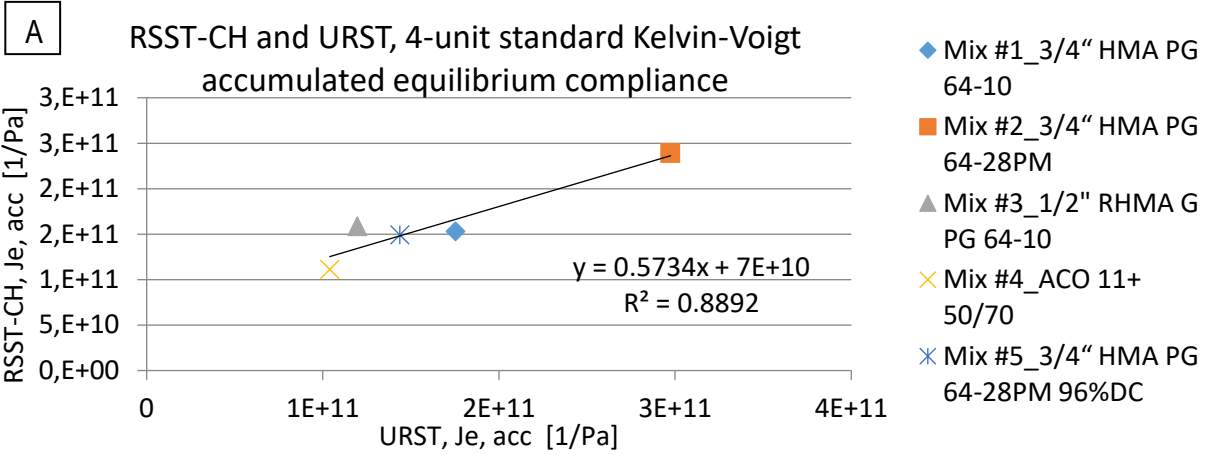


Figure 5. 4-Unit standard Kelvin-Voigt discrete retardation spectrum of Mix#1 3/4" HMA PG64-10

Mix #1 3/4" HMA PG64-10		Mix #2 3/4" HMA PG64-28PM		Mix #3 1/2" RHMA G PG64-10		Mix #4 ACO 11+ 50/70		Mix #5 3/4" HMA PG64-28PM, 96%DC	
RSST-CH	URST	RSST-CH	URST	RSST-CH	URST	RSST-CH	URST	RSST-CH	URST
Retardation time, τ_v [s]:									
2.822E+07	9.865E+06	1.862E+07	2.683E+07	7.639E+07	4.285E+07	9.731E+06	1.950E+07	2.059E+07	2.648E+07
1.666E+07	1.026E+07	1.690E+07	2.117E+07	2.765E+07	2.468E+07	9.749E+06	1.715E+07	1.495E+07	1.016E+07
1.542E+07	2.177E+07	2.027E+07	3.118E+07	1.435E+07	1.324E+07	1.425E+07	1.395E+07	1.544E+07	1.599E+07
5.606E+06	1.351E+07	1.362E+07	2.878E+07	5.286E+06	9.114E+06	1.046E+06	6.167E+06	5.061E+06	1.288E+07
Spectral compliance magnitude, J_a [1/Pa]:									
1.000E+01	4.000E+00	1.000E+01	4.000E+00	1.000E+01	4.000E+00	1.000E+01	4.000E+00	1.000E+01	4.000E+00
1.049E+02	2.623E+01	1.194E+02	4.253E+01	3.289E+02	7.304E+01	1.811E+02	4.746E+01	1.229E+02	3.933E+01
9.549E+02	4.264E+02	1.270E+03	5.805E+02	1.877E+03	8.989E+02	1.015E+03	6.020E+02	1.057E+03	5.599E+02
1.400E+04	1.000E+04	1.400E+04	1.000E+04	1.400E+04	1.000E+04	1.400E+04	1.000E+04	1.400E+04	1.000E+04
Instantaneous compliance, J_g [1/Pa]:									
1.630E+08	4.564E+07	3.503E+07	6.538E+07	1.577E+08	2.789E+08	4.009E+08	8.440E+07	3.105E+07	1.098E+07
Accumulated equilibrium compliance, J_e, acc [1/Pa]:									
1.53E+11	1.75E+11	2.39E+11	2.97E+11	1.58E+11	1.20E+11	1.11E+11	1.04E+11	1.49E+11	1.44E+11
Cycles to 5% PSS [-]:									
1.370E+06	6.195E+07	4.019E+08	1.901E+11	4.288E+05	2.758E+06	2.937E+04	3.440E+05	1.843E+06	3.339E+07

Table 1. List of determined material characteristics from RSST-CH and URST

2.7. Žák, J., On Laser Scanning, Pavement Surface Roughness and International Roughness Index in Highway Construction, 2016.

Authors' contribution percentage:

100% Žák, J.

On laser scanning, pavement surface roughness and international roughness index in highway construction

Josef Zak^a

^aDepartment of Road Structures, CTU in Prague, Prague, Czech Republic, josef.zak@fsv.cvut.cz

The paper reports data from the research project where the objective was to develop and validate a tool that would be publicly available and would leverage the point cloud data commonly acquired on sites to calculate the pavement surface properties such as the International Roughness Index and Roughness. To do so, a unique RIRI program was written in Python to streamline the point cloud data analysis. The program is publicly available under the GNU General Public License. Further, the paper presents data from three test sections where the developed methodology was used to calculate the pavement smoothness properties from a point cloud and compared to classical, reference, methodologies, such as the rod and level and precise levelling. The paper focuses on the variability and precision of all methodologies. It was found that the Pearson type IV distribution is a fitting descriptor for histograms calculated with the help of Freedman and Diaconis's law from rectified slopes and roughness values with regard to its fitness and use of its parameters for the pavement surface smoothness description.

Keywords: Asphalt, Durability, Safety, Software, Testing

1. Introduction

The choice of a proper pavement construction technology has always been a task combining engineer's knowledge and experience. The goal is to effectively construct a desired pavement layer while meeting all standardized requirements, design criteria and contracting agencies' demands. However, many disorders whose occurrence is linked to an improper mix design, errors in the mix production, its water content, and mistakes in the laydown process, such as the temperature loss, paver stops, improper compaction, result in an immediate decrease of the constructed layer quality. One of the criteria for a flexible pavement is its surface smoothness. It has a significant effect on the surface water runoff and the ride quality, and, most importantly, traffic safety [1]. Some of these disorders are present right after the layer construction, and some of them take their effect when traffic loading and weather conditions occur during the pavement's lifetime. Janoff suggested, in his extensive work [2] based on the data collected over ten years from more than 400 test sections, that the initial smoothness is related to the pavement long-term roughness and durability in regard of the pavement cracking and overall deterioration. These

findings are today proved by the mechanical analysis addressing the effect of flexible pavement viscoelasticity in relation to dynamic loading increased with the pavement surface roughness [3]–[7].

It was proved by [8] that highway users judge the condition of a highway by the riding experience when they travel over the highway. The pavement surface smoothness is an important parameter for road users not only from the perspective of their riding experience, but it is also one of the determinants of road user cost, as indicated in [8]. The need to measure the pavement surface smoothness led to the development of devices ranging from very simple and still in use devices like the rod and level, profilographs, where the Californian profilograph may be mentioned as one of the early developed and still in use devices. Further, with the advances in technology, the need led to many developed automated devices to measure the pavement smoothness [9], [10].

The wearing course roughness has been used in many project specifications over the US and European countries to set pay adjustments based on the desired threshold. Nowadays, even in Public-Private-Partnership schemes and advanced design-build projects, roughness is one of the specifically set quality criteria. Furthermore, advanced design techniques and the use of construction machine control systems help to achieve these contract requirements [11].

Although the definition of smoothness indicators varies over states and countries from the International Roughness Index (IRI), the Profilograph Index (Pri), the Mean Roughness Index (MRI), the Quarter-car Index, the root-mean-square vertical acceleration and the rod and level surface smoothness measurement (roughness), whose review may be found in [12]–[16], the value of smoothness should be well recognized as a useful indicator of the pavement serviceability performance and the quality of pavement layers should be periodically checked.

2. Methodology

The ability to use 3D laser scan data acquisition systems for the pavement profile properties determination was already proven by others [17]. However, the use of laser-based devices in civil construction is increasing. The laser technology is used for construction machines' navigations, surveying, the construction progress monitoring and quantity checks. The goal of the research project was to develop and validate an applicable methodology which would allow leveraging the already recorded point cloud data and provide feedback to contractors, laboratories and contracting agencies on the constructed layer smoothness, without a need for extra single purpose measurements. The other goal was also to validate a free to use and modify tool that may be used at the construction site and by participating laboratories.

2.1. Test sections

Three test sections were selected to demonstrate the applicability of the RIRI program and acquired point cloud data to measure the pavement surface smoothness. The test sections were selected so that the range from smooth roads to rough pavement surfaces would be covered within the research project scope.

The first test section is a two-lane urban road. The selected section is 510.00m of a straight urban road, with no intersections or driveways. This test section was expected to have the smoothest pavement surface properties. The laser scan measurements together with the rod and level and precise levelling were done two days after the pavement wearing course laydown.

The second test section is an arterial road, with a high traffic capacity, a four-lane expressway with one lane dedicated for parking in each direction. The total length of the test section is 1.618.00m. The surface course was laid down using the total station machine control system. The wearing course can be classified as an open graded surface. The test section is in a highly urbanized area so the semi-open graded wearing course was placed for the purpose of noise pollution reduction. Both measurements, the laser scan and the classical rod and level and precise levelling, were done two months after the new wearing course placement.

The third section is a cement stabilized base course of wye (railway triangular junction). The layer surface properties were measured two days after its placement. This test section is expected to have the roughest properties regarding the environment conditions, stabilized layer maximal nominal aggregate size and the fact that it is not a pavement wearing course. The length of this test section is 160.00m. The methodology scheme can be seen from figure 1.

The surfaces were cleaned from loose particles with road sweepers before the surface properties data were acquired on the site.

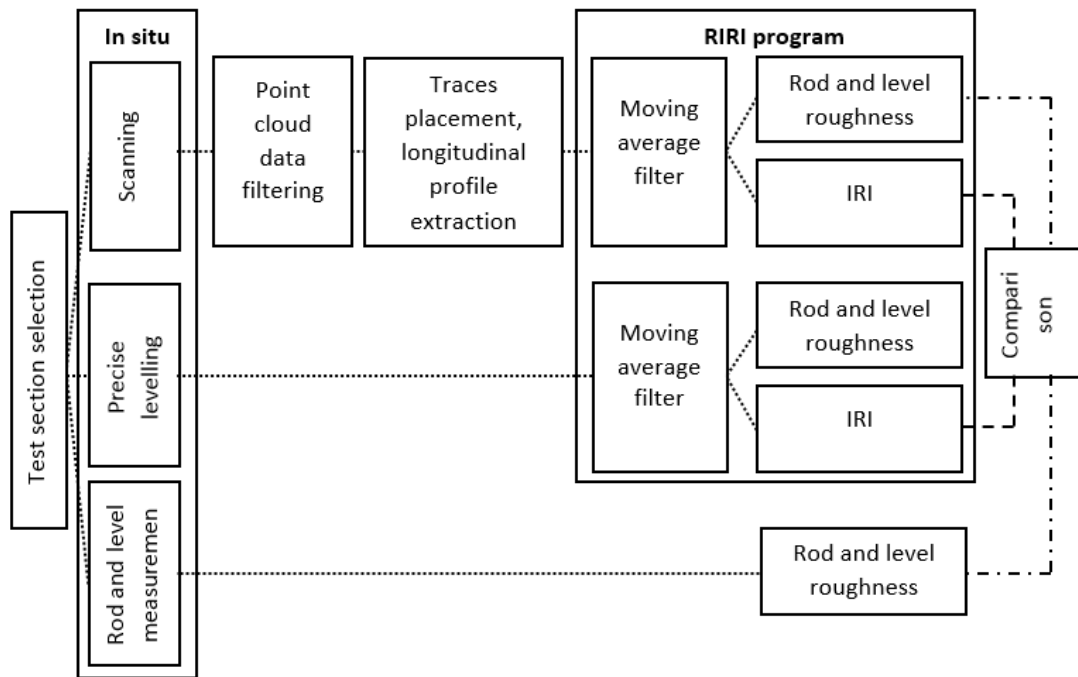


Figure 1: Research project methodology scheme

2.2. International Roughness Index

Two pavement profile characteristics to address the pavement surface smoothness were selected. IRI was recognized by the World Bank as a superior criterion for the pavement smoothness measurement [8] and for its spread use over states, European countries and its inclusion in the Czech national standard [18], and the proposed European standard [19] was selected as the main further considered surface smoothness index.

IRI was computed from a longitudinal road profile measurement using a virtual response type system, the quarter-car simulation, running at a speed of 80 km/h. The quarter-car simulation was applied on the longitudinal profile derived from the filtered longitudinal profile. The longitudinal profile was created from the 3D surface by positioning the alignment in the desired trace of the profile. The profile was filtered with a moving average so that the filtered profile used for further analysis would contain points with a 0.25m spacing. The so called RIRI tool was used to calculate rectified slopes for each longitudinal profile point by applying the quarter-car simulation. IRI was calculated from point cloud data based on:

- Each IRI is computed from a single longitudinal road profile.
- From each test section, five longitudinal profiles were created by placing five parallel alignments.

- The spacing between the alignments was 0.25m and they were always created within pavement lines.
- The filtered point cloud data had a point density higher than 100 points/m², so that the maximal sampling interval criterion of 125 mm, in [19], was met.
- The 3D laser scan resolution is 0.2mm.
- The created longitudinal profile was smoothed with a moving average whose base length is 250 mm.
- The smoother longitudinal profile is assumed to have a constant slope between the sampled elevation points.
- IRI is calculated from the smoothed longitudinal profile using a quarter-car simulation, with specific parameter values, at a simulated speed of 80 km/h.
- The simulated suspension motion is plotted in the form of a rectified slope linearly accumulated and further divided by the length of the profile to calculate IRI.

To validate the acquired data precision and their usability for the pavement index calculation, the longitudinal elevation profile was measured with precise levelling in the right wheel path of the outer pavement lane. The points from precise levelling were already taken with a 0.25m spacing so that the smoothing step could be omitted during the data processing. This longitudinal profile was used as an input file to the RIRI program to calculate the accumulated rectified slope and IRI.

2.3. Roughness

Roughness under the rod and level was measured at each test section. The rod and level measurements were done in one trace located in the outer lane right wheel path for all test sections. The measurements were taken only in one trace for each section due to the labour cost and the limited time window.

The roughness under the rod and level was calculated from point cloud data for the same five traces as used for the IRI calculation in each test section. The placement of these five traces, in the outer lane right wheel path for all test sections, was determined from the laser scan data only.

3. RIRI program

To streamline the point cloud data analysis, the so called RIRI program was written in the Python language [20]. In order to allow for the program's public use, the RIRI graphical user interface was developed as part of the research project. The program is capable to filter the input data with a moving average so that the filtered longitudinal profile with points with a 0.25m spacing is obtained for further analysis. The principle of the quarter-car simulation is further applied on the filtered longitudinal profile and the rectified

slope is calculated for each point. These data can be plotted in a chart, see figure 2. The plotted figures allow zooming and the location of areas where the computed values are of interest. Any profile data may also be imported into the RIRI program as an ASCII file, to perform IRI and the rod and level analysis. The roughness output or IRI output files are generated together with created plots, so that the data may further be used to locate the desired areas where the Roughness and IRI values vary from the desired threshold in any other program.

One of the broadly known tools for the pavement profile analysis is the ProVALsoftware [21]. However, the ProVAL licence does not allow modifying the source code, thus it would not allow us to achieve the desired goals. The RIRI program was developed with the aim of being of the greatest possible use to the public, and the best way to achieve this was to make it free software which everyone could use, redistribute and modify. Unlike ProVAL, the RIRI program is licenced under the General Public Licence [22]. The program is available at permalink: <http://d2051.fsv.cvut.cz/riri.htm>

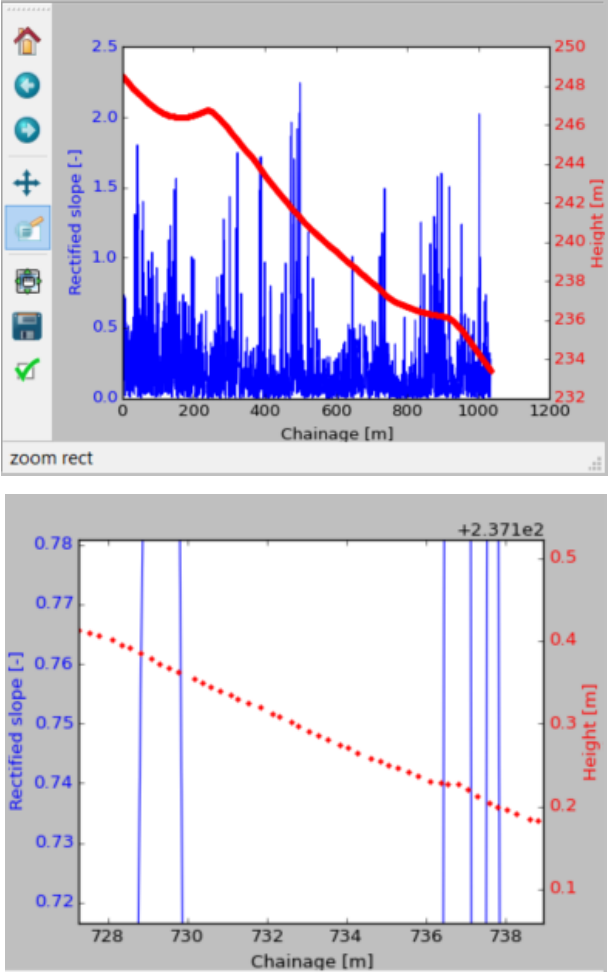


Figure 2: IRI plot in the RIRI program and data zoom

4. Test data interpretation and application

4.1. IRI

Figure 3 shows the comparison between the rectified slopes calculated from the laser scan and the rectified slopes calculated from the precise levelling of the first test section. It is troublesome to judge on the proposed method's validity only from the rectified slope plot and IRI as the rectified slope average. In figure 4, a typical Box-and-Whisker plot for the calculated rectified slope, and also for the first test section may be seen. Box-and-Whisker plot characteristics are further listed in table 1. The laser scan data acquisition provides a lower rectified slope variability as is also seen from the smaller interquartile range of all rectified slopes calculated for the profiles from point cloud data.

As may be seen all rectified slope values have a high variability and contain outliers. These outliers refer to construction disorders mentioned in the introductory paragraph, thus they have an importance for the quality of the pavement structure hence they will be further studied together with IRI. The position of the outliers and its detail may be located using the RIRI program as shown in figure 2.

Another descriptor, a histogram, may be used to distinguish the surface smoothness characteristics in terms of calculated rectified slopes. In this way, the density distribution functions may be used to compare the calculated rectified slopes if the traces used for data acquisition are not identical. Because each filtered longitudinal profile contains more than 400 values and the outliers are also of our interest, Freedman and Diaconis's law is chosen to set the non-oversmoothed histogram class width rather than the commonly used Sturges' law [23]–[25]:

$$h = 2(IQ)n^{-1/3} \quad (1)$$

where h is a class width, IQ is the sample interquartile range.

The Pearson type IV distribution function was used to estimate the shape of the rectified slope density distribution [26]:

$$P(x) = \frac{a}{\left[1 + \frac{4 * (x - b)^2 \left(2^{\frac{1}{a}} - 1\right)}{c^2}\right]^a} \quad (2)$$

where x is an independent variable, the rectified slope class, a is the amplitude, b is the centre of the Pearson type IV distribution, c is the full width at half maximum and d is the Pearson type IV distribution parameter.

The following abbreviations are used in figures and tables: i -th test section trace (T_i), rectified slope (RS), laser scanning (LS), precise levelling (PS), average values from five traces (AT) and Pearson product-moment correlation coefficient (PCC).

Data approximation may be seen in figures 5 and 6. The so called average trace may be used as a suitable representative trace, when all Box-and-Whisker plot parameters for the rectified slopes obtained from point cloud data are compared, see figure 4. The same trend, where the rectified slopes calculated from point cloud data exhibit a lower variability than the rectified slopes calculated from point cloud data, is evident from the data from all test sections. The Pearson type IV distribution parameters are listed in table 1.

It is proved that the rectified slopes and IRI ($r = 0.94$) obtained from point cloud data correlate well with those measured with a classical methodology.

The Pearson type IV distribution is capable to approximate the rectified slope's histograms well as may be seen from the coefficient of determination ranging from 0.89 to 0.65. The parameters like the amplitude, the centre position and the full width at half maximum of the Pearson type IV distribution also have very good correlations when both methodologies are compared. This implies that the Pearson type IV distribution is a fitting descriptor for the calculated rectified slopes histogram and that both methodologies used to obtain these data have a good correlation.

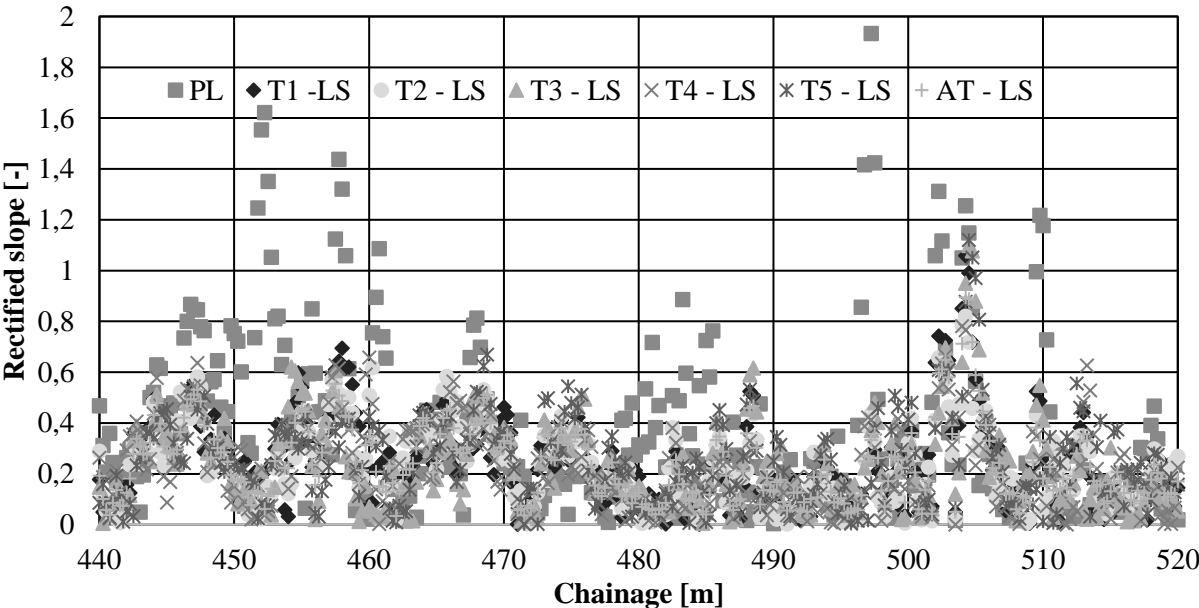


Figure 3. Rectified slope over a selected test section length, test section # 1

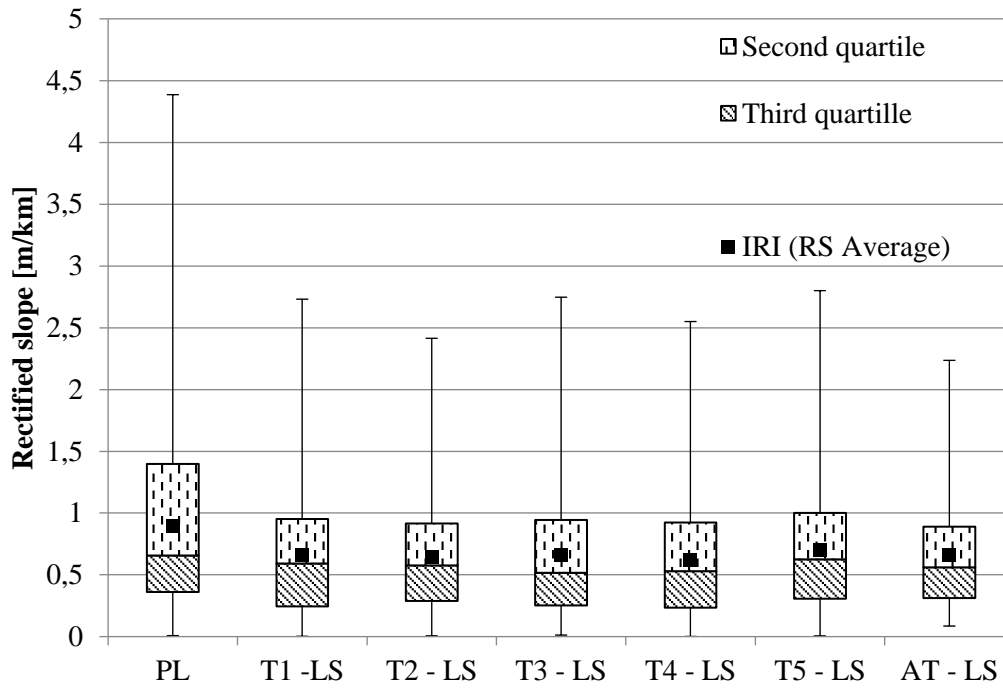


Figure 4. Box-and-Whisker plot, Rectified slope and IRI, test section # 1

	Test section #1		Test section #2		Test section #3		PCC between PL and AT - LS
	PL	AT - LS	PL	AT - LS	PL	AT - LS	
IRI (RS Average)	0.894	0.657	4.662	2.004	6.346	4.190	0.94
Standard Deviation	0.715	0.437	4.377	1.447	5.099	2.730	0.91
Min	0.008	0.086	0.006	0.074	0.074	0.076	-0.39
Q1	0.362	0.312	1.618	0.951	2.403	2.214	0.95
Median	0.657	0.560	3.480	1.688	5.086	3.578	0.95
Q3	1.398	0.890	6.051	2.529	9.320	5.502	0.96
Max	4.386	2.236	28.008	9.593	26.792	15.599	0.87
Bottom	0.362	0.312	1.618	0.951	2.403	2.214	0.95
Third quartile	0.295	0.248	1.862	0.737	2.683	1.363	0.97
Second quartile	0.741	0.330	2.571	0.842	4.234	1.924	0.97
Pearson type IV distribution parameters							
a	46.127	11.841	11.381	0.539	17.268	0.627	0.99
b	0.475	0.261	4.110	3.856	1.802	4.212	0.72
c	0.170	0.011	1.380	0.871	6.105	1.976	0.97
d	0.330	0.879	0.030	0.077	0.600	0.002	-0.05
r2 CoefDet	0.871	0.679	0.815	0.603	0.848	0.888	-

Table 1. Comparison of Rectified Slope and IRI and Parameters of Pearson Type IV Distribution

4.2. Roughness

The measured roughness is usually expressed in the form of a histogram where the x axis is the roughness depth in millimeters and the y axis is the number of occurrences. The pavement quality specifications then allow the roughness depth under a certain threshold. If the same data analysis principle as the one used for the IRI comparison is used, by fitting these histograms in equation 2 we obtain the parameters of the Pearson type IV distribution. The parameters and correlations between both methodologies are presented in table 2.

It is believed that the third test section exhibits such high roughness due to the layer maximum nominal aggregate size of 32mm. Even if this layer is well compacted, the porosity of the surface is partly captured when point cloud data are acquired with the laser scan.

From the values of the coefficient of determination, it may be concluded that the Pearson type IV distribution fits well with the measured roughness. Further, when we look at the PCC values, it may be concluded that both techniques, the laser scanning and the rod and level, are capable to determine comparable results of the surface roughness.

The correlation between the a parameter of the Pearson type IV distribution suggests that both methodologies are capable to determine a comparable amplitude. However, b is negative in two test sections, thus the high correlation of the b parameter does not imply the correlations of mean values as they have to be positive from the principle of measurement.

	Test section #1		Test section #2		Test section #3		PCC between PL and AT - LS
	PL	AT - LS	PL	AT - LS	PL	AT - LS	
Pearson type IV distribution parameters							
a	1598.81	249.53	36.42	43.67	11.46	128.10	0.91
b	-0.522	1.451	2.584	1.830	-22.851	-0.037	1.00
c	0.050	0.711	0.700	0.035	2.050	0.004	-0.78
d	0.522	0.999	0.868	0.227	0.024	0.172	0.16
r ² CoefDet	0.857	0.990	0.903	0.769	0.769	0.868	-

Table 2. Comparison of roughness described with Pearson type IV distribution

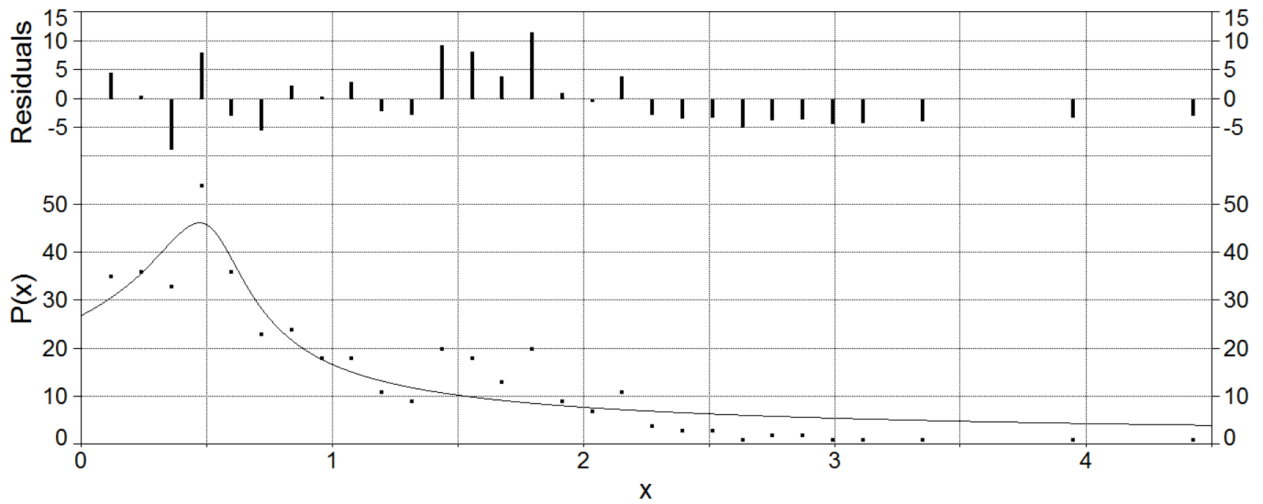


Figure 5. Rectified slope histogram approximated with Pearson type IV distribution, PL, test section # 1

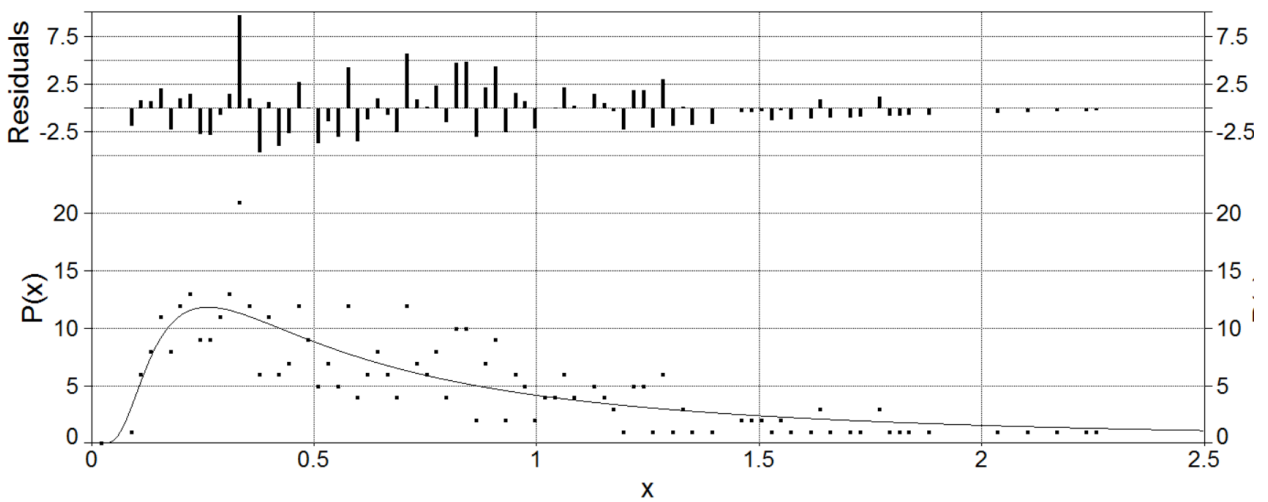


Figure 6. Rectified slope histogram approximated with Pearson type IV distribution, AT – LS, test section # 1

5. Conclusion

The objective of the research project was to develop a free to use and modify program capable to calculate IRI and roughness properties of pavement layers from point cloud data and statistically evaluate whether the point cloud data commonly acquired on sites are so high-quality that they can be used for the surface smoothness parameters calculation. The comparison was done with the methods broadly used to measure pavement roughness – rod and level and IRI – precise levelling. The following are the key conclusions and findings from this study:

The most important conclusion from this project, in the authors' opinion, is that the point cloud data commonly acquired on the site may be used to calculate the surface smoothness properties such as IRI and roughness. The standard deviation of IRI calculated from a point cloud was found to be lower than the standard deviation of IRI calculated from the longitudinal profile measured with precise levelling.

This was done with comparison to classical methodologies for measuring roughness – the rod and level measuring and precise levelling to measure the pavement profile and calculate IRI.

It was found that the average rectified slope from five parallel traces on a point cloud is the suitable criterion when both methodologies are compared. The average trace provides sufficient accuracy when the average rectified slope (IRI) needs to be used and when the rectified slope variability is of interest.

It has been found that the RIRI program is a useful tool for streamlining point cloud data analysis and it may be used for the pavement surface IRI and roughness calculations. The program contains a data viewer that helps to locate sections with a reduced surface quality in regard of smoothness and take appropriate further actions.

The histogram descriptor was used to analyze the rectified slope and roughness. Class widths were determined using Freedman and Diaconis's law. The Pearson type IV distribution was found to provide a reasonable approximation of both rectified slope and roughness histograms. The distribution parameters may be used for the data comparison.

Acknowledgements:

This publication was supported by the European social fund within the framework of implementing the project "Support of inter-sectoral mobility and quality enhancement of research teams at the Czech Technical University in Prague", CZ.1.07/2.3.00/30.0034. Period of the project's realization 1.12.2012 – 30.6.2015.

6. References

- J. Zak, J. Stastna, L. Zanzotto, and D. MacLeod, "Laboratory Testing of Paving Mixes – Dynamic Material Functions and Wheel Tracking Tests," *Int. J. Pavement Res. Technol.*, no. 6, pp. 147–154, 2013.
- M. S. Janoff, *Pavement Smoothness*. National Asphalt Pavement Association, 1996.
- A. Chabot, O. Chupin, L. Deloffre, and D. Duhamel, "ViscoRoute 2.0 A Tool for the Simulation of Moving Load Effects on Asphalt Pavement," *Road Mater. Pavement Des.*, vol. 11, no. 2, pp. 227–250, Jun. 2010.
- E. Y. G. Chen, E. Pan, T. S. Norfolk, and Q. Wang, "Surface Loading of a Multilayered Viscoelastic Pavement," *Road Mater. Pavement Des.*, vol. 12, no. 4, pp. 849–874, Dec. 2011.
- J. Zak, J. Stastna, J. Vavricka, K. Milackova, L. Kasek, and L. Zanzotto, "Poisson's Ratio of Hot Asphalt Mixtures Determined by Relaxation and Small Amplitude Oscillation Tests," *J. Test. Eval.*, vol. 43, no. 2, 2014.

- J. Zak, C. L. Monismith, and D. Jarušková, "Consideration of Fatigue Resistance Tests Variability in Pavement Design Methodology," *Int. J. Pavement Eng.*, vol. 2014, no. 8, pp. 1–6, 2014.
- H.-L. Xu, Y. Yuan, T.-J. Qu, and J.-R. Tang, "Dynamic model for a vehicle-pavement coupled system considering pavement roughness," *J. Vib. Shock*, vol. 19, no. 33, pp. 152–156, 2014.
- M. W. Sayers, T. D. Gillespie, and W. D. O. Paterson, "Guidelines for Conducting and Calibrating Road Roughness Measurements." The World Bank, Washington, D.C., U.S.A., 1986.
- B. Choubane, R. L. McNamara, and G. C. Page, "Evaluation of high-speed profilers for measurement of asphalt pavement smoothness in Florida," *Transp. Res. Rec.*, no. 1813, pp. 62–67, 2002.
- C. L. Monismith, "Flexible Pavement Analysis and Design-A Half-Century of Achievement," in *Geotechnical Engineering State of the Art and Practice*, American Society of Civil Engineers, 2012, pp. 187–220.
- M. Prikryl, L. Kutil, and J. Zak, "3D Laser Scanning Measurement Technology, Sweden Road 41 (Väg 41) Bergham-Gullberg," in *Asphalt Pavements 2011*, 2011, pp. 23–32.
- G. Boscaino and F. G. Praticó, "A classification of surface texture indices of pavement surfaces," *Bull. Lab. Ponts Chaussees*, vol. 234, pp. 17–34, 2001.
- H. M. Chemistruck, Z. R. Detweiler, J. B. Ferris, A. A. Reid, and D. J. Gorsich, "Review of current developments in terrain characterization and modelling," *Proc. SPIE— Int. Soc. Opt. Eng. Int. Soc. Opt. Eng.* Bellingham WA USA, 2009.
- M. W. Sayers and S. M. Karamihas, "The little book of profiling." University of Michigan, MI, USA, 1998.
- W. J. Wilde, "Implementation of an International Roughness Index for Mn/DOT Pavement Construction and Rehabilitation, Report MN/RC-2007-09." Research Services Section, Minnesota Department of Transportation, St. Paul, USA, 2007.
- M. Willet, G. Magnusson, and B. W. Ferne, "FILTER experiment – Theoretical study of indices, FEHRL Tech. Note 2000/02." Transport Research Laboratory, Crowthorne, Bershire, UK, 2000.
- J.-R. Chang, K.-T. Chang, and D.-H. Chen, "Application of 3D Laser Scanning on Measuring Pavement Roughness," *J. Test. Eval.*, vol. 34, no. 2, pp. 83–91, 2006.
- CSN 736175, "Measurement and evaluation of pavement surface roughness." Czech Office for Standards, Metrology and Testing, 2009.
- prEN 13036-5: 2014(E), "Road and airfield surface characteristics — Test methods — Part 5: Determination of longitudinal unevenness indices." European Committee for Standardization (CEN), 2014.
- Python Software Foundation, "Python Language Reference, version 2.7." .
- The Transtec Group Inc, "ProVal, User's Guide 3.5." 2015.
- Free Software Foundation, "GNU General Public License." 2007.
- D. Freedman and P. Diaconis, "On the histogram as a density estimator:L 2 theory," *Z. Für Wahrscheinlichkeitstheorie Verwandte Geb.*, vol. 57, no. 4, pp. 453–476, Dec. 1981.
- R. J. Hyndman, "The problem with Sturges' rule for constructing histograms." Monash University, Australia, 1995.
- H. A. Sturges, "The Choice of a Class Interval," *J. Am. Stat. Assoc.*, vol. 21, no. 153, pp. 65–66, 1926.
- K. Pearson, "Mathematical Contributions to the Theory of Evolution. XIX. Second Supplement to a Memoir on Skew Variation," *Philos. Trans. R. Soc. Math. Phys. Eng. Sci.*, vol. 216, no. 538–548, pp. 429–457, Jan. 1916.

2.8. Šroubek, F., Šorel, M., Žák, J., Obr, V., Precise International Roughness Index Calculation, 2020

Authors' contribution percentage:

40% Šroubek, F.

30% Šorel, M.

20% Žák, J.

10% Obr, V.

Precise International Roughness Index Calculation

Filip Šroubek^a, Michal Šorel^a, Josef Žák^b, Vítěk Obr^c

^aThe Czech Academy of Sciences, Institute of Information Theory and Automation, Pod Vodarenskou vezi 8, Prague, Czech Republic. Email: sroubekf@utia.cas.cz

^bCTU in Prague, Faculty of Civil Engineering, Department of Construction Management and Economics, Thakurova 7, Prague, Czech Republic.

^cControl System CA, Inc., Suite 850, 10655 Southport Road SW, Calgary AB T2W 4Y1, Canada.

Roadway infrastructure management focuses on quality of the road surfaces which influences the pavement longevity and riding quality. The road surface quality can be expressed in many ways from which the International Roughness Index has been recognized widely around the developed countries. This paper summarizes the derivation of International Roughness calculation and proposes a new numerical method for its computation. Compared to original Sayers's method, it does not use iterative approximation, which makes it much faster for non-uniformly sampled road data. The method can be used for arbitrary polynomial model of segments between elevation samples. The method utilizes modern geoinformation technologies for collecting and processing data, such as LIDAR that generate point clouds with billions of points in large scale applications. Except the Fortran code listed in the original paper, the code for the original algorithm has not been publicly available and most researchers relied on the ProVAL software with several limitations, including uniform sampling, the lack of automation, and little control over the influence of resampling methods and the initialization of the quarter-car simulation procedure. We provide Matlab codes for both the original method and the algorithm newly proposed in this paper.

1. Introduction

One of the criteria for a flexible pavement is its surface smoothness. The smoothness is tracked by the road maintenance agency and perceived by the road users. It was proved in [18] that highway users judge the condition of a highway by the riding experience when they travel over the highway. The pavement surface smoothness is an important parameter for road users not only from the perspective of their riding experience, but it is also one of the determinants of road user cost, as indicated in [18]. The choice of a proper pavement reconstruction design and technology has always been a task combining engineer's knowledge and experience. Many aspects that embeds empirical approach in pavement design persist in the asphalt pavement industry till today [13]. The engineer's goal is to effectively design and construct a desired pavement layer while meeting all standardized requirements, design criteria and contracting agencies' demands. However, many disorders whose occurrence is linked to an improper mix design,

errors in the mix production, its water content, and mistakes in the laydown process, such as the temperature loss, paver stops, improper compaction, result in an immediate decrease of the constructed layer quality happen during the construction. Some of these disorders are present right after the layer construction, and some of them take their effect when traffic loading and weather conditions occur during the pavement's lifetime. Thus in terms of pavement reconstruction, the engineer's challenge is even tougher when taken into account pavement deterioration caused by climatic conditions, traffic loading, subgrade deterioration [17].

The road smoothness has a significant effect on the surface water runoff and the ride quality, and, most importantly, traffic safety [27]. Janoff suggested, in his extensive work [10] based on the data collected over ten years from more than 400 test sections, that the initial smoothness is related to the pavement long-term roughness and durability in regard of the pavement cracking and overall deterioration. These findings are today proved by the mechanical analysis addressing the effect of flexible pavement viscoelasticity in relation to dynamic loading increased with the pavement surface roughness [3, 6, 26, 25, 28].

The need to measure the pavement surface smoothness led to the development of devices ranging from very simple and still in use such as the rod and level, profilographs, where the Californian profilograph may be mentioned as one of the early developed and still in use devices [21]. With the advances in technology, several automated devices were developed to measure the pavement smoothness [7, 13] including smartphones and other inexpensive sensors[11, 4].

The asphalt layer roughness has been used in many project specifications over the US and European countries to set pay adjustments based on the desired threshold. Nowadays, even in Public-Private-Partnership schemes and advanced design-build projects, roughness is one of the specifically set quality criteria. Furthermore, advanced design techniques and the use of construction machine control systems help to achieve these contract requirements [15].

Although the definition of smoothness indicators varies over states and countries from the International Roughness Index (IRI), the Profilograph Index (Prl), the Mean Roughness Index (MRI), the Quarter-car Index, the root-mean-square vertical acceleration and the rod and level surface smoothness measurement (roughness), whose review may be found in [14, 2, 5, 19, 23, 24], the value of smoothness should be well recognized as a useful indicator of the pavement serviceability performance and the quality of pavement layers should be periodically checked.

Light detection and ranging (LiDAR) and photogrammetry are the advanced geoinformation technologies that are able to capture the highway surface geolocation in large scale. Both LiDAR and photogrammetry

are methods that generate point clouds with billions of points. These big data can be utilized to address the IRI as is one of the key smoothness indication for the highway management [28].

2. Contributions

In this paper, we propose a novel method to compute IRI from elevation measurements taken at arbitrary regular intervals and possibly also any irregular intervals. We provide implementation of the method in the Matlab programming language.

Our work was motivated by the need to implement the computation of IRI as a software package component developed in our research institute. The software package utilizes the point cloud data captured by LiDAR. The code for the original algorithm in a computer language suitable for our purposes (Matlab or Python) was not publicly available and the only free option was ProVAL software [16], which has several limitations. ProVAL has only a graphical user interface, which means that repeated IRI computation cannot be automated. ProVAL works only with uniform sampling of elevation profiles. In the non-uniform case, the user must first resample data on a uniform grid, which inevitably influences the value of IRI subsequently computed. Finally, the code of the software is not available, which complicates more elaborate analysis of smoothness. For example, if we want to analyze the influence of the quarter car model initialization in the IRI computation.

The IRI computation, as described in the World bank proposal [18] and later in [20], solves an inhomogeneous linear ordinary differential equation modeling the motion between sprung and unsprung masses of a car moving by a constant speed along a measured section of the road.

In the original approach, the equation is solved by the state transition method. As an alternative, we propose a solution based on the method of variation of constants [22]. This approach gives the same results but offers greater flexibility and speed, especially for non-uniform sampling of input road profile. Ability to use non-uniform sampling can be useful in several situations. For example, elevation profile generated by intersection of a wheel path with edges of a triangulated point cloud has irregularly spaced samples. Another situation is a measurement with imprecise odometer, which systematically over or underestimates distance, and we want to rectify the results.

While non-uniform sampling is in theory possible even in the original method, the iterative computation of the exponential of the transition matrix makes the computation impractical, which also explains why this option is not available in ProVAL. Similarly to the original solution, IRI can be computed efficiently by the proposed method both for overlapping (floating-window mode) and non-overlapping road sections. Finally, in contrast to the original algorithm, which requires linear segments between road samples, the

proposed method can incorporate any polynomial model without increasing computational requirements. While this is partially a theoretical advantage, because IRI assumes piece-wise linearity by definition, this could be useful in the research of IRI alternatives.

To summarize, the proposed solution works with equal efficiency for

- uniform and non-uniform sampling of the road profile,
- overlapping and non-overlapping road sections,
- any polynomial model of road segments between samples.

We also provide the code of the proposed method in Matlab, which is suitable for computing IRI automatically on large set of road profiles.

3. International Roughness Index

This section contains a concise summary of the IRI definition based mainly on [18, 20].

IRI is computed from a single longitudinal profile, represented by a sequence of elevation measurements. The sample interval should be no larger than 300mm for accurate measurements. According to [20], a vertical resolution of 0.5mm is suitable for all situations. The slope of the road between samples is assumed to be constant.

The computation consists of three steps.

1. the profile is smoothed by a box filter of length 250mm
2. the ride of an ideal car (Golden Car) is simulated using the quarter-car model [8] at a speed of 80km/h.
3. IRI of a road section is defined as an accumulated suspension motion divided by the length of the section.

The quarter-car car model using Newton's laws of motion is described by four first-order differential equations, which can be written in matrix form as

$$\frac{dx}{dt} = x' = Ax(t) + bh(t) \quad (1)$$

with an initial condition $x(0) = x_0$. Quantities x , A and b are defined as follows:

$$x(t) = [z_s(t), z_{s'}(t), z_u(t), z_{u'}(t)]^T ,$$

$$A = \begin{bmatrix} 0 & 1 & 0 & 0 \\ -k_2 & -c & k_2 & c \\ 0 & 0 & 0 & 1 \\ k_2/u & c/u & -(k_1 + k_2)/u & -c/u \end{bmatrix} ,$$

$$b = [0,0,0, k_1/u]^T ,$$

where $z_s(t)$, $z_u(t)$ and $h(t)$ are height of sprung mass, height of unsprung mass and profile elevation, respectively. The parameters for the *Golden Car* model are defined as $c = 6.0$, $k_1 = 653$, $k_2 = 63.3$ and $u = 0.15$. Time derivatives are indicated with a prime mark. Time is related to a longitudinal distance by the simulated speed of vehicle

$$t = x/V ,$$

where x is longitudinal distance and V is the simulated forward speed defined as 80 km/h for the IRI. Vector $x(t)$ contains four state variables (height and speed of sprung and unsprung mass) that completely describe the simulated system in time.

The IRI of a section of length L is defined as

$$IRI = \frac{1}{L} \int_0^{L/V} |z_{s'}(t) - z_{u'}(t)| dt , \quad (2)$$

that is as an accumulation of the absolute suspension motion (distance of sprung and unsprung masses) divided by L . A common approach is to divide the road profile into segments of constant length (common length's are $L = 20m$ or $L = 100m$) and the IRI is calculated in each segment separately. An alternative is computation in each profile sample by a moving window of length L .

IRI is linear in two senses. First, the definition (2) implies that the average IRI of two segments of the same length equals the IRI of the segments taken together. Second, multiplication of the elevation input data by a scalar constant results in the multiplication of IRI by the same value. This comes from the linearity of both (1) and (2).

4. Proposed solution

The proposed solution is based on the method of variation of constants; see [22] Chapter 3.4. Using this method, IRI problem (1) has an analytical solution $x(t)$, which is the sum of a general solution $x_h(t)$ of the associated homogeneous system $x'(t) = Ax(t)$ and a particular solution $x_p(t)$ of the nonhomogeneous system: $x(t) = x_h(t) + x_p(t)$. Let $M(t)$ be a fundamental (also called principal) matrix with columns that correspond to the solution of the homogeneous system, i.e. $M'(t) = AM(t)$. The fundamental matrix is constructed from eigenvalues and eigenvectors of A ; see e.g. [12] Chapter 5.7. The constant form of A guarantees that $M(t)$ is invertible for every t . The solution of the associated homogeneous system that satisfies the initial condition is $x_h(t) = M(t)M(0)^{-1}x_0$. The general solution of (1) is then given by

$$x(t) = M(t)M(0)^{-1}x_0 + M(t) \int_0^t M(s)^{-1}bh(s)ds. \quad (3)$$

The integral in the second term can be calculated analytically for certain forms of $h(t)$ and this allows us to express the general solution explicitly. An example of the form that allows explicit solution are piecewise polynomials. In practice, the road profile is sampled and h is a discrete variable represented as a sequence $\{h_i\}_{i=0}^N$, where h_i is the profile elevation at distance x_i and time $t_i = x_i/V$. We assume that $\{x_i\}$ is an increasing sequence with $x_0 = 0$ and $x_N = L$. Note that the sampling need not be uniform. Let $p(t|c_i)$ denote a polynomial function defined by a set of coefficients c_i . The function is set to zero everywhere except on the interval $\langle t_{i-1}, t_i \rangle$. The number of coefficients in c_i depends on the polynomial degree and the coefficient values are calculate from $\{h_i\}$ and $\{t_i\}$ according to the used interpolation method. The polynomial interpolation of $\{h_i\}$ is expressed as $h(t) = \sum_i p(t|c_i)$ and then the integral can be calculated analytically on every interval $\langle t_{i-1}, t_i \rangle$ by a function

$$F(t_{i-1}, t_i, c_i) \equiv \int_{t_{i-1}}^{t_i} M(s)^{-1}bp(s|c_i)ds.$$

We used Matlab Symbolic Math Toolbox to find the analytical expression for F .

The general solution of (1) at time t for a polynomial interpolation of the profile sequence $\{h_i\}$ and the corresponding time samples $\{t_i\}$ is given by

$$x(t) = M(t)(M(0)^{-1}x_0 + \sum_{k=1}^K F(t_{k-1}, t_k, c_k) + F(t_K, t, c_{K+1})), \quad (4)$$

where the index K is such that $t_K < t \leq t_{K+1}$.

We are often interested only in the discrete solution $x_i \equiv x(t_i)$ at time samples $\{t_i\}_{i=1}^N$, which is the special case of the above equation,

$$x_i = M(t_i)(M(0)^{-1}x_0 + \sum_{k=1}^i F(t_{k-1}, t_k, c_k)). \quad (5)$$

The IRI is then approximated by a discrete form of (2), i.e.

$$IRI \approx \frac{1}{L} \sum_{i=1}^N |x_i(2) - x_i(4)|(t_i - t_{i-1}), \quad (6)$$

where $x_i(2)$ and $x_i(4)$ are the second, z_{sr} , and the forth, z_{ur} , element of the vector $x(t_i)$, respectively.

Since IRI (6) is a sum of contributions from individual time intervals, the dense computation by the moving window can be computed very efficiently – IRI in the next road section is nothing else than just the IRI value from the previous section plus the contribution of the new time interval $t_{N+1} - t_N$, minus the contribution of the interval $t_2 - t_1$.

The final aspect of the IRI definition we should mention is the initialization of the simulation. In [20], the initial state of simulation is recommended to be set using the average slope over the first $L_0 = 11m$. In our case, this corresponds to the time $T_0 = L_0/V$ to travel the distance L_0 so that

$$x_0 = [h(0), (h(T_0) - h(0))/T_0, h(0), (h(T_0) - h(0))/T_0].$$

Nevertheless, at 80km/h even the best initialization influences simulation for about 20m, which means that ideally the simulation should be started at least 20m before the start of the measurement. In addition, even if IRI is computed on non-overlapping profile segments, the simulation should be run for entire profile without re-initialization for each segment. This is a natural behavior of a real vehicle going without any interruptions.

5. Experiments

To check correctness of the proposed algorithm, we implemented also the original Sayers's methods and verified that both give exactly (to the machine precision) the same results. Next, we compared the IRI values computed by the proposed algorithm and ProVAL application on a number of elevation profiles. As an example, we show this comparison for a profile of a damaged road acquired by a mobile LIDAR system.

In Fig. 1, we compare IRI in sections of 20m. We can see that the values provided by ProVAL are close to those from our algorithm (1.5% relative error). Similarly, in Fig. 2, we show the same comparison for segments of length 1m. Since IRI is averaged on much smaller segments, their values tend to differ more than for longer IRI segments. Interestingly, ProVAL seems to systematically “undershoot” peak values of IRI. The next experiment demonstrates the ability of the proposed algorithm to work with arbitrary

sampling including irregularly sampled data. We show that resampling necessary in the standard method [20] smooths the elevation profile and consequently lowers the value of IRI. For this purpose, we randomly generated 200 continuous elevation profiles with $IRI = 1$ according to the Gaussian one-parametric model with fixed waviness $w = 2$ as described in the ISO standard 8608 [9, 1]. These profiles have the same power spectrum but each profile and each frequency has different random phase. An example of such profile is shown in Fig. 3. To completely eliminate the influence of the initialization, we constructed the profiles to be periodic with period $20m$ and measured IRI on the last $20m$.

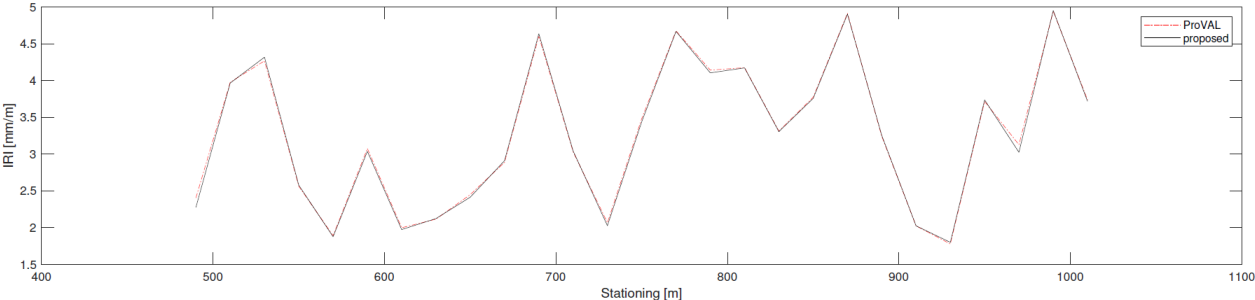


Figure 1. Comparison of IRI values computed by ProVAL and the proposed algorithm for non-overlapping segments of length 20m. Elevation data were sampled with 0.25m interval from a triangulation of a LIDAR point cloud.

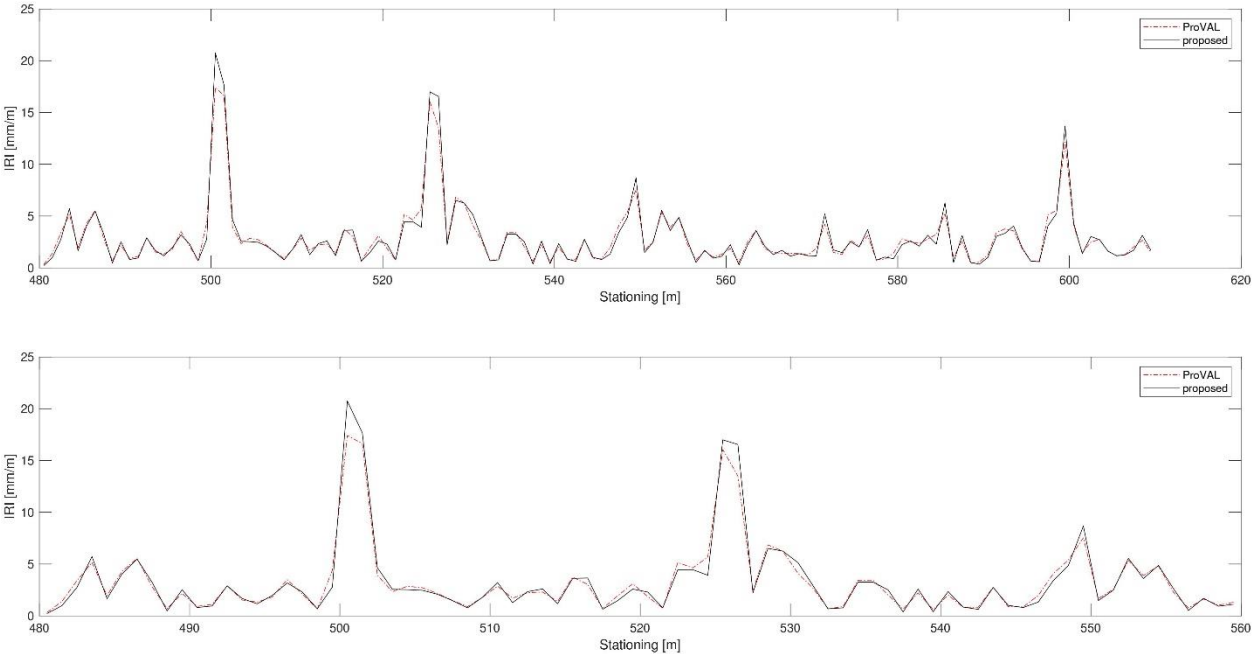


Figure 2. Comparison of IRI values computed by ProVAL and the proposed algorithm for non-overlapping segments of length 1m. Elevation data were sampled every 0.25m. Both graphs show the same data on different scales.

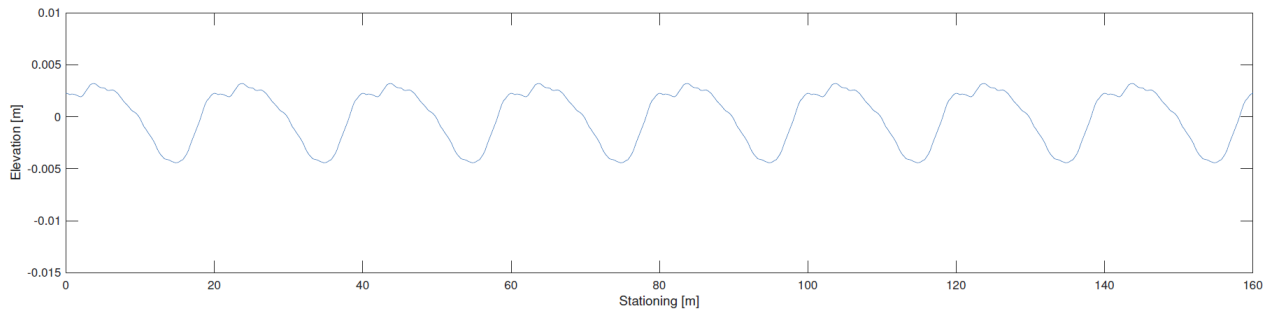


Figure 3. An artificial road with $IRI = 1$. This is an example of one road generated in the experiment demonstrating the influence of resampling. These roads are intentionally made periodic to completely eliminate the influence of initialization.

Let us assume that we need to compute IRI on a 20m interval with a sampling step 0.25m but the samples are mistakenly taken shifted by 0.125m, i.e. half of the sampling interval. Assume that this shift is known. Whereas the standard method [20] first requires resampling to correct positions, the proposed method computes IRI directly for arbitrary coordinates. Results are shown in Table 1, where they are compared with the IRI of the continuous profile. The table summarizes the mean value of IRI, the root means square error of IRI estimation and the maximum error over the set of 200 profiles. Table 2 shows the results of an analogous experiment but for a larger sampling step of 0.5m. Note that in these experiments the numbers for the correct sampling and the proposed method are same to three decimal places and differ in the fourth decimal place not shown in the tables.

Method	mean IRI	RMSE	Max. error
Continuous profile	1	0	0
Correct sampling	0.996	0.004	0.009
Resampling	0.990	0.011	0.020
Proposed direct method	0.996	0.004	0.009

Table 1. Resampling errors for sampling step 0.25m.

Method	mean IRI	RMSE	Max. error
Continuous profile	1	0	0
Correct sampling	0.985	0.016	0.033
Resampling	0.967	0.035	0.070
Proposed direct method	0.985	0.016	0.033

Table 2. Resampling errors for sampling step 0.5m.

We see that resampling causes lower IRI by smoothing the elevation profile. Even for step 0.25m, i.e. less than the recommended 0.3m [20], the error can achieve 2% of the IRI value with the average error about 1%. For a slightly longer step of 0.5m, the maximum error rises to 7% and the average error to 3.5%. A rule of thumb in these experiments is that resampling approximately doubles the error caused by discrete sampling of the profile. For more dense sampling, the error becomes negligible, yet it should be taken into account for sampling steps around the recommended value of 0.3m.

6. Conclusion

The asphalt layer roughness is being used in many projects specifications over the US and European countries to assess quality of pavements. The newly proposed computation method allows superior utilization of three-dimensional (3D) big data such as light detection and ranging (LiDAR) point clouds to compute IRI.

Moreover these technologies allow the IRI computation even in urban areas where the conventional measurement techniques can not be utilized and LiDAR is more frequently used, and billions of points are stored, to capture the area for mapping purposes. The method allow the utilization of these data for the IRI calculation thus pavement management.

The proposed method works with arbitrary even non-uniform sampling of elevation profiles, which avoids resampling that otherwise causes underestimation of the IRI value. For non-uniform sampling of road profile, the method is significantly more efficient than the original method [19].

The code of the proposed method is provided in Matlab at GitHub. We verified that for reasonably long segments, around 20m, the code gives results very close to those computed by ProVAL and can be used as its alternative for all practical purposes.

Acknowledgements:

The work reported here has been conducted as part of the research project "Implementation of Industry 4.0 principles during production and repairs of constructional layers of surface transportation" supported by Ministry of Industry and Trade of the Czech Republic.

7. References

- K. Bogsjö, K. Podgórski, and I. Rychlik. Models for road surface roughness. *Vehicle System Dynamics*, 50(5):725–747, 2012.
- G. Boscaino and F. Pratico. A classification of surface texture indices of pavement surfaces. *Bulletin Des Laboratoires Des Ponts et Chaussees*, 234:17–34, 2001.
- A. Chabot, O. Chupin, L. Deloffre, and D. Duhamel. Viscoroute 2.0 a tool for the simulation of moving load effects on asphalt pavement. *Road Materials and Pavement Design*, 11:227–250, 06 2010.
- A. Chatterjee and Y. Tsai. Training and testing of smartphone-based pavement condition estimation models using 3d pavement data. *Journal of Computing in Civil Engineering*, 34(6):04020043, 2020.
- H.M. Chemistruck, Z.R. Detweiler, J.B. Ferris, A.A. Reid, and D.J. Gorsich. Review of current developments in terrain characterization and modeling. In Dawn A. Trevisani, editor, *Modeling and Simulation for Military Operations IV*, volume 7348, pages 190 – 201. International Society for Optics and Photonics, SPIE, 2009.
- Ewan Y.G. Chen, Ernian Pan, Timothy S. Norfolk, and Qiang Wang. Surface loading of a multilayered viscoelastic pavement. *Road Materials and Pavement Design*, 12(4):849–874, 2011.
- Bouزيد Choubane, Ronald McNamara, and Gale Page. Evaluation of high-speed profilers for measurement of asphalt pavement smoothness in florida. *Transportation Research Record*, 1813:62–67, 01 2002.
- J. Howe, Jeffrey Chrstos, Richard Allen, Thomas Myers, Dongchan Lee, Chi-Ying Liang, David Gorsich, and Alexander Reid. Quarter car model stress analysis for terrain/road profile ratings. *International Journal of Vehicle Design*, 36, 01 2004.
- ISO8608. ISO 8608 : Mechanical Vibration, Road Surface Profiles, Reporting of Measured Data: International Standard. International Organization for Standardization, ISO, 1995.
- M.S. Janoff. Pavement smoothness. Information Series 53. National Asphalt Pavement Association, 1996.
- V. Khalifeh, A. Golroo, and K. Ovaici. Application of an inexpensive sensor in calculating the international roughness index. *Journal of Computing in Civil Engineering*, 32(4):04018022, 2018.
- D.C. Lay, S.R. Lay, and J.J. McDonald. *Linear Algebra and Its Applications* (5th Edition). Pearson, 2016.
- Carl L. Monismith. Flexible pavement analysis and design-a half-century of achievement. In *Geotechnical Engineering State of the Art and Practice*, pages 187–220, 2012.
- Peter Mucka. International roughness index specifications around the world. *Road Materials and Pavement Design*, pages 929–965, 06 2016.
- M. Prikryl, L. Kutil, and J. Zak. 3d laser scanning measurement technology, sweden road 41 (väg 41) bergham-gullberg. In *Asphalt Pavements*, pages 23–32, Prague, 2011. Pragoprojekt.
- ProVAL. Profiler viewing and analysis software (version 3.6.).
- Dawid Rys and Piotr Jaskula. Effect of overloaded vehicles on whole life cycle cost of flexible pavements. In *Testing and Characterization of Asphalt Materials and Pavement Structures*, pages 104–117. Springer, 07 2018.
- M. W. Sayers, T. D. Gillespie, and W.D.O. Paterson. Guidelines for conducting and calibrating road roughness measurements. Technical Report WTP46, The World Bank, Washington, D.C., USA, 1986.
- M. W. Sayers and S.M. Karamihas. *The Little Book of Profiling*. University of Michigan, MI, USA., 1998.
- M. W. Sayers. On the calculation of international roughness index from longitudinal road profile. *Transportation Research Record*, 1501:1–12, 1995.
- L. Scofield, S. Kalavela, and M. Anderson. Evaluation of california profilograph. *Transportation Research Record*, 1348:1–7, 1992.

- G. Teschl. Ordinary Differential Equations and Dynamical Systems. Graduate studies in mathematics. American Mathematical Soc., 2012.
- W. James Wilde. Implementation of an international roughness index for mn/dot pavement construction and rehabilitation. Technical Report MN/RC-2007-09, Minnesota State University, Minnesota Department of Transportation, St. Paul, USA, 2007.
- M. Willet, G. Magnusson, and B.W. Ferne. Filter experiment – theoretical study of indices. FEHRL Tech. Note 2000/02, 2000.
- H.L. Xu, Y. Yuan, T.J. Qu, and J.R. Tang. Dynamic model for a vehicle-pavement coupled system considering pavement roughness. *Journal of Vibration and Shock*, 33(19):152–156, 2014.
- J. Zak, Carl L. Monismith, and Daniela Jaruskova. Consideration of fatigue resistance tests variability in pavement design methodology. *International Journal of Pavement Engineering*, 16(1):91–96, 2015.
- J. Zak, J. Stastna, L. Zanzotto, and D. MacLeod. Laboratory testing of paving mixes-dynamic material functions and wheel tracking tests. *International Journal of Pavement Research and Technology*, 6(3):147–154, May 2013.
- J. Zak. On laser scanning, pavement surface roughness and international roughness index in highway construction. In *E&E Congress*, Prague, Czech Republic, 2016.